Centrifugal recovery of embryonic stem cells for regenerative medicine bioprocessing

Ju Wei Wong

Department of Biochemical Engineering

University College London

A thesis submitted for the degree of

Doctor of Philosophy

September 2008

To my parents

Poh Poh and *Judy*

For their love, unconditional support and untold sacrifices and without whom, none of this would have been possible.

Acknowledgements

It is a pleasure to thank the many people who made this thesis an enjoyable experience.

First and foremost, I would like to express my thanks and gratitude to Professor Mike Hoare for his invaluable support, guidance and encouragement throughout the course of my graduate studies. He has been instrumental in fostering a culture of intellectual challenge, rigour and discovery. He taught me how to ask questions and express my ideas. He showed me different ways to approach a research problem and the need to be patient, yet persistent and open to accomplish my goals. I would also like to thank my advisor Professor Chris Mason for his scientific knowledge, advice and providing insightful discussions and suggestions for my research.

A number of colleagues and fellow graduate students have played some kind of role in my research and time here at UCL. In this regard, I am indebted to Diana for her idiot proof masterclasses in stem cell biology and laboratory techniques, Emily, Spyros, Simon, Alex, Ioannis, Charo and especially Alfred, Minal and Emma for making tea, coffee and things interesting, and also for their immeasurable perspective on laboratory and result related issues.

I would also like to take this opportunity to thank Julia Markusen who together with Chris, encouraged me to apply for graduate school. To partially bankroll graduate school, I am very grateful to Professor Peter

Dunnill and Professor Nigel Titchener-Hooker whom together with Professor Mike Hoare were instrumental in helping me secure my Overseas Research Scholarship Award. In cultivating an interest in research and eventually pursuing graduate school, I am grateful to Professor Miranda Yap who kindly kept me "off the streets" during my summer holidays as an undergraduate in Singapore by allowing me to "loiter" in her labs. In those labs, I would like to thank Kathy, Victor, Danny and Yang for keeping me busy with animal cell culture stuff.

A good support system outside of college is essential to surviving the insanity associated with graduate school. I would not have made it through graduate school without the love, support, compassion, friendship and kindness of all my friends in Singapore and London. In this regard, I would like to thank Gene, Gina, Irene, Nick, Su, Yvonne, the Pryors, Smé-dawg, Nick 'Slake my thirst' Millar, François, Aussie Nick, the Parrishes, Fleur, Vic, the Busutills, the Baulks and Mark. I can only apologise to the others whom I have failed to list, but would like to reassure them that I am very thankful. I would also like to thank Dingo the pogonophobe.

Last but certainly not least, my love, thanks, and heartfelt gratitude to my parents, immediate and extended family. They have been a constant source of love, support, patience and encouragement, and for this I owe them more than than they will ever know.

Ju Wei
August 2008

Abstract

In order to realise the potential of embryonic stem (ES) cells as a regenerative medicine, it is crucial that economical, robust and scalable bioprocesses be established. Because bioprocesses irrevocably define the safety and efficacy of any biologically derived product, an understanding of the the impact of the engineering environment on ES cells is sought. This thesis uses murine ES cells as a mimic for ES cell types that will be used in cell based regenerative medicine applications to examine the bioprocessing impact of centrifugal recovery cells. A micro scale-down approach was used to examine the effects of centrifugal force, centrifugation time and process temperature on both the yield and biological characteristics of cells subjected to batch centrifugation. When subjected to centrifugation, mES cell loss and cell damage does not appear to occur during the settling or cell pelleting. In general, 5—25% of cells are lost during pellet resuspension to recover the centrifuge cells. The level of cell loss is determined by a combination of centrifugal force, centrifugation time and process temperature. The extent of damage of the remaining cells (i.e. cells not lost during resuspension) is minimised at lower processing temperatures. It is hypothesised that at low processing temperatures, cell loss is minimised due to weak cell-to-cell contact and are thus less susceptible to damage caused by the shear environment generated to disperse the collected cell pellet.

The concept of Windows of operations was also applied to evaluate an optimal set of centrifuge operating conditions that results in minimal

cell loss and cell damage. The process visualisation tool indicates that operating the centrifuge at 5–9 mins × 300–500 g will result in maximum cell recovery at 4, 21 and 37^{o}C process temperatures. The influence of centrifugation on the biological characteristics of mES cells revealed changes in proliferative capacity, pluripotency and differentiation status when exposed to varying levels of centrifugal force. mES cells exposed to increasing levels of centrifugal force up to 2,000 g progressively lost pluripotency. The pluripotency potential of cells exposed to 3,000 g of centrifugal force was not significantly different from un-centrifuged mES cells. Differentiating mES cells exposed to increasing levels of centrifugal force exhibited increased cell proliferation and a possibility of early induction of endoderm and mesoderm differentiation. Although limited in some areas, the results strongly suggest that restricting exposure to no more than low levels of centrifugal force is necessary to safeguard the stability of the desired mES cell characteristics. Overall, the insight gained from the work accomplished serves to create and establish an awareness of the challenges faced within the arena of whole cell bioprocessing for regenerative medicines.

Contents

List of Figures

List of Tables

Chapter 1

Regenerative Medicine Bioprocessing

1.1 Introduction

The diffusion of regenerative medicine as a field of study and product technology has gained momentum in recent years, and is at the vanguard of modern human healthcare. Its burgeoning status is driven by the clinical desire for new therapies and a continual further understanding of cell biology as the field progresses. This thesis will highlight the requirement to develop robust and scalable bioprocesses to facilitate the translation and proliferation of (cell-based) regenerative medicines as the field ventures from a research based activity into the domain of human healthcare. The focus of this thesis is to investigate the impact of bioprocessing on cells, in particular the centrifugal recovery of embryonic stem cells. This thesis will conclude with a discussion of the work accomplished and suggest new and exciting opportunities for regenerative medicine bioprocessing research.

1.2 Regenerative medicine

Regenerative medicine is an emerging multidisciplinary field of study within biotechnology which has the capacity to create a new paradigm in healthcare, especially where chronic and degenerative diseases are concerned. Regenerative medicines seek to eliminate the debilitating effects of trauma, diseases or degeneration by restoring lost native function and structure. In contrast, molecular medicines such as analgesics, antibiotics and antibodies treating arthritis and cancer ameliorate and manage symptoms of the condition over multiple doses, and cannot in general regenerate tissue (Mason & Dunnill, 2008b). The crucial distinguishing features of a regenerative medicine are: (1) the absence of fibrosis and scarring at the repair site (Yannas, 2001); (2) regeneration is anatomical consistent and are capable of remodeling (Yannas, 2004); and (3) normal tissue function is established or restored.

Before the published editorial by Mason & Dunnill (2008a) providing a brief description of regenerative medicine, there were many differing interpretations of

what it should be (Daar & Greenwood, 2007). This confusion and lack of consensus is due to the multidisciplinary nature of regenerative medicine and is not helpful. In order to facilitate understanding and advocacy across all levels of comprehension and interest, a clear and unified definition of regenerative medicine encompassing the differing opinions has to be established (Mason & Dunnill, 2008a). The following definition of a regenerative medicine is based on the aforementioned distinguishing features of regenerative medicine. Therapies promoting regenerative medicine can principally be differentiated into four mutually exclusive, collectively exhaustive strategic areas. These areas are underpinned by the presence and absence of two related determinants: cells and scaffolds (Fig. 1.1). Each strategic area is briefly outlined in the following four sub-sections: (1) molecular medicines; (2) biomaterials engineering; (3) cell therapy; and (4) tissue engineering.

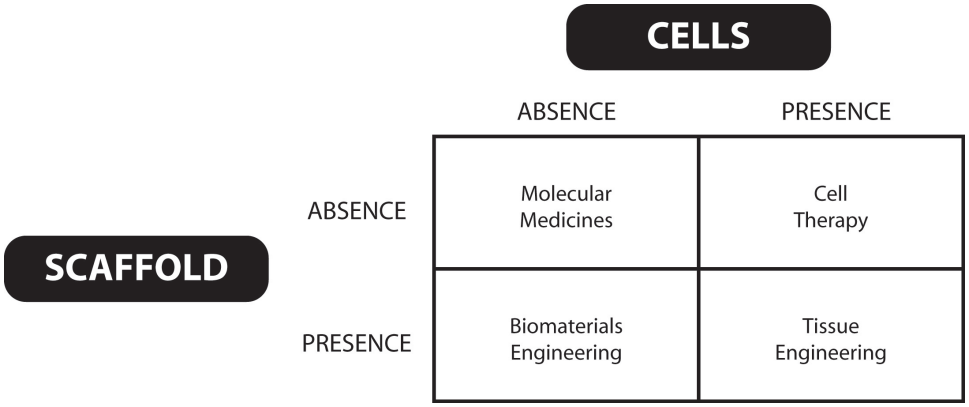

Figure 1.1: The regenerative medicine matrix. Four mutually exclusive strategic approaches to clinical therapy as defined by the absence or presence of cells and scaffolds.

1.2.1 Molecular medicines

In general, molecular medicines are unable to regenerate tissue, nevertheless there are exceptions in this category. Synthesised in multi-stepped bioprocesses and administered exogenously, these molecules seek to trigger, mimic or control the innate regenerative capacity of the patient to restore lost tissue function. For instance:

1. Cytokines and hormones form a dynamic network of signaling (glyco)proteins that play vital roles in homeostasis, physiology and development. When administered as a therapy, they stimulate tissue regeneration or mimic developmental processes. Two examples within this category of therapy are given: (1) recombinant human erythropoietin (rHuEPO) is a synthetic analogue of the naturally occurring hormone erythropoietin (EPO) which is responsible for regulating erythropiosis, and has successfully been used in the treatment of hematological and ontological disorders (Ng *et al.*, 2003); and (2) transforming growth factor $\beta 3$ (TGF-$\beta 3$) when introduced into the periphery of a healing adult wound mimics the fetal wound healing response, resulting in a diminished inflammatory response and reduced scarring (Shah *et al.*, 1992).

2. Nucleic acids when administered as a gene replacement or silencing therapy. In gene replacement therapy, functional copies of a mutated gene are delivered to affected cells via a vector to establish or restore normal function. For example, visual function was improved in patients with Leber's congential amaurosis after exogeneous cDNA was introduced to correct gene mutations (Bainbridge *et al.*, 2008). RNA interference (RNAi) has the sequence-selective specificity to silence genes in order to promote regeneration of tissue (Cheema *et al.*, 2007), and to inactivate disease causing gene expression, particularly in gene related disorders that are not amendable to conventional treatments. For example, silencing of Apolioprotein B (ApoB) expression. Elevated levels

of ApoB is correlated with a high risk of coronary artery disease (Soutschek *et al.*, 2004; Zimmermann *et al.*, 2006).

3. Chemical molecules that influence cell fate such as Reversine. Reversine is a small molecule purine derivate capable of dedifferentiating lineage committed myoblasts into progenitor cells capable of proliferating and redifferentiating into adipocytes and osteoblasts (Chen *et al.*, 2004). Whilst strictly not a molecular medicine, the value of such molecules is worth mentioning as they are crucial in the campaign to understand stem cell biology and its future as a successful medicine (Ding & Schultz, 2004).

1.2.2 Biomaterials engineering

This is a branch of material science concerned with the fabrication of biomimetic substrates capable of supporting cell attachment and/or cell proliferation. Biocompatible and biodegradable scaffolds have been developed (Table 1.1) to provide mechanical strength, and to mimic the 3-dimensional (3D) bio-physical and chemical cues of natural extracellular matrix (ECM). The role of ECM is crucial as it provides the substrate for cells to attach and it orchestrates tissue organisation and remodeling (Aumailley & Gayraud, 1998). Scaffolds can be directly implanted into the defect site as a histo-conductive substrate for surrounding cells to infiltrate and proliferate (*in vivo* tissue engineering), or seeded with cells and cultured in a bioreactor to form tissue for grafting (*in vitro* tissue engineering) (see Section 1.2.4 for Tissue Engineering). With time the seeded scaffolds would degrade into non-toxic components and be replaced by native ECM produced by the cells, thus supporting tissue regeneration (Freyman *et al.*, 2001). The structural organisation of a scaffold is pivotal in its effectiveness as an ECM mimic and can be dissected into, macro– (10^{-1}–10^{-3} m), micro– (10^{-3}–10^{-6} m), and nano– (10^{-6}–10^{-9} m) scale features, which together promote cell adhesion, proliferation and migration, tissue formation and even cell differentiation (Engel *et al.*, 2008; Lee *et al.*, 2008). The macro-scale structure relates to the overall anatomical shape of the scaffold to fit its purpose—to match defect site configuration or bioreactor dimensions. The micro-scale structure relates to its general topology and scaffold pore size, its distribution and interconnectivity. Together the macro– and micro–scale features influence mass transport of nutrients and wastes within the scaffold (Hollister, 2005), cell proliferation, cell migration and tissue ingrowth (Moore *et al.*, 2004). The nano-scale structures relate to substrate surface nano-features that control cell behaviour: cell adhesion; cell locomotion; cell orientation/morphology; cell signaling; transcription activity; gene expression and cytoskeleton reorganisation (Bursac *et al.*, 2007; Stevens & George, 2005).

Equally important are the bulk properties of the scaffold. Tensile strength, its stiffness (i.e. Young's modulus, E), rate of degradation and surface properties influence its overall performance. Mechanical strength is demanded in applications where high loadings are encountered. Structural tissue mimics such as bone must be load-bearing during the regenerative process (Adachi *et al.*, 2006), at the same time should not completely shield ingrowing tissue from the mechanical stresses crucial in directing tissue development. Material stiffness modulates the elastic environment of the cells and phenotypic changes of cells with respect to the surrounding elasticity have been reported (Engler *et al.*, 2006). The rate of degradation of a scaffold is controlled by its chemistry and its *in vivo* degradation mechanism (e.g. hydrolytic or enzymic degradation). The mechanical strength of a scaffold is specified by its degradation rate, thus it has to be carefully considered during design in order to promote optimal tissue regeneration. As noted earlier, the nano-scale surface features control cell behaviour, as can modifications made to the surface. The charge density, derivatisation with protein motifs (Massia & Hubbell, 1990) are equally crucial in modulating cell adhesion, survival, growth and proliferation (Hubbell, 1995; Jiao & Cui, 2007; Wilson *et al.*, 2005).

Table 1.1: Polymeric material used for scaffolds in regenerative medicine applications. Adapted from Seal *et al.* (2001).

Polymer Classification	Advantages	Disadvantages
Synthetic		
Polyesters (e.g. PGA & PLA)	Adjustable degradation rates by varying polymer chemistry. Monomeric components can be metabolised and surface can be derivitised to enhance cell attachment.	High degradation rates can result in a local depression of pH. Inflammation and foreign body reactions have been observed *in vivo* due to persistent particulate (500–700 nm) degradation debris (Cordewener *et al.*, 2000).
Polyethylene oxide	Highly biocompatiable injectable gel (20% w/v) and can be crossed-linked with exposed to UV light.	Gel can experience rapid diffusion and poor mechanical stability after injection. *In vivo* cross-linking of polymer is difficult.
Natural		
Alginate	Easily molded and cross-linked by Ca^{2+} into a stable structure to entrap cells. Can be derivitised with materials indigenous to the human body.	Leaching of Ca^{2+} from cross-linked alginate diminishes structural integrity. Alginate is not native to the human body and thus potentially immunogenic.
Collagen	Present in most types of connective tissue in the human body and is an excellent structural matrix protein.	16 different types of collagen. Only types I and II are sufficient in abundance to be of utility in regenerative medicine applications. Collagen type influences cell phenotype and proliferation.
Hyaluronan	Abundant in cartilaginous ECM and can be co-polymerised with esters to form a hybrid material with increased biocompatibility and tailored degradation rates. Degradation products are highly biocompatiable.	Highly water soluble, rapid readsorption and tissue clearance times.
Fibrin gels	Exploits wound healing chemistry to cast gels; 3-D fibrinogen networks are cross-linked by factor XIIIa. Non-cytotoxic and highly biocompatible.	Lacks the mechanical stability to be casted into structures. Highly susceptible to enzyme degradation, especially *in vivo* resulting in rapid degradation rates.
Chitosan	Highly abundant polysaccharide. Relatively biocompatible, biodegradable and does not elicit a strong immune response.	Not proven as an effective regenerative medicine scaffold and requires further investigation and development.

1.2.3 Cell therapy

The direct application of cells to prevent, treat or attenuate illness is described as a cell therapy. The use of cells in this manner is not novel and is well established in bone marrow and blood transfusions in treating immunological and haematological disorders. Potential therapeutic areas including cartilage damage, corneal repair, nerve repair, diabetes, neurological disorders and reconstructive/asethetic surgery (Dunnett *et al.*, 2001; Elliott *et al.*, 2007; Horas *et al.*, 2003; Lima *et al.*, 2006; Nesic *et al.*, 2006; Shortt *et al.*, 2007; Weiss *et al.*, 2007). These cells are normally expanded *in vitro* prior to implantation.

The safety, efficacy and success of any cell-based regenerative medicine is contingent on the judicious selection of both cell source and type, and its *in vitro* bioprocessing before being administered to the patient. In tissue engineering applications, where cells are administered together with a scaffold, the material that constitutes the scaffold has to be selected carefully. Cells used in regenerative medicine applications should be capable of proliferation whilst maintaining the desired phenotype and biological function throughout bioprocessing. Cells may also be modified *in vitro* prior to usage (Chen *et al.*, 2003; Pollock *et al.*, 2006). The sources of cells used can be autologous, allogenic and xenogenic in origin.

1. Autologous cells. Cells are harvested from the patient, and are returned to the same patient. Cells are either harvested from a site away from the point of trauma, or at a time point prior to treatment. Grafted autologous cells have the advantage of avoiding immune-mediated rejection responses, thus eliminating the use of immunosupressive drugs. Its limitations on its use include: insufficient useful or undamaged cells during harvesting, or harvested cells lack the proliferative capacity to be therapeutically viable.

2. Allogenic cells. Cells are harvested from a donor rather than the recipient patient. Allogenic cells have the advantage of being more readily available

at short notice, but the recipient's immune response may have to be attenuated with immunosupressive drugs. Ideally, these drugs should help the host become more tolerant or adapt to the foreign antigens in the allogenic cells without any adverse side effects (Gorantla *et al.*, 2000). However, this is not the case in practice. These drugs reduce systemic immunity, thereby increasing the risk of infection and cancer in the long term and do not completely eliminate the risk of chronic rejection. Cells derived from the brain, eye and fetal sources or transplanted into these areas appear to enjoy a degree of immune privilege (Green & Ware, 1997).

3. Xenogenic cells. Cells harvested from a donor of another species. Their consideration will be omitted from this discourse as their use has been unpopular in clinical practice, and their commercial potential is outweighed by the following risks: zoonotic infection (Boneva & Folks, 2004; van der Laan *et al.*, 2000); immune-mediated hyperacute rejection responses; greater risk of opportunistic infection due to the use of higher doses of immunosupressive drugs; subtle differences in metabolic functions and the ethical considerations debating the beneficence of its use.

The type of cell used in a regenerative medicine rests upon on its clinical application, relative abundance and its ability to be cultured in bulk *in vitro*. Cells may be terminally differentiated somatic cells, adult or embryonic stem cells. Terminally differentiated somatic cells such as fibroblast, smooth muscle cells, keratinocytes and chondrocytes confer tissue specific characteristics and are amiable to *in vitro* culture techniques as are adult stem cells. Both terminally differentiated somatic cells and adult stem cells however have a finite replicative capacity and experience replicative senescence (Bruder *et al.*, 1997; Hayflick, 1979). As a result, the rate of cell proliferation *in vitro* is an important determinant in selecting the type of cell to be used in a regenerative medicine (Shieh & Vacanti, 2005). Cells such as

neurons and cardiomyocytes have a low (or zero) rate of proliferation *in vitro*, as a consequence are unsuitable as a therapeutic choice. An alternative strategy is thus required to make up sufficient numbers of these cells for therapy within an appropriate timeframe. A potential solution is offered in the form of embryonic stem cells, not only to manufacture cells with a poor rate of proliferation but also for cell types not available due to degeneration, disease or defect. Adult and embryonic stem cells are further described in Section 1.4.

1.2.4 Tissue engineering

Tissue engineering is a collective term describing the understanding and integration of science from many diverse areas such as biomaterials, developmental and cell biology, engineering sciences, surgical and clinical practice (Langer & Vacanti, 1993). It is based on the tenet of allying a suitable biomaterial with pertinent cell types under favorable conditions *in vitro* to synthesise neo-tissue. This is acheived by shaping of a biocompatiable and biodegradable material into the desired 3D geometry to form a scaffold that provides the appropriate bio-physical and chemical milieu for cell attachment and tissue synthesis. The scaffold is seeded with cells and allowed to grow and mature in a bioreactor nourished by tissue culture medium, eventually forming a living functional tissue substitute ready for grafting (Atala *et al.*, 2006; Sherwood *et al.*, 2002). Examples of tissue engineered bladder, blood vessels, kidney, reproductive organs, skin and urethra for clinical application are given in Atala (2004) and Metcalfe & Ferguson (2007). The building of complex 3D tissues composing of multiple cell types and its associated small scale functional features (e.g. intestinal villi, renal corpuscle and nephron), its vascularisation and *in vitro* culture are major challenges in this area.

In situ organogenesis and tissue sythensis is a consequence of highly orchestrated spatial and temporal cell signaling processes. These signaling processes can vary in intensity and originate from cell-to-cell contact, cell-to-scaffold/ECM contact or arrive in the form of soluble factors such as hormones and cytokines. The current understanding of these processes is in its infancy but fast growing thus potentially allowing the construction of complex tissues *in vitro*. The study on skin and peripheral nerve synthesis by Yannas (2004) may provide clues and general rules for progress in this area.

An effective nutrient supply and distribution is another crucial factor in the construction of large and complex tissues. Under static conditions cell growth on scaffolds occur within 1 millimetre from the liquid-scaffold interface as the transport

of oxygen, essential nutrients and cellular waste products are limited to diffusional transport (Dunn, 2008). To overcome this limitation, there exist three vascular based strategies to supply the required nourishment to support cell growth and proliferation in large tissue constructs: (1) utilising the pre-existing vascular beds of the host or graft, however this approach is only suited to thin tissue constructs such as skin (O'Ceallaigh *et al.*, 2007); (2) encouraging the growth of blood vessels by using angiogeneic factors such as vascular endothelial growth factor (VEGF), fibroblast growth factor (FGF) and platelet-derived growth factor (PDGF) (Lokmic & Mitchell, 2008; Soker *et al.*, 2000); and (3) building into the scaffold a blood distribution system. Hoganson *et al.* (2008) discusses the applications of pre-formed scaffold embedded channel system for liver and lung tissue engineering.

1.3 Bioprocessing

Since the development of recombinant DNA techniques in the 1970s, the diffusion of modern biotechnology on the global stage has transformed agriculture, healthcare and economic systems in many countries throughout the world. It is one of the most enabling industrial innovations in recent times driven by scientific discovery and technological innovation in order to satisfy a market need. It has led to the introduction of a large number of products with many diverse applications (Giovannetti & Jaggi, 2007). Crucial to the manufacturing of these products is the field of *bioprocessing*. Conceptually, a bioprocess is an industrial scale sequential multi-step procedure used to synthesise, recover, isolate, purify, polish and formulate a product that is a derivative of a biological system. A bioprocess is customarily divided into upstream and downstream processing. All upstream and downstream unit operations interact very strongly with each other and the choice of unit operation significantly influences overall bioprocess performance (Zhou & Titchener-Hooker, 1999).

The safety and efficacy of any biological product is singly determined by its identity (Kuhlmann & Covic, 2006) and during its manufacture, the bioprocess uniquely specifies the product. Differences in manufacturing procedures can affect the product and ultimately the consumer (Casadevall *et al.*, 2002). Detecting changes in product identity attributed to changes in bioprocess is compounded by its biological complexity. Product identity changes will go undetected if they occur beyond its understanding or analytical means (Chirino & Mire-Sluis, 2004). In order to mitigate these risks, manage process variations and product heterogeneity, the manufacture of biological products for healthcare applications operate within highly structured environments governed by strict operational procedures (e.g. current good manufacturing practice (cGMP), total quality management (TQM)) and process controls.

The success of a bioprocess is measured by the safety and efficacy of its product and its commercial profitability. Crucial to the success of any bioprocess is a detailed

qualitative understanding of the bioprocess environment at the design stage so that any issues that arise can be addressed. This is achieved by examining the performance of a particular unit operation and how it integrates within the entire process. Appreciation of the variations within the many interacting variables, how they are accumulated and their influence on the product will assist in establishing acceptable operational ranges and set-points. A qualitative understanding of the bioprocess environment also aids in establishing suitable manufacturing in-process monitoring and control strategies, and identify critical process variables. Titchener-Hooker *et al.* (2008) discusses a micro biochemical engineering approach to bioprocess design and is especially useful where large quantities of material are not readily available.

1.3.1 Whole cell bioprocessing

The emerging field of *whole cell bioprocessing* is driven by the increasing amount of basic science research and number of potential therapies entering clinical trials. Whole cell bioprocessing refers to the idea that live cells are a major constituent of the final product and are omnipresent throughout the entire bioprocess — from cell procurement from a donor source, to its expansion and isolation in culture, storage and when implanted into a patient (Mason & Hoare, 2007). Cells at every stage of the bioprocess have to be maintained in a satisfactory state to ensure product quality, safety and efficacy.

In a review by Kemp (2006), the author traces the history and success of regenerative medicine to date of pioneers and early adopters within the field. Whole cell bioprocessing is an evolution of the well established bioprocess industry that has developed successful process for products derived from the culture of cells. Whilst sharing some sharing some fundamental conceptual bioprocess frameworks and fundamental engineering tenets with traditional bioprocesses, whole cell bioprocessing has many distinguishing characteristics (Mason & Hoare, 2007). For example: the

omnipresence of cells in the bioprocess (as mentioned above); reduced nutritional and gas transport to cells when fabricated into neo-tissue; short shelf-life during transportation or storage due to unique nutritional and oxygen demands; where cells are used, the homogeneity and potency of a given population of therapeutic cells, scalability of bioprocess, cell source contamination and process sterility issues (Dunn, 2008; Klein *et al.*, 2006). These unique characteristics of a whole cell bioprocess impose significant biochemical engineering challenges at various levels of its management and execution. An editorial by Mason & Hoare (2006), the authors emphasise the need to draw from experiences within and beyond the field of biotechnology to facilitate the commercial development and exploitation of whole cell bioprocesses. For instance, process automation to facilitate throughput and product consistency and the adoption of management information systems (MIS), enterprise resource planning (ERP) systems and manufacturing execution systems (MES) to support and manage manufacturing and business decisions.

From a biochemical engineering perspective, robust and scaleable whole cell bioprocesses need to be developed in order to fulfill their market potential, and a list of desirable whole cell bioprocess characterisitcs is provided in Mason & Hoare (2006)

1.3.2 Bioprocess conditions

One of the most crucial aspects in the development of cell based regenerative medicines is its bioprocessing environment. As noted earlier, any biologically derived product is defined by the process, this maxim takes on a greater significance where cells are themselves the final product. The bioprocessing of cells for regenerative medicine exposes them to a diverse range of conditions and gradients such as gas and nutrient concentrations, osmolarity, pH, temperature, hydrostatic pressure, shear conditions, relative centrifugal force and interfacial gas-liquid phenomena. As animal cells are recognised to be delicate and susceptible to physical and biochemical

cues from its surroundings (Al-Rubeai *et al.*, 1995; Papoutsakis, 1991), its bioprocessing conditions present unique challenges during manufacture. When exposed to undesirable conditions damage to cells occur. Damage may result in loss of cells or cell viability (see Section 3.3.1 for detailed description). More subtle to cell damage are changes in cell physiology such as metabolism, protein synthesis, proliferation rates, apoptotic profile, phenotype, genotype, karyotype and epigenetic profile (Al-Rubeai & Singh, 1998; Lin *et al.*, 2005; Seow *et al.*, 2001). The effects of cell damage influence overall bioprocess productivity and product safety and efficacy. As a consequence it is crucial to take into consideration the likely sources of damage and curb unwanted cell damage by minimising its exposure to such influences.

1.3.2.1 Temperature

Temperature is one of the many key factors that determine cell survival. When exposed to temperatures above physiological, animal cells are rendered non-viable (Westra & Dewey, 1971) mainly due to the denaturation of cytoplasmic proteins which are essential in maintaining normal cellular function. However, when exposed to sub-physiological temperatures above freezing, animal cells have been shown to adapt to these changes in a variety of ways. Cells are known to be able to recover from hypothermic conditions without suffering long term consequence and this has been exploited in the transport of organs and cells in transplant medicine. Cells lines have also been induced to become cold-tolerant (Glofcheski *et al.*, 1993; Russotti *et al.*, 1996). Three levels of sub-physiological temperatures can be specified: moderate (33–25°C), mild (20–16°C) and severe (10–4°C) hypothermia, and its effect on cultured cells is described in detail in Hunt *et al.* (2005). Briefly, hypothermic exposure has been shown to disrupt cell cytoskeleton, suppress protein synthesis and modify cellular membanes (Fujita, 1999; Waugh, 1982). Depending on severity of exposure (e.g. time and temperature) and cell type, apotosis can be prevented or induced (Perotti *et al.*, 1990; Rauen *et al.*, 2000; Sakurai *et al.*, 2005). Cells rewarmed

from hypothermic conditions to physiological have been reported to be apoptotic (Healy *et al.*, 2006; Rauen *et al.*, 2000) and express heat shock proteins (Liu *et al.*, 1994). Heat shock proteins are a group of proteins which are expressed when cells are exposed to elevated temperatures or subjected to environmental stress. Exposing cells to hypothermic temperatures have been demonstrated as a manufacturing strategy to increase protein of interest yields in culture (Chong *et al.*, 2008; Fox *et al.*, 2004) or to help schedule the scaling up of manufacturing seed trains (Hunt *et al.*, 2005).

Under bioprocess conditions exposure to freezing temperatures is lethal to unprotected cells. During cryopreservation of cells for long term storage, measures are taken to avoid cell damage (via solute concentration, dehydration and intra-/extracellular ice formation) by controlling the velocity of cooling in the presence of a cryopreservant (e.g dimethyl sulfoxide (DMSO) or glycerol) (Gao & Critser, 2000; Mazur, 1970)

1.3.2.2 Hydrodynamic environment

The hydrodynamic forces found within a bioprocess can trigger a variety of stress responses in animal cells including cell necrosis and cell loss (Zoro *et al.*, 2008). These forces occur in every aspect of a cell based regenerative medicine bioprocess: from cell biopsy, to its culture in vessels, primary recovery, pipe transfer and pumping, and eventually when returned back to the patient. The term *shear damage* is widely used in bioprocessing to describe the hydrodynamic forces that results in cell damage. Although in some instances, cell damage is not entirely ascribed to shear rate or shear force (Chisti, 2001). Cell sensitivity to shear damage has been reported in both laminar and turbulent flow regimes and the level of cell damage incurred is related to the mean bursting cell membrane tension and growth phase (Born *et al.*, 1992). Under laminar shear stresses, damage varies considerably from 0.2×10^3—100 N m^{-2} with substantial damage occurring from 100—350 N m^{-2} (Born *et al.*,

1992). It is difficult to define shear forces in turbulent flow and thus are usually expressed as a local or average power dissipation rate (W kg^{-1} or m^2 s^{-3}) which is independent of flow regime. In turbulent flow average power dissipation rates up to 2×10^4 W kg^{-1} were presumed to interact with cells via appropriately sized eddies that cause membrane distortions that increase membrane tension and surface energy, and consequently cell disruption (Zhang *et al.*, 1993). Eddie sizes approximating the cell diameter or smaller (Kawase & Moo-Young, 1990; Kunas & Papoutsakis, 1990), distort the membrane and when membrane bursting tension and bursting surface energy are exceeded, cells are disrupted (Zhang *et al.*, 1993). Eddies larger than the cell entrain the cell without causing damage (Maa & Hsu, 1996). Cells entering a contractile flow regime (equivalent to extensional flow (Taylor, 1934)) will experience compression perpendicular to the direction of flow, whilst simultaneous experiencing extension in the direction of the flow. Animal cells introduced into contractile flows have been reported to withstand energy dissipation rates up to 10^4—10^5 W kg^{-1} (Ma *et al.*, 2002). Cell damage due to un-submerged and submerged jets are described in Chan *et al.* (2006) and MacLoughlin *et al.* (1998). Whilst the work in either study was not carried out with animal cells, the cell damage mechanisms are relevant and can be applied. Bubble disengagement at the bulk liquid-gas interface has been associated with animal cell damage in culture (Chisti, 2000). During the collapse of a disengaging bubble, regions of high strain rates develop at the liquid-gas interface (Garcia-Briones & Chalmers, 1994). Depending on bubble size, energy dissipation rates of bubbles disengaging at the surface range between 1×10^1—1×10^7 W kg^{-1} with smaller bubbles generating higher energy dissipation rates (Boultonstone & Blake, 1993).

1.3.3 Primary recovery

The separation of cells from its suspending liquor is an important criteria in specifying overall bioprocess yield in cell based bioprocesses. The conservation of cells

during separation is crucial in regenerative medicine applications, and necessary to avoid inordinate intracellular product loss or extracellular product contamination in protein bioprocessing. In order to separate and concentrate cells, centrifugation and tangential flow microfiltration are in competition. A third, the adsorption of cells in an expanded bed exists as a proof of concept and requires considerable development for industrial deployment (Halperin *et al.*, 1984).

Continuous flow disc stack and multi-bowl centrifugation are the most common forms of centrifugal cell separation in the bioprocess industry because they combine low running costs with high throughput (Pilot scale: 10—100s L hr^{-1} and industrial scale: $> 1,000$ L hr^{-1}) and uncomplicated process and operational development (Hutchinson *et al.*, 2006). Traditionally used to separate microbial cells and protein aggregates, they are increasingly used to separate fragile animal cells (Lander *et al.*, 2005; Lightfoot & Moscariello, 2004). However, their high operational speeds are also associated high levels of cell disruption generating sub-cellular particles (Kempken *et al.*, 1995). The high shear regions encountered at the feed zones in both centrifuge types are the cause of cell damage (Boychyn *et al.*, 2000; Maybury *et al.*, 1998). Boychyn *et al.* (2001, 2004) modeled these feed zones with computational fluid dynamics (CFD) to characterise the energy dissipation rates. A maximum energy dissipation rate of 2 $\times 10^5$ W kg^{-1} was determined for a disc stack centrifuge operating at a flowrate of 15—80 L h^{-1} and at 167 rps, and 6 $\times 10^5$ W kg^{-1} and 12 $\times 10^5$ W kg^{-1} were determined for a multi-chamber bowl centrifuge under flooded and partially-flooded (70%) conditions respectively. Cell damage can also occur in centrifuges with solids discharge capability. The collected cells are either scraped from the collection bowl or ejected violently from the bowl into an adjoining collection chamber at speeds up to 100 m s^{-1} (Chan *et al.*, 2006).

The use of tangential flow microfiltration for large-scale separation of animal cells has been limited due to shear environment induced cell damage within the filtration module (Maiorella *et al.*, 1991). Performance of tangential flow microfiltration is

gauged on filtrate flux rates across the filtration membrane, and the accumulation of a concentration of cells and cell debris (concentration polarisation effect) coupled with membrane fouling are the governing phenomena that limits performance of the filtration module (Belfort *et al.*, 1994). The most common method employed to improve transport performance across the membrane involve adjusting fluid flow characteristics within the filtration module. This is achieved by providing local high shear rates or inducing Taylor or Dean Vortices (Vanreis & Zydney, 2007), to reduce the effects of concentration polarisation and fouling. However, in doing so, the susceptibility of animal cells to shear damage has to be considered. Maiorella *et al.* (1991) identified a critical wall shear rate (3,000 s^{-1}) at which cell damage will occur for a range of animal cell types. To deploy tangential flow microfiltration as a harvesting operation for animal cells, process conditions at which cell damage is minimal has to be established; van Reis *et al.* (1991) describes the scale-up development of an animal cell tangential flow microfiltration unit capable of processing 5,000 L $hour^{-1}$.

The use of centrifugation and tangential flow microfiltration is also found in clinical apheresis, where low volumes (0.25—1 L) of precious cells are processed. Apheresis describes any procedure in which blood is withdrawn from a donor and separated into its constituent components to be retained or transfused into a recipient. As an emerging field with very specific needs, it is likely whole cell bioprocessing will borrow heavily from both clinical apheresis and industrial cell separation processes to adopt an effective primary recovery scheme.

1.3.4 Windows of operation

The concept of windows of operation was first described by Woodley & Titchener-Hooker (1996) as a bioprocess design tool. It has been applied in various scenarios to frame critical operating parameters in a graphical format to facilitate analysis and

bioprocess design decisions (Blayer *et al.*, 1996; Zhou & Titchener-Hooker, 1999). Bioprocesses and the unit operations they are made up from, have many interacting variables and often have to be considered simultaneously for a desired level of performance (Salte *et al.*, 2006). A window of operation is a graphical visualisation of an optimum operating region within this multivariable parameter space as defined by the system's governing process constraints and correlations.

Building a windows of operation requires the identification of process and system constraints that may either be quantitative or qualitative. Subsequently, two common variables between the relationships that govern the interdependencies between the constraints have to be identified and established as the axes of the window (Fig. 1.2). The shape and not just the area of a plotted window of operation is indicative of bioprocess or operational robustness. The concept of windows of operation can be extended into a 3D parameter space by identifying three common variables amongst the relevant constraints and is termed volumes of operation (King *et al.*, 2004).

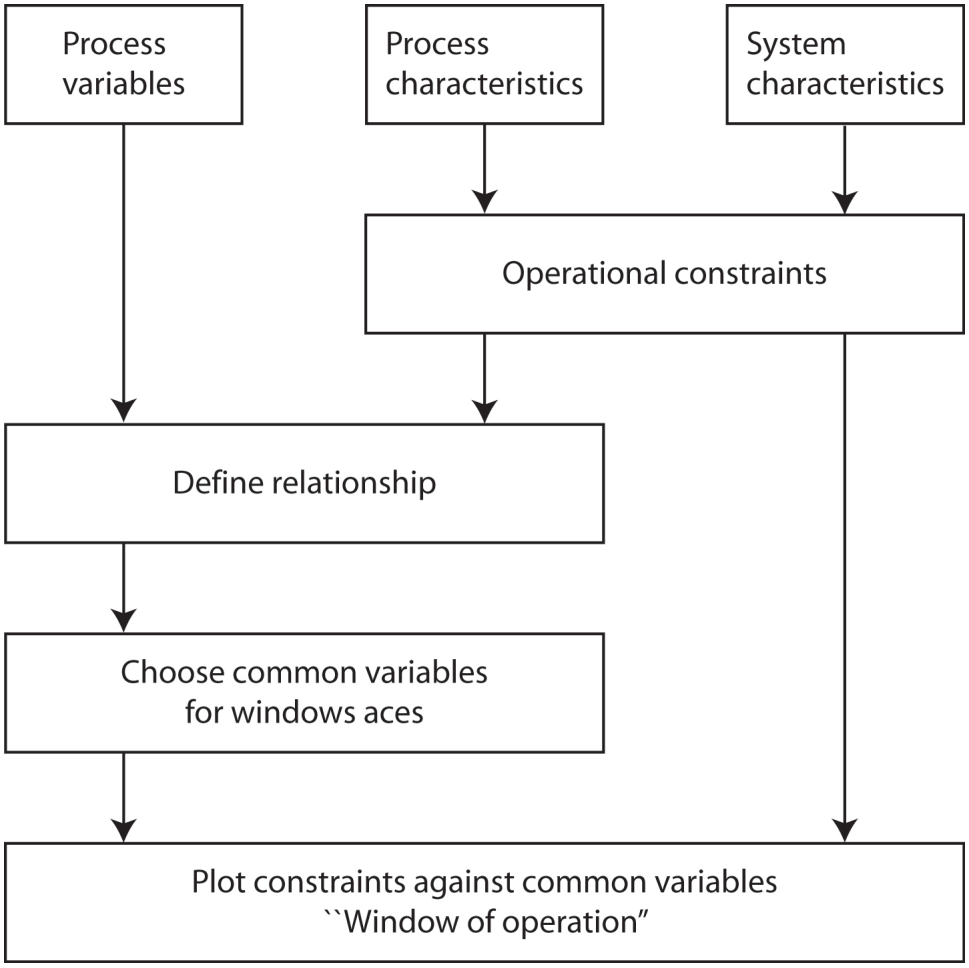

Figure 1.2: Building a window of operation. Reproduced from Woodley & Titchener-Hooker (1996).

1.4 Stem cells

Stem cells are cells that are capable of: (1) self-renewal, (2) the plasticity to differentiate into a range of specialised cell types, and (3) immortality–capable of undergoing unlimited expansion. The capacity for self-renewal and differentiation is underpinned by symmetrical or asymmetrical stem cell division and is the mechanism used to maintain an appropriate number of required cell types (Morrison & Kimble, 2006). Stem cells not only specify the starting material for organs and tissues in embryogenesis, they are also responsible for their continual maintenance, renewal and growth throughout ontogeny (Zandstra & Nagy, 2001). Because of these unique properties, stem cells represent an unlimited and renewable source of cells for cell therapy for regenerative medicine (Améen *et al.*, 2008; Lerou & Daley, 2005; Tögel & Westenfelder, 2007).

1.4.1 Adult stem cells

Adult stem cells (ASCs) are lineage specific cells that are found in various tissues throughout the body and are responsible for tissue homeostasis and its regeneration after damage. They reside in niches within tissue, and are specified by the highly specialised niche cells that regulate their proliferation and differentiation (Sneddon & Werb, 2007). Major adult stem cell populations have been found in niches within the eye (Dua *et al.*, 2005), in the gastrointestinal tract (Brittan & Wright, 2002), in skin for hair (Oshima *et al.*, 2001) and within the bone marrow (Dazzi *et al.*, 2006) and are reviewed in Moore & Lemischka (2006). *In vitro*, ASCs are incapable of long-term self renewal, this is in contrast to their behavior *in vivo* where continual self-renewal is essential in maintain life-long homeostasis (Mountford, 2008). This discrepancy in behaviour is attributed to the strict regulatory controls of the stem cell niche environment has over adult stem cell proliferation and differentiation (Trounson,

2006). The current inability to maintain and control ASC proliferation over extended periods of time in culture limits their potential in research and therapy.

1.4.2 Embryonic stem cells

Pluripotent embryonic stem (ES) cells are most commonly derived from the inner cell mass (ICM) of preimplantation embryos and *in vitro* fertilisation (Evans & Kaufman, 1981; Thomson *et al.*, 1998). Alternative methods of ES cell-like cell derivation can be found in Takahashi & Yamanaka (2006) (e.g. induced pluripotent stem cell (iPS)) and Chen *et al.* (2003) (e.g. nuclear transfer ES cells (ntESC)). ES cells are capable of long-term undifferentiated expansion *in vitro* (Amit *et al.*, 2000) and do not appear to undergo replicative senescence (Zeng & Rao, 2007), whilst maintaining the potential to differentiate into the three primary germ layer lineages and germline cells (Aflatoonian & Moore, 2006). The three primary germ layers consist of the ectoderm, mesoderm and endoderm and they give rise to all the tissue and organs during organogenesis: Ectoderm, the outer most primary germ layer develops into the nervous system and epithelial tissue; Mesoderm, the middle primary germ layer develops into muscle, blood and connective tissue; and, Endoderm, the inner most primary germ layer develops into the respiratory tract and the gut. Germline cells include the sex cells (e.g. egg and sperm) and the gametocytes.

In situ the ICM from which ES cells are derived from rapidly differentiate leading to the development of the embryo. As a consequence, pluripotent ES cells are an artefact of their *in vitro* environment (Avery *et al.*, 2006). Oct4, Nanog and Sox2 have been identified as key transcriptional factors in maintaining pluripotency in both mouse and human ES cells within the self-renewal signaling cascade (Avery *et al.*, 2006; Wobus & Boheler, 2005).

1.4.2.1 Mouse embryonic stem cells

The first mouse embryonic stem (mES) cell lines were derived from the ICM of mouse blastocysts (Evans & Kaufman, 1981) and cultured on mitotically inactivated embryonic fibroblast cells (MEF or feeder layers) in order to maintain mES cell pluripotency *in vitro*. These cells can be expanded indefinitely *in vitro* to give relatively homogenous and undifferentiated mES cell populations (Smith, 2001). Because mES cell pluripotency could only be maintained when cocultured with MEFs, it was reasoned that some extrinsic factor exist to either suppress differentiation or promote self-renewal. This factor was identified to be leukemia inhibitory factor (LIF) (Williams *et al.*, 1988), and the LIF\STAT3 signaling pathway has been established to play a central role in maintaining mES cells pluripotency (Boeuf *et al.*, 1997). Addition of LIF to non-serum free culture medium enables feeder free culture of mES cells. When mES cells are introduced into embryos and implanted, they give rise to chimeras exclusively descended from ES cells (Nagy *et al.*, 1993; Wang *et al.*, 1997).

More recently, pluripotent stem cells derived from the epiblast layer (epiblast stem cell or EpiSC) of post-implantation mouse embryos has been established (Brons *et al.*, 2007). Although EpiSC cells display the key features of a stem cell (e.g. self-renewal, plasticity and immortality), they are distinct from mES cells in their epigenetic state and signals that control their differentiation, and share key defining features with human ES cells (Tesar *et al.*, 2007).

1.4.2.2 Human embryonic stem cells

The techniques used to derived mES cells proved critical in establishing human ES (hES) cells from pre-implantation embryos. Like mES cells, hES cells can be maintained in a pluripotent state when cocultured on feeder layers. In contrast, unlike mES cells, LIF is unable to maintain hES cells in a pluripotent state when

cultured in feeder free conditions. The precise action of MEF layers in maintaining plurpotency in hES cells has yet to be elucidated, however some hES cell lines have been successfully cultured in animal free conditions (Lu *et al.*, 2006), ECM derived preparations (Ludwig *et al.*, 2006) or conditioned medium supplemented with bFGF. The activin A\TGF$\beta$ signaling pathway is essential for hES cell self-renewal (Beattie *et al.*, 2005).

1.4.2.3 Induced pluripotent stem cells

Induced pluripotent stem (iPS) cells are pluripotent cells that that have been derived from reprogramming somatic cells with introduced ectopic transcription factors. In mouse fibroblast iPS cells, these factors have been identified to be *Oct4*, *Sox2*, *c-Myc* and *Klf4* (Takahashi & Yamanaka, 2006), and in human fibroblast iPS cells these factors are *OCT4*, *SOX2*, *NANOG* and *LIN28* (Takahashi *et al.*, 2007). iPS cells have also been recently derived from hepatocytes (Aoi *et al.*, 2008), mature B lymphocytes Hanna *et al.* (2008) and pancreatic β cells (Stadtfeld *et al.*, 2008). iPS cells exhibit the morphology and growth properties of ES cells and express ES cell marker genes (Takahashi & Yamanaka, 2006). Although the derivation of iPS cells from somatic cells circumvents the controversial use of embryos, the derivation efficiency is low when compared to hES cell derivation protocols ($<$0.1 % vs. $\sim$ 20 %).

1.5 Investigational objectives

Although ES cells represent an unlimited source of of cells for cell based regenerative medicines, they are themselves not the therapy. Grafting pluripotent ES cells directly into a host risks the formation of teratomas –tumor like cell masses containing cells belonging to all three primary germ layers– and immune rejection responses. The ability of ES cells to form teratomas *in vivo* is a defining characteristic of pluripotent ES cells. The therapeutic cells are differentiated derivatives of the original population of ES cells and can exist either as terminally differentiated somatic cells or as lineage committed precursor cells.

Within any bioprocess that exploits the properties of ES cells for therapy, a distinction between the source of ES cells and its subsequent differentiation can be made to facilitate operations. Where ES cells are grown to required numbers whilst still maintaining their pluripotent properties, these operations may be classified as *expansion operations*. *Expansion operations* provide the necessary starting material for *differentiation operations* where ES cells are directed towards the required cell phenotype. This distinction between the different operations are exemplified in Figure 1.3. With *expansion* or *differentiation operations*, there exist a variety of unit operations and handling procedures to achieve a specific bioprocess target. It is likely that centrifugation will be employed to facilitate ES cell expansion and differentiation procedures.

This thesis examines the impact of centrifugal recovery of mES cells and centres about the use of a laboratory scale bench top centrifuge fitted with swing-out rotors. mES cells were selected as a mimic for ES cell types that will be used cell based regenerative medicines. The overall objective of this thesis is to carry out fundamental underpinning work on centrifugation within a regenerative medicine bioprocessing framework to enable its application in the production of cell based therapies. Current literature relating to centrifugation performance during recovery

of cells relate to shear damage predictions using computational fluid dynamics, scaling issues or operational efficiency issues to separate cells from the liquor for protein recovery. There is a distinct absence of literature related to ES cell centrifugation and how centrifugation conditions might affect ES cell properties; this is largely due to the lack of developments in this areas. The work accomplished potentially reveals important bioprocess design implications specific to centrifugation for regenerative medicine processing. In this thesis, the impact of centrifugal recovery on ES cells are segregated into two distinct areas: (1) the physical impact of centrifugation on mES cells; and (2) the impact of centrifugation on the phenotype of mES cells. Preliminary studies involving the centrifugation of human neonatal foreskin derived fibroblast aided in the development of a suitable and robust experimental schema.

Figure 1.3: Simplified process flow diagram for the bioprocessing of ES cell based regenerative therapies. Although ES cells represent an unlimited source of cells for therapy, they are themselves not directly applied as a treatment. Differentiated derivatives of the original population of ES cells constitute the final product. Thus, the entire bioprocess maybe distinguished between ES cell *expansion operations* or ES cell *differentiation operations*. *Expansion operations* are associated with the culture and maintenance of pluripotent ES cells to supply the starting material for *differentiation operations*.

1.5.1 The physical impact of centrifugation on mES cells

This study seeks to examine the impact of centrifugation of mES cells by quantifying the level of cell damage incurred. Millilitre volumes of mES cell suspensions representative of routine cell harvesting operations were exposed to a range of centrifugal force (0—3000 g) and centrifugation time (0—100 mins) at 4, 21 and 37°C process temperature. Two key measures of cell damage, overall cell concentration and cell viability were monitored before and after centrifugation to provide the necessary information to characterise cell damage in relation to the bioprocessing conditions. Windows of operation will be generated based on the cell damage data to visualise an area of available operating conditions for centrifugation when subject to user defined constraints. A mixture of theoretical and experimental work will be used to deliver the proposed window of operation.

1.5.2 The impact of centrifugation on the phenotype of mES cells

This study examines the influence of centrifugation on two defining characteristics of stem cells; pluripotency and differentiation potential. Millilitre volumes of mES cells were exposed to a range of centrifugal force (0—3000 g) and returned to culture. The impact of centrifugation on mES cell pluripotency and differentiation potential were monitored in a feeder free monolayer culture and static suspension embryoid body (EB) culture system respectively. Changes in cell phenotype were tracked through green fluorescent protein (GFP) and gene expression.

Chapter 2

Materials and Methods

2.1 Introduction

The research in this thesis centers around the use of millilitre (mL) scale experiments of feeder free murine embryonic stem (mES) cells. Experimental design is to provide a representation of actual scale processes to investigate the impact of batch centrifugation on the cell properties.

2.2 Equipment and cell culture

This section describes the centrifuge equipment and cell culture technique used throughout this investigation.

2.2.1 Centrifuge equipment

An Eppendorf 5810R temperature controlled laboratory bench-top centrifuge is used, fitted with the A-4-62 rotor and swing out buckets. Cell suspensions were centrifuged in 2 mL micro-centrifuge tubes containing a machined acrylic insert (Fig. 2.1). The insert aids in the definition and partitioning of the sediment and the supernatant fraction. It also aids in minimising the disturbances to the sedimented cells during aspiration of the supernatant. Due to the presence of the insert within the micro-centrifuge tube, its maximum working volume is reduced to 1.7 mL.

2.2.2 Cell culture

Oct4-GiP ES cells (Stem Cell Sciences plc, Edinburgh, UK) (hereafter known as *Oct4*-GFP) made on a pure 1290la background expressing resistance and cytoplasmic green fluorescence protein (GFP) under the direct regulator control of the mouse *Oct4* gene (Ying *et al.*, 2002) were cultured on 0.1% (w/v) porcine gelatin (Sigma-Aldrich, Poole, UK) coated T-flasks (Iwaki, Funabashi, Japan) and maintained in

Glasgow Minimum Essential Medium (GMEM) (Sigma-Aldrich, Poole, UK) containing: 10% (v/v) foetal bovine serum (FBS) (Invitrogen, Paisley, UK), and supplemented with 0.1 m M 2-β-mercaptoethanol (BDH, Poole, UK); 1× minimum essential medium with non-essential amino acids (MEM NEAA) (Invitrogen, Paisley, UK); 1mM sodium pyruvate (Invitrogen, Paisley, UK); 2 mM L-glutamine (Invitrogen, Paisley, UK); and 10^6 units L^{-1} leukemia inhibitory factor (LIF) (Chemicon, Watford, UK). All cell cultures were incubated at 37°C, with a 7% CO_2 content in air. Sub-confluent monolayers of cells were routinely passaged at a 1 in 8–10 split ratio every two days. Dissociation of cells was achieved by removing the spent media, and washing the cells with Dulbeccos phosphate-buffered saline (DPBS) (Sigma-Aldrich, Poole, UK), and incubating for 4 minutes with 0.025% (v/v) trypsin (Invitrogen, Paisley, UK), supplemented with 1% (v/v) chick serum (Sigma-Aldrich, Poole, UK) and 0.3 mM ethylenediaminetetraacetic acid (EDTA) (BDH, Poole, UK) in DPBS. Dissociated cells were subsequently quenched with complete media and pelleted at 280 g × 3 min ready for passaging or resuspended in complete medium ready for experimentation.

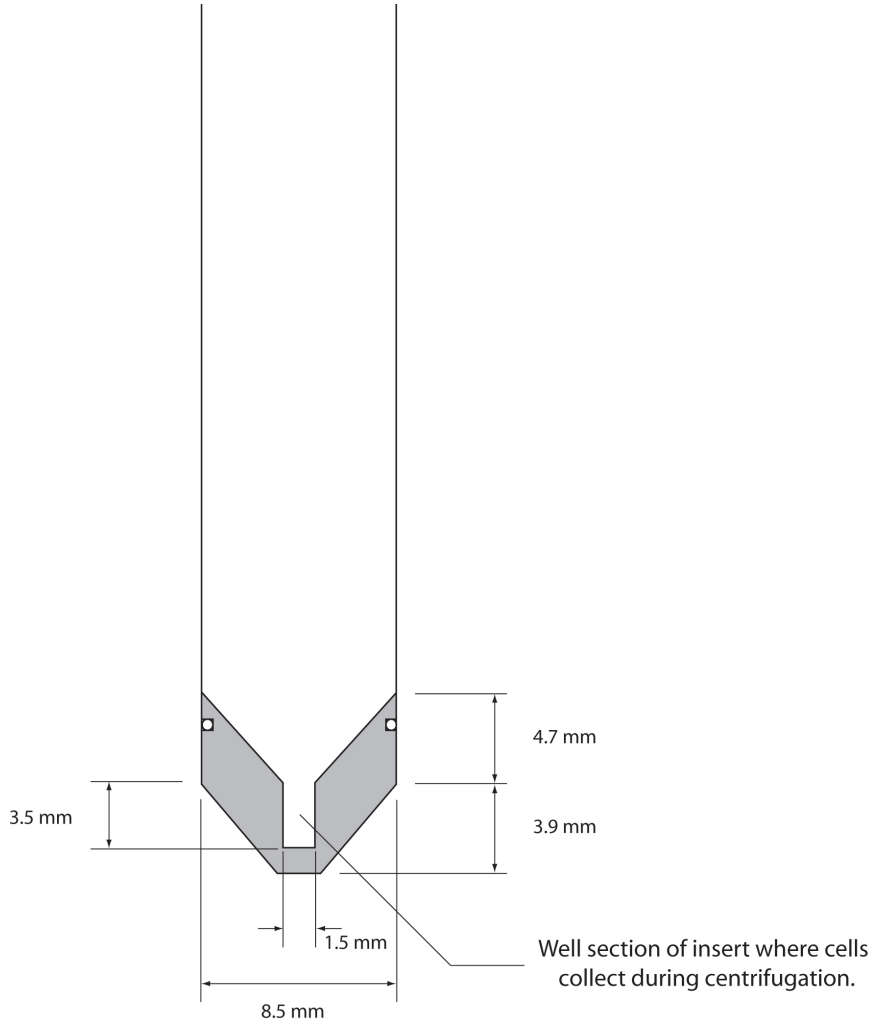

Figure 2.1: Cross-sectional view of 2 mL centrifuge tube with machined acrylic insert. The centrifuge tube has a working volume of 1.7 mL and acrylic insert aids in the partitioning and definition of the supernatant and sediment fractions. Proportions are drawn to scale.

2.2.3 Cell enumeration and GFP expression measurement

Cell enumeration and GFP expression measurement was accomplished using bench top flow cytometry. Samples were analysed using the Guava EasyCyte Plus System (Guava Technologies, Stamford, UK) with the bundled ExpressPlus software, v3.x. Cell enumeration was achieved using Guava Technologie's proprietary cell counting dye, ViaCount Flex Reagent, to determine cell numbers and cell viability. ViaCount Flex Reagent consists of a proprietary formulation of propidium iodide (PI) and a membrane permeable DNA stain; the differential permeability of each dye within the cells when detected by the instrument is able to identify nucleated cells and distinguish between viable and non-viable cells. For cell enumeration, monodispersed cell suspension samples were diluted with DPBS to within the range of the detection rate of the instrument (10 to 500 events per μL) to give a volume of 197 μL. 3 μL of ViaCount Flex Reagent was then mixed into the diluted cell suspension to make up a total sample volume of 200 μL and allowed to incubate at room temperature for 5 minutes before analysis. GFP fluorescence was measured concurrently during enumeration on the PM3 channel of the instrument. For GFP expression analysis, a gate was placed around the viable cell population to identify GFP-positive and -negative populations (GFP^+ and GFP^- respectively). The GFP-positive population from control samples were further gated into 50% high and 50% low expression areas (Fig. 2.2 A). As a results of the placed gates, GFP expression for a viable cell population can be labeled as: negative, high and low. The GFP settings from each control sample were applied across all other samples to evaluate shifts in expression within the GFP-positive cell populations (Fig. 2.2 B). Percentage yield of *Oct4*-GFP expression on viable cells is calculated according to the following formula:

$$Y_{GFP} = \frac{C_{GFP}}{C_V} \times 100 \tag{2.1}$$

Where Y_{GFP} is the yield of *Oct4*-GFP expressing cells as a percentage (%) and C_{GFP}

is the concentration of cells expressing *Oct4*-GFP (cells mL^{-1}). All experimental samples were analysed in triplicates or more, with data presented as a mean $\pm$ 2 standard error (SE). Statistical significance was determined using the two-tailed Student's t test. Significant differences between groups are declared and denoted as: * when $p < 0.05$; and ** when $p < 0.01$.

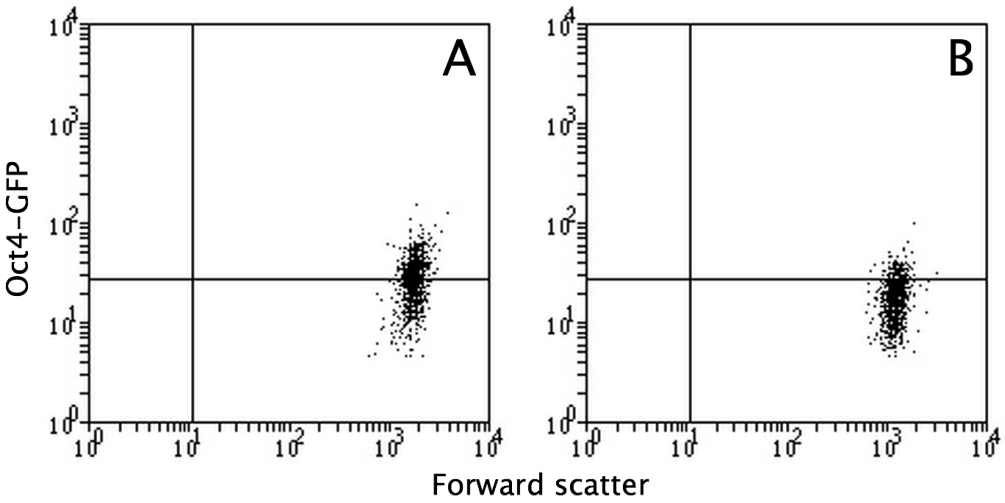

Figure 2.2: *Oct4*-GFP expression analysis using the Guava EasyCyte Plus bench top flow cytometer. GFP^+ expressing cells from control samples were identified and gated into 50% high and 50% low expressing areas (Panel A). Gate settings from the control samples were applied to treated samples to evaluate shifts in GFP^+ expression (Panel B). In this example, 51% of GFP^+ cells were recorded as high GFP^+ in the control sample, and 14% of GFP^+ cells were recorded as high GFP^+ in the treated sample. The difference in values indicate a loss in high GFP^+ expressing cells.

2.3 Physical impact of centrifugation on mES cells

This section of the chapter will first describe the theoretical considerations used in the characterisation of the physical impact of centrifugation on mES cells and the construction of a suitable window of operation. This is followed by the methods describing how experimental data was obtained.

2.3.1 Theoretical considerations

2.3.1.1 Clarification

When allowed to stand under the influence of gravity over time, particles suspended within a fluid will settle out of solution due to the density difference between the solid and liquid phases. This process is called clarification and can be accelerated by applying a centrifugal force to increase the particle settling velocity. To measure clarification performance, the Sigma concept of *equivalent settling area* is commonly used, and is an index of area that is equivalent to that of a settling tank capable of the same particle separation performance under the influence of gravity (Ambler, 1961). Sigma concept is based on the Stoke's definition of settling velocity of a particle and assumes particles are present as single spheres in a dilute suspension and that settling is unhindered. Stoke's particle settling velocity is defined as:

$$u_s = \frac{d^2 g}{18\mu}(\rho_p - \rho_f) \tag{2.2}$$

where u_s is the terminal settling velocity of the particle (m s^{-1}), d is the diameter of the particle (m), g is the acceleration due to gravity at sea level (9.81 m s^{-1}), μ is the viscosity of the fluid the particle is moving through (N sm^{-2}), ρ_p and ρ_f are the particle and fluid density respectively (kg m^{-3}).

The clarification capacity, C, (m s^{-1}) of as centrifuge is defined as:

$$C = \frac{V}{t_c \cdot \Sigma_{lab}} \tag{2.3}$$

where V is the volume (m^3) of suspension being centrifuged, t_c, is the overall centrifugation time (s), and Σ_{lab}, is the theoretical equivalent separation area (m^2) for recovery of 100% of particles for a laboratory bench top centrifuge corrected for acceleration and deceleration phases as derived by Maybury *et al.* (2000):

$$\Sigma_{lab} = \frac{V \cdot \omega^2 \cdot (3 - 2x - 2y)}{6g \cdot ln\left(\frac{2r_2}{r_2 + r_1}\right)} \tag{2.4}$$

where ω is the rotor angular velocity (s^{-1}), x is the fraction of the overall time for acceleration, and y is the fraction of the overall time for deceleration of the rotor. r_1 and r_2 are the radii (m) of the surface of the centrifuge liquor and the base of the centrifuge tube respectively. The relationship between ω and RCF is given by:

$$RCF_{max} = \frac{\omega^2 \cdot r_2}{g} \tag{2.5}$$

where RCF_{max} is the maximum relative centrifugal force (g) and g is the acceleration due to gravity at sea level (9.81 m s^{-2}). The fraction of mES cells recovered, F, for a given clarification capacity is given by:

$$F = 1 - \frac{N_1}{N_0} \tag{2.6}$$

where N_0 and N_1 are the total cell counts in the supernatant before and after centrifugation respectively. Clarification performance of the centrifuge is determined by plotting F against clarification capacity on a probability-log scale.

2.3.1.2 Cell recovery

Cell recovery after centrifugation was evaluated on a basis of cell numbers and % cell viability. High cell numbers and % cell viability recovered are desirable as this indicates a low level of cell damage during the centrifugation. % cell viability, ν, is given by:

$$\nu = \frac{C_V}{C_V + C_N} \times 100 \tag{2.7}$$

where C_V is the viable cell concentration (cells mL^{-1}), and C_N is the non-viable cell concentration (cells mL^{-1}).

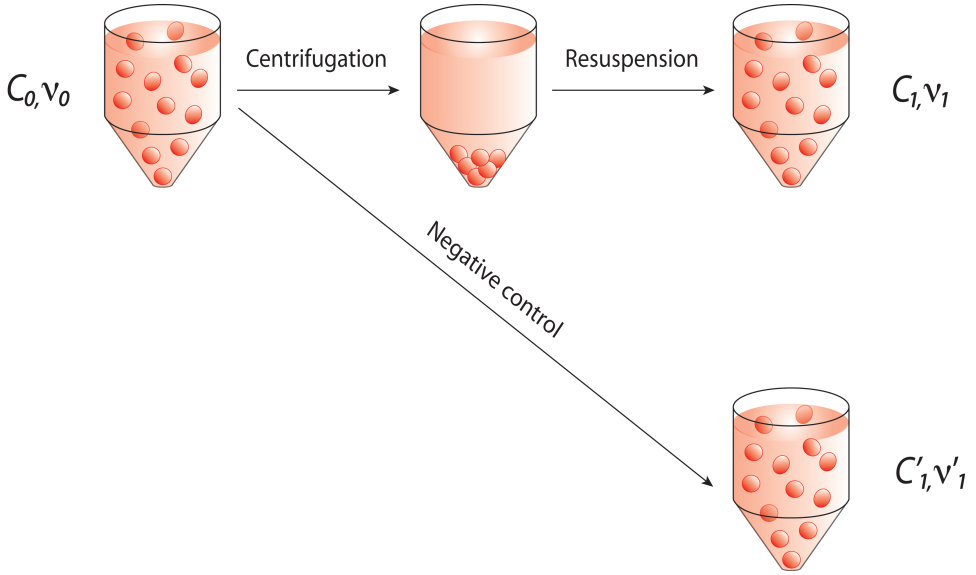

Figure 2.3: Schematic representing the millilitre scale batch centrifugation procedure used to investigate the impact of centrifugation on mES cells. Cell suspensions of known cell concentration (C_0) and cell viability (ν_0) are subjected to centrifugation. The collected cell pellet is subsequently resuspended back into a known volume of liquor under constant resuspension conditions. The cell concentration (C_1) and cell viability (ν_1) of the resuspended liquor is evaluated and is used to determine the impact of centrifugal force and centrifugation time on cell recovery. The cell concentration (C'_1) and cell viability (ν'_1) of uncentrifuged control samples of equivalent time-temperature history are evaluated in parallel. Cell concentrations were evaluated using bench top flow cytometry. Experiments were carried out at three different process temperatures, 4, 21 and 37°C.

Figure 2.3 represents the millilitre scale batch centrifugation procedure used to investigate the impact of centrifugation on cells. For cell recovery calculations, this can be distinguished between a *process* and a *centrifugation* metric. The difference between either metric lies within how time is considered within the system for a given set of centrifugation conditions (RCF, T and t_c). The *centrifugation* metric takes into account the overall processing time for centrifugation and thus ignores cell gains or losses due to time-temparature exposure. On the other hand, the *process* metric accounts for all effects including holding time, centrifugation time and cell resuspension losses. For instance, the fraction of cells lost from the *process*, F_P, is defined as:

$$F_P = \frac{C_0 - C_1}{C_0} \tag{2.8}$$

and the fraction of cells lost after *centrifugation*, F_C, is defined as:

$$F_C = \frac{C_1' - C_1}{C_1'} \tag{2.9}$$

where C_0 is the initial concentration of total cells (cells mL^{-1}) in the sample before centrifugation, C_1 is the final concentration of total cells (cells mL^{-1}) in the sample after centrifugation, and C_1' is the final cell concentration of uncentrifuged cells exposed to an equivalent time-temperature history as C_1.

Similarly, calculations made on a % viability basis, ν, to determine the physical change in state of cells during centrifugation can be defined for a *process*, $F_{P,\nu}$, and *centrifugation*, $F_{C,\nu}$, metric and are given in equations (2.10) and (2.11):

$$F_{P,\nu} = \frac{\nu_0 - \nu_1}{\nu_0} \tag{2.10}$$

and,

$$F_{C,\nu} = \frac{\nu_1' - \nu_1}{\nu_1'} \tag{2.11}$$

where ν_0 is the initial cell viability (%) in the sample before centrifugation, ν_1 is the final cell viability (%) in the sample after centrifugation, and ν_1' is the final cell viability (%) of uncentrifuged cells exposed to an equivalent time-temperature history as ν_1.

2.3.1.3 Window of Operation

The Window of Operation developed presents information with regards to centrifuge performance and is constructed with a minimum acceptable level of clarification and fraction of cell viability lost in mind. The two common performance criteria identified in batch centrifugation that directly govern the interdependencies within the system are *time* (t), i.e. overall centrifugation time (t_c) characterised by time taken for the centrifuge bowl to accelerate from rest to a set RCF value, the hold time at the set value and the time taken for the centrifuge bowl to decelerate from the set RCF value to rest, and *relative centrifugation force* (RCF). These two dimensions define the multivariable parameter space within which the window of operation lies.

For clarification, the clarification performance, F, of a centrifuge is governed by the relationship between the variables, C, t_c and RCF and are specified in Equations (2.3) and (2.4). When combined these give:

$$t_c = \frac{6g \cdot ln\left(\frac{2r_2}{r_2+r_1}\right)}{C \cdot \omega^2 \cdot (3 - 2x - 2y)} \tag{2.12}$$

Equation (2.12) represents the relationship between RCF and t_c for a user defined minimum acceptable level of clarification (C).

For cell recovery, the *Fraction of cell viability lost* is used to construct the second minimum acceptable criteria used to characterise centrifuge performance. The fraction lost in % cell viability data sets from the cell recovery experiments were plotted in 3D Cartesian coordinates ($x = t, y = RCF$ and $z = \Delta\nu$) for each temperature condition, and imported into the surface fitting package. Three non-linear sigmoid mathematical functions were explored to find a model to fit profile of each data set; the functions were:

$$\Delta\nu = \left(1 - e^{-a \cdot t_c \cdot RCF^n}\right)^m \tag{2.13}$$

$$\Delta\nu = \tanh^m \left(a \cdot t_c \cdot RCF^n\right) \tag{2.14}$$

$$\Delta\nu = \frac{\left(a \cdot t_c \cdot RCF^n\right)^m}{\left(a \cdot t_c \cdot RCF^n\right)^m + 1} \tag{2.15}$$

where a, m and n are fitted coefficients and $\Delta\nu$ is the fraction change in % cell viability. The relationship between $\Delta\nu$ and the two dimensions (RCF and t) that define the multivariable parameter space is embodied in each function and they represent the constraint that defines the limit of available centrifuge operating conditions for a given user defined level of $\Delta\nu$. Each function satisfies the limit conditions:

$$\Delta\nu = 0\,,\ t_c = 0 \qquad \Delta\nu = 0\,,\ RCF = 0 \tag{2.16}$$

$$\Delta\nu \to 1\,, t_c \to \infty \quad or \quad RCF \to \infty \tag{2.17}$$

and have the profile:

$$\frac{\delta\Delta\nu}{\delta t_c} = 0\,,\ t_c = 0 \qquad \frac{\delta\Delta\nu}{\delta RCF} = 0\,,\ RCF = 0 \tag{2.18}$$

Surface fitting was achieved using a non-linear least square algorithm executed in MATLAB® (v7.3) to determine the value of coefficients in the proposed model. The fitting algorithm was programmed to assume convergence when the difference between successive iterative approximations was $< 1 \times 10^{-100}$. The *goodness of fit* for each function explored was evaluated through the *coefficient of determination* (R^2) value given by:

$$R^2 = 1 - \frac{\sum_{i=1}^{n} \left(\nu_i - f\left(\Delta\nu_i\right)\right)^2}{\sum_{i=1}^{n} \left(\nu_i - \bar{\nu}\right)^2} \tag{2.19}$$

where ν_i is the actual fraction change in % cell viability for a given set of centrifugation conditions, $f\left(\Delta\nu_i\right)$ is the predicted fraction change from the sigmoid expressions evaluated, and $\bar{\nu}$ is the average of the predicted values.

2.3.2 Experimental design

The study of the physical impact of centrifugation is broken down into three major experimental studies: (1) clarification; (2) cell recovery; and (3) cell damage, and seeks to characterise different aspects of the centrifugation procedure by varying a combination of RCF, T or t_c. Cell suspensions for each study were prepared as described.

Harvested mES cell suspension were adjusted to 4, 21 or 37°C and a concentration of 1×10^6 cells mL^{-1} to provide the monodispersed cell suspension feedstock for centrifugation. Feedstocks of $< 95\%$ cell viability as determined by flow cytometry (see Section 2.2.3) were excluded from the studies. 1.7 mL of feedstock was then aliquoted into the 2 mL micro-centrifuge tube containing a machined acrylic (see Section 2.2.1 for description) insert ready for centrifugation.

2.3.2.1 Clarification

Cell suspensions at 21°C were subjected to the following centrifugation conditions: for a constant t series, t = 2 min, for RCF = 40, 60, 100, 160, 200 and 240 g; for a constant RCF series, RCF = 30 g, for t = 2, 4, 6, 10, 14, 16 and 20 min. After centrifugation, the number of cells remaining in suspension within the supernatant fraction was determined. Supernatant is defined as all the liquor contained within the main cylindrical body and conical section of the centrifuge tube; sediment (together with its entrained liquor) is defined as the cell pellet found within the well section of the machined insert within the 2 mL centrifuge tube. The influence of temperature on clarification was determined at 4 and 37°C for centrifugation conditions that achieve high levels of F (> 85%).

2.3.2.2 Cell recovery

Cell suspensions at 4, 21, and 37°C were subjected to the following centrifugation conditions: for a constant t series, t = 20 min, for RCF = 100, 200, 500, 1,000, 2,000 and 3,000 g; For a constant RCF series, RCF = 200 g, for t = 2, 5, 10, 20, 50 and 100 mins. After centrifugation, the collected cell pellet is resuspended back into the same volume of liquor *in situ* and the cell density determined. The resuspension regime is capable of dispersing the pelleted cells into a mono-dispersed cell suspension and was kept constant across all cell pellet samples. The regime is defined as follows using standard Gilson P1000 and P200 pipettors and pipette tips:

1. remove 1 mL of the supernatant from the tube,
2. with a 200 μL pipette tip, with pipettor set at 200 μL, gently triturate pellet over 20 cycles,
3. with a 1,000 μL pipette tip, with pipettor set at 500 μL, gently triturate pellet over 20 cycles,

4. replace 1 mL of the withdrawn supernatant, and gently triturate a final 5 cycles with a 1,000 μL pipette tip, with pipettor set at 1,000 μL.

Gentle trituration refers to a situation where the pipettor's push button was manually cycled smoothly at a frequency approximating 1 cycle per second. Control samples (5–7 mL) were exposed to the same time and temperature combinations, and were mixed every 30 minutes using trituration with a standard 10 mL serological pipette to minimise cells settling out of solution.

2.3.2.3 Cell damage

The centrifugation procedure can be broken down into a *settling* phase, where cells settle out of solution and are collected in a pellet at the bottom of the tube when centrifuged, and into a *resuspension* phase, where the collected cell pellet is dispersed into a monosuspension in a volume of liquid (Fig. 2.3). Harvested cell suspensions were centrifuged at 3,000 g $\times$ 20 mins at 4, 21 and 37^oC. Samples of culture medium immediately after the *settling* phase and *resuspension* phase were assayed for lactate dehydrogenase (LDH) activity using the CytoTox-ONE^{TM}Homogeneous Membrane Integrity Assay (Promega UK, Southhampton, UK). Pelleted cells were resuspended according to the regime outlined in Section 2.3.2.2. Negative control uncentrifuged cell suspension were assayed alongside. Briefly, 100 μL of sample culture medium was loaded into 96 black untreated microwell optical bottom plates (Nalge Nunc International, New York, USA) and incubated with an equal volume of CytoTox-ONE^{TM}Reagent at 22 ^oC for 10 minutes. After incubation, the reaction was quenched with 50 μL of supplied Stop Solution. The plates were measured in a Tecan Sapphire II fluorometric plate reader (Tecan UK Ltd, Reading, UK) with a 550/600 nm excitation/emission set point and a $\pm$20 nm bandpass. Background fluorescence of cell free culture medium was also measured. The values reported are expressed in relative fluorescence units (RFU).

2.4 The impact of centrifugation on the phenotype of mES cells

2.4.1 Experimental design

The following series of experiments were designed to investigate: (1) the impact of centrifugation on mES cell pluripotency; and (2) the impact of centrifugation on the differentiation potential of mES cells. Cell suspension feedstocks for centrifugation studies were prepared in 2 mL centrifuge tubes as described in Section 2.3.2 on page 47.

2.4.1.1 Undifferentiated expansion of mES cells study

Undifferentiated monolayer cultured *Oct4*-GFP cells were harvested as described in Section 2.2.2 and resuspended in complete medium adjusted to 21°C. Cell suspension feedstocks were centrifuged at 500, 1,000, 2,000 and 3,000 g for 3 minutes. The collected pellets were resuspended into a mono-dispersed cell suspension using the pipetting regime outlined in Section 2.3.2.2 and plated onto pre-gelatinised 6 well plates at 10,000 viable cells cm^{-2}. Cultures were incubated under standard conditions and culture medium for 2 days. Control cultures, i.e. not centrifuged, exposed to the same ambient conditions and pipetting regimes were prepared alongside.

2.4.1.2 EB expansion and differentiation study

Undifferentiated monolayer cultured *Oct4*-GFP were harvested as per Section 2.2.2 and resuspended in LIF free complete medium. The cell suspension was subsequently subjected to centrifugation at 21°C for 20 minutes at 500, 1,000, 2,000 and 3,000 g. Cell pellets obtained were dispersed back into the supernatant *in situ* and adjusted to 5×10^5 viable cells mL^{-1} for static suspension culture inoculation. The

centrifuged cells were plated onto non-tissue culture treated PS vented 94 × 15 mm petri dishes (Greiner Bio-One Ltd, Gloucestershire, UK) with a final inoculation volume of 15 mL. Cells were incubated at 37°C, with a 7% CO_2 content in air for 8 days in suspension culture with medium exchanges every 2 days. Medium exchanges were achieved by allowing embryoid bodies (EBs) to gravity settle in 25 mL centrifuge tubes for 15 minutes. 1 mL EB samples were taken from each culture every 2 days and dissociated with 0.1% trypsin (see Section 2.2.2 for preparation) before flowcytometric analysis. 20 phase contrast images of cultures were taken on days 4 and 8 for each condition for image analysis. Control cultures, i.e. not centrifuged, exposed to the same ambient conditions and pipetting regimes were prepared alongside.

2.4.2 Analytical techniques

2.4.2.1 Growth rates and doubling times

Growth rates and doubling times were calculated based on the exponential growth phase of the culture. The specific growth rate is given by the following equation:

$$\mu = \frac{ln(C_2) - ln(C_1)}{t} \tag{2.20}$$

and doubling time is given by:

$$t_d = \frac{ln(2)}{\mu} \tag{2.21}$$

where C_2 and C_1 is the viable cell concentration at the end and start of the exponential growth phase (viable cells mL^{-1}), μ is the specific growth rate of the culture ($hours^{-1}$) and t_d is the culture doubling time (hours).

2.4.2.2 EB image analysis

Phase contrast images of EBs were acquired every two days through the course of the static suspension culture. (Nikon Eclipse TE2000-U inverted microscope equipped with a Nikon SD-Fi1 camera (Nikon UK Ltd, Surrey, UK) and a 4× objective lens). Resolution of the images obtained were 1,280 × 960 pixels, corresponding to a field of view of 2,190 × 1,620 millimeters. EBs were analysed using ImageJ processing and analysis software v1.38x (available for download at: http://rsb.info.nih.gov/ij/ , US National Institutes of Health) to count the number of EBs present and determine their diameter. Imaged EBs with an area smaller than 1,250 μm^2 were excluded from analysis. This was to exclude background cell debris, single cells and small cell aggregates.

2.4.2.3 Reverse transcription polymerase chain reaction and quantitative polymerase chain reaction

Total RNA was isolated from cell pellets using the RNAqueous Kit® (Applied Biosystems, Warrington, UK) according to manufacturer's instructions and contaminating genomic DNA was degraded using TURBO DNA-*free*™Kit (Applied Biosystems, Warrington, UK). A NanoDrop™1000 spectrophotometer (Thermo Fisher Scientific, Leicestershire, UK) was used to assess RNA quantity and quality ($A_{260}/A_{280} > 1.8$). First strand random decamer primed cDNA was synthesised by using the RETROscript® Kit (Applied Biosystems, Warrington, UK) as described by the supplier.

For reverse transcription polymerase chain reaction (RT-PCR) analysis, synthesised cDNA was amplified in 25 μL volumes using the BIOTAQ™Core Kit (Bioline Ltd, London, UK) and individual primer pairs for specific gene markers (Table 2.1). After an initial 3 minutes denaturing step at 94.0°C, reactions were cycled through 25—30 rounds of 94.0°C for 25 seconds for denaturing, annealing temperature range

of 55.0—60.0°C for 20 seconds, and extension at 72.0°C for 45 seconds. This was followed by a final extension time of 5 mins. PCR products obtained were analysed by agarose gel electrophoresis on 2.5% agarose gels stained with SafeView^{TM}Nucleic Acid Stain (NBS Biologicals Ltd, Cambridge, UK). The size of the amplification bands was estimated using HyperLadderII (Bioline Ltd, London, UK. *No reverse transcription controls* and *no template controls* were included to monitor for contamination.

Quantitative polymerase chain reaction (qPCR) was performed in a Mastercycler® ep *realplex*^{4} (Eppendorf, Cambridge, UK) with QuantiTect®SYBR® Green RT-PCR Master Mix (Qiagen, West Sussex, UK) and QuantiTect® Primer Assay (Qiagen, West Sussex, UK) for specific gene markers (Table 2.1) with the following cycling conditions: an initial activation step 95.0°C for 15 minutes followed by 40 cycles of 94.0°C for 15 seconds, 55.0°C for 30 seconds and 72.0°C for 30 seconds. Melting curve analysis of the PCR products were performed to verify their specificity. The relative expressions of gene targets were normalised to *β-actin* and calculated using the $2^{-\Delta\Delta C_T}$ method (Livak & Schmittgen, 2001). Amplification efficiency representative for each gene specific QuantiTect® Primer Assay kit was determined using 10-fold dilution standard curve. For all gene targets investigated, the average efficiency was 0.998 with a $< 10\%$ coefficient of variance.

Table 2.1: List of gene specific targets for RT-PCR and qPCR. RT-PCR primer pair sequences are depicted in 5′ to 3′ direction.

RT-PCR			
Gene	Accession #	Primer sequence	Amplicon (bp)
Oct4	NM_013633	F: CAGCCAGACCACCATCTGTC	138
		R: GTCTCCGATTTGCATATCTCCTG	
Nanog	NM_028016	F: TTGCTTACAAGGGTCTGCTACT	106
		R: ACTGGTAGAAGAATCAGGGCT	
Rex1	NM_009556	F: TGGAAGCGAGTTCCCTTCTC	128
		R: GCCGCCTGCAAGTAATGAG	
β-actin	NM_007393	F: CAACGAGCGGTTCCGATG	67
		R: GCCACAGGATTCCATACCCA	
qPCR			
Gene		QuantiTect® Primer Assay Cat. #	
Oct4		QT00109186	
Nanog		QT01076334	
Utf1		QT00252112	
Sox17		QT00160720	
T		QT00094430	
Tubb3		QT00124733	
β-actin		QT01136772	

Chapter 3

Results and Discussion: Physical Impact of Centrifugation on mES Cells

3.1 Introduction

Two major sets of results are reported in this chapter and they relate to the study of centrifuge clarification performance (see Section 3.2) and cell damage during centrifugation (see Section 3.3). The results obtained were used to construct a Window of Operation defining an optimum operating region for centrifugation of mES cells.

3.2 Centrifuge clarification performance

Centrifuge clarification performance was established based on a cell concentration of 1×10^6 cells mL^{-1}. The inverse relationship between clarification capacity (C) and fraction of total cells (total cells = viable cells + non-viable cells) recovered (F) is shown in Figure 3.1 and this represents the clarification performance of the batch centrifuge when operated at 21°C. Clarification capacity limits were established empirically to correspond to a useful range of F values ($\sim$ 30–95 %). The clarification capacity was adjusted by varying time (t = 2–20 mins) at constant RCF (g = 30) conditions, and varying RCF (RCF = 40–240 g) at constant time (t = 2 mins) conditions. Establishing limits on the clarification capacity was useful in avoiding over-centrifugation of the cell suspension as the mES cells could be sensitive to the mechanical forces applied. In contrast, under-centrifugation of the cell suspension would result in a significant loss of mES cells to the suspending liquid resulting in poor clarification. The range of centrifugal conditions examined was between 60–600 $g$mins. In order to achieve a minimum of 90% recovery in cells, samples have to be exposed to a minimum of 300 $g$mins (i.e. top 3 F-values for either series examined). For example, 300 $g$mins is equivalent to centrifugation at 150 g × 2 mins or 100 g × 3 mins.

Imposing a linear relationship on the data set yields a satisfactory fit (R^2 = 0.873). The trend of data points where $F > 0.8$ indicates higher levels of cell recovery requires a disproportionately greater level of centrifugation when compared

to lower levels of cell recovery. This is likely to be an artifact of the assumptions used when applying Sigma concept. Sigma concept is based on Stoke's definition of settling and assumes unhindered settling of a spherical particle within a homogenous gravitational field. In practice, the cells in suspension are a distribution of sizes about a mean cell size of 13 μm (measured using Cedex HiRes automated cell counter), and settling is hindered due to the high concentration of cells accumulating at the bottom of the tube. The centrifugal field within the centrifuge tube is not homogenous because: (1) we assume constant centrifugal acceleration based on $\frac{\omega^2 \cdot r_2}{g}$ (see Eqn. (2.5)), where r_2 is the outer radius of the centrifuge tube, and (2) the direction of centrifugal forces within the tube do not act in parallel to the walls of the tube, resulting in a proportion of cells that collide with the tube walls due to the radiality of the centrifugal force. The calculated clarification capacity (C) for a 99% recovery of cells is 7.77×10^{-7} m s^{-1} and is based on the linear fit. This value will be used in a following section (see Section 3.4) to construct a Window of Operation. Incidentally, the maximum value of F that can be determined experimentally is 0.99 or 99.0%, and is imposed by the detection limit of the Guava Instrument.

As the fraction of mES cells recovered is calculated from the cells remaining within the supernatant fraction (see Eqn. (2.6)), no comments will be made on the state of mES cells collected in the cell pellet at this juncture. This is addressed in Section 3.3.2 as cells could be viable or rendered non-viable or destroyed by the applied centrifugal force. Throughout the experiment it was noticed that the cell pellets became more tightly packed as centrifugal force and time were progressively increased ($C \rightarrow 10^{-7}$ m s^{-1}). In order to minimise disturbances to the cell pellet collected by flow eddies generated during sampling, the supernatant from each centrifuge tube was carefully removed using a pipette. In particular, with the pipette tip held below the fluid meniscus, supernatant was withdrawn gently from the cylindrical and conical sections of the centrifuge tube only. No fluid was withdrawn from the well section of the machined acrylic insert which contains the cell pellet.

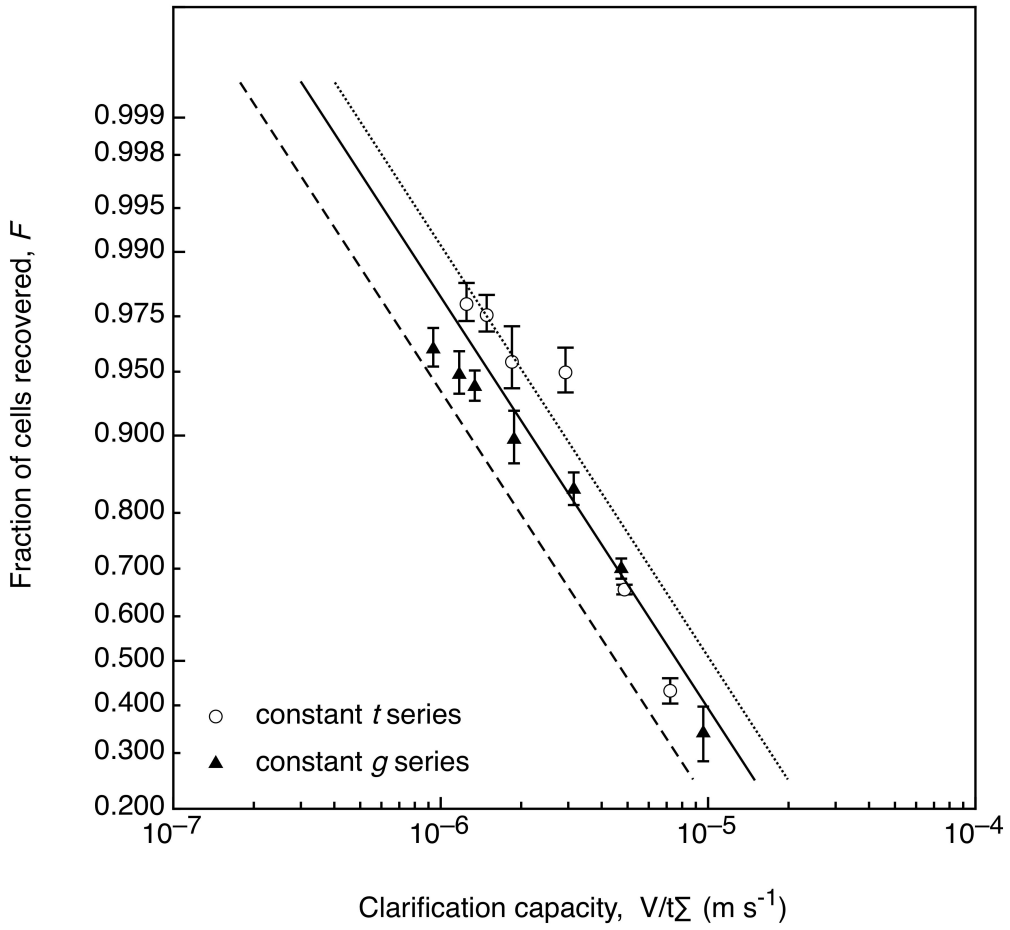

Figure 3.1: Centrifuge clarification performance determined on a total cells basis (viable and non-viable cells). Cell suspensions at 21°C were centrifuged by varying time at constant RCF ($g = 30$) conditions (▲), and varying RCF at constant time ($t = 2$ mins) conditions (○). F, fraction of cells recovered was evaluated on the number of cells that remained in the supernatant fraction of the liquor. The solid line represents a linear fit for all experimental data points ($R^2 = 0.873$), the dashed and dotted lines are the 4 and 37°C corrections for this line. The calculated C value for a 1% loss in recovered cells is 7.77×10^{-7} m s^{-1}. Results are mean ± 2SE for 6 independent samples for each centrifugation condition.

3.2.1 Theoretical analysis of cell settling in centrifugal field

In this subsection, a simple model for cell settling in a centrifugal field was developed using Equation (2.2) and the results from Figure 3.1. Centrifuge clarification performance data was transformed into a log-normal distribution by plotting changes in fraction of cells recovered (dF) against an appropriate range of clarification capacity values (C) which were divided into 100 equal steps (Fig. 3.2A). The distribution obtained corresponds to a range of $0.001 \leq F \leq 0.999$ values and was established from the linear fit of the experimental data points in Figure 3.1. The gradient of the linear fit line determines the shape of the distribution; a steep gradient results in a narrow spread and a shallow gradient results in a broad spread.

As clarification capacity (C) and Stoke's terminal settling velocity of a particle (u_s) are dimensionally similar (m s^{-1}), Figure 3.2A also depicts the distribution of settling velocities of cells within the centrifugal field (cells are assumed to behave like spherical particles). In addition, it also represents the distribution of cell sizes within the population of cells subjected to centrifugation as u_s is proportional to cell size (i.e. $C \propto u_s \propto d$). Using Equation (2.2), the mean cell size of the cell population can be determined from the information presented in Figure 3.2A and literature values. For example, the expected mean cell diameter of the cell population corresponds to a 50% recovery in cells. Thus, when $F = 0.5$, $C = 7.67 \times 10^{-6}$ m s^{-1} and this corresponds to the peak observed in the distribution (Fig. 3.2A). Feeding $C = 7.67 \times 10^{-6}$ m s^{-1} and literature values for μ, ρ_p, ρ_f, and solving for d in Equation (2.2) ($\mu_{21^oC} = 0.979 \times 10^{-3}$ N sm^{-2}, and $\Delta\rho = 20$ kg m^{-3}), the mean cell diameter was calculated to be 13 μm. This value is concordant with the known mean cell diameter of *Oct*4-GFP cell populations.

The distribution of cell settling velocities at 4 and 37^{o}C process temperatures were determined using Equation (2.2) and varying fluid viscosity (Fig. 3.2B) ($\mu_{4^oC} = 1.969 \times 10^{-3}$ N sm^{-2} and $\mu_{37^oC} = 0.692 \times 10^{-3}$ N sm^{-2}). A decrease in process temperature from 21 to 4^{o}C results in a corresponding decrease in cell settling velocities.

This is due to the increase in viscous drag associated with the decrease in process temperature. The effect of viscous drag on cell settling velocities is decreased when the process temperature is raised from 4 to 37^{o}C. The effects of temperature on cell physiology and cell size were assumed to be negligible. The distributions obtained for 4 and 37^{o}C process temperatures were mapped onto the probability-log centrifuge clarification performance plot (Fig. 3.1) and maybe used to predict clarification performance at various process temperatures (Table 3.1).

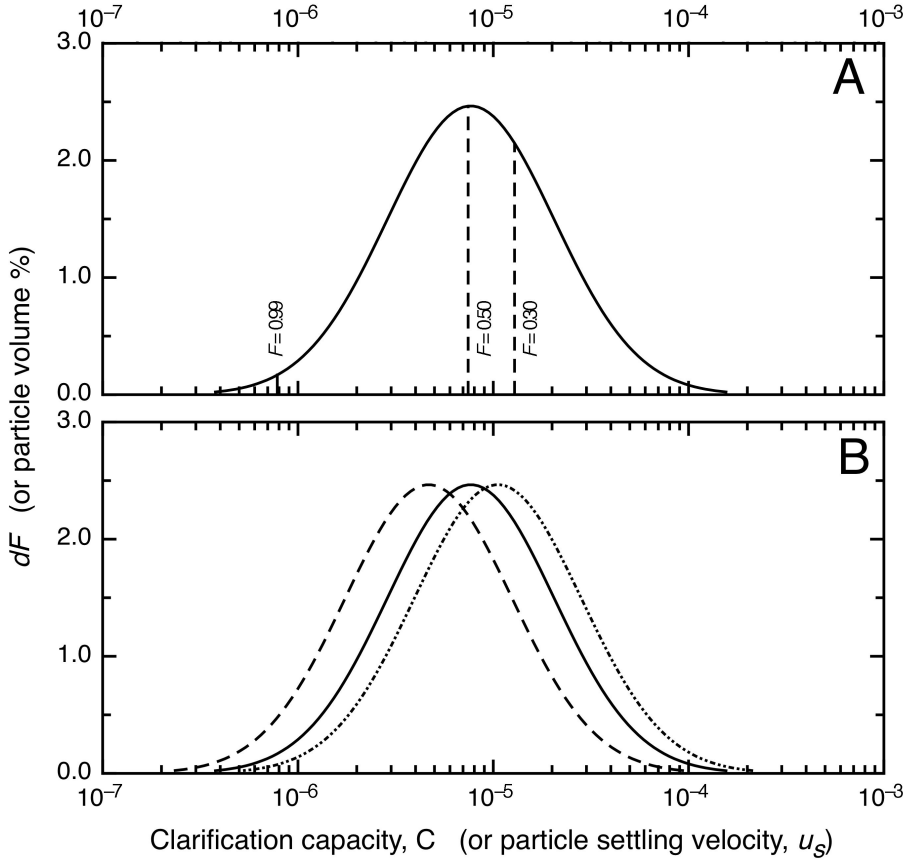

Figure 3.2: The clarification capacity distribution was obtained by plotting changes in fraction of cells recovered (dF) against an appropriate range of clarification values (C) which were divided into 100 equal steps (Panel A). As C and Stoke's particle settling velocity, u_s are dimensionally similar, the distribution obtained is also indicative of the cell size distribution. Although only experimental data was available for F values within a range of ∼0.30–0.99, the distribution represented corresponds to $0.001 \leq F \leq 0.999$ values. The influence of process temperature was assumed only to affect fluid viscosity and the clarification capacity distribution was corrected accordingly using Equation (2.2) (Panel B). The solid line represents the distribution at 21^{o}C, and the dashed and dotted lines are the 4 and 37^{o}C corrections for this line.

3.2.2 Influence of temperature variations

The influence of process temperature variation on clarification performance at high levels of cell recovery ($F > 85\%$; 30 g $\times$ 10 mins; $\Sigma = 1.88 \times 10^{-6}$ m s^{-1}) is summarised in Table 3.1. The table also includes predicted cell recovery values at the various process temperatures examined. Temperature was assumed to only affect the viscosity of the suspending liquor within the system and its effect on cell physiology to be negligible. Statistical testing (two-tailed Student's t test) to a 95% confidence revealed that the difference in F between 21 and 4°, and 21 and 37° were not significant. The temperature-viscosity profile for complete medium was assumed to be equivalent to that of water (Radisic *et al.*, 2005), and corrections for 4 and 37 °C to the 21°C fitted line were made and plotted in Figure 3.1 (see Section 3.2.1). All but one of the data points are spread between in the 4 and 37°C degree boundaries, further reinforcing that temperature variations do not have a significant effect on clarification performance. This analysis was confined to high levels of cell recovery not because the influence of temperature at low levels of cell recovery are large on F, but because low levels of cell recovery in practice are not desirable. The predicted F values for three process temperatures examined varied no more than 7% from the obtained experimental value. Although simple, the clarification model was able to give fairly accurate results because it was informed with experimental data (i.e. 21^{o}C F data) and the contributions of fluid viscosity changes with respect to temperature variations were significant.

Table 3.1: Table summarising the influence of temperature on clarification performance of the centrifuge operating at fixed Sigma value of 1.88×10^{-6} m s^{-1} at high cell recoveries ($F > 85\%$). There were no significant differences between operations at 21 and 4 °C, and 21 and 37° at the 95% level of confidence. The table also includes predicted F values generated from the simple clarification model developed. The differences between predicted and experimental F values ($\leq 7\%$) suggest that the model is able to give fairly accurate predictions. Results are mean ± 2SE for 6 independent sample for each condition.

	F		
Temperature (°C)	Predicted	Experimental	p-value
4	0.814	0.876 ± 0.0114	0.160
21	0.923	0.896 ± 0.0240	–
37	0.957	0.938 ± 0.0105	0.0527

3.3 Centrifugal cell recovery

This section examines the effect of centrifugal force, centrifugation time and the associated cell pellet resuspension procedure on mES cells during processing. For every centrifuged cell sample exposed to a combination of centrifugal force, time and process temperature, an equivalent (uncentrifuged) control sample was assessed in parallel. Each sample was evaluated for *Fraction of cells lost* and *Fraction of cell viability lost* as measures of cell damage. The former metric is indicative of the absolute recovery of all cells detected (viable and non-viable cells) after centrifugal processing, and the latter is indicative of the change in state of cells from that particular sample.

The influence of time and temperature on the control samples are shown in Figure 3.3. Note that on the expanded y-axis scale positive values reflect an overall loss in cell numbers or cell viability, and negative values reflect an overall gain in cell numbers or cell viability. Differences between initial and final values for cell numbers and cell viability for each condition were tested to the 95% level of confidence and hence are highlighted as significant changes from the initial sample. Only 4 samples showed such a significant change.

A significant gain in total cells (Fig. 3.3 A) and a significant loss in cell viability (Fig. 3.3 B) at 100 minutes of all three of the holding temperature was registered. A significant loss in cell viability was also observed in the sample held for 50 mins at 37°C. Results for the remaining control samples suggest that experiments to study the effects of recovery conditions on the cells can be assessed as having the same initial cell concentrations and viabilities as the initial start material at least for hold time up to 20 minutes and possibly up to 50 minutes for 4 and 21°C. The use of lower temperatures does not significantly affect cell concentration and viability.

The results for *Fraction of cells lost* and *Fraction of cell viability lost* for centrifuged mES cell samples is presented in Figure 3.4 and Figure 3.5 respectively

(Note the difference in y-axis scale between Fig. 3.3; 0—0.1, and Fig. 3.4 and 3.5; 0—1.0).

Both measures of cell damage were further evaluated on a *process* (Panels A & B in Fig. 3.4 and 3.5) and a *centrifugation* (Panels C & D in Fig. 3.4 and 3.5) basis. The difference between evaluation on a *process* and *centrifugation* basis lies within how time is considered with in the system for a given set of centrifugation conditions and is detailed in Section 2.3.1.2. Briefly, the *centrifugation* metric take into account the overall processing time for centrifugation and thus ignores cell gains or losses due to time-temperature exposure. On the other hand, the *process* metric accounts for all effects including holding time, centrifugation time and cell resuspension losses.

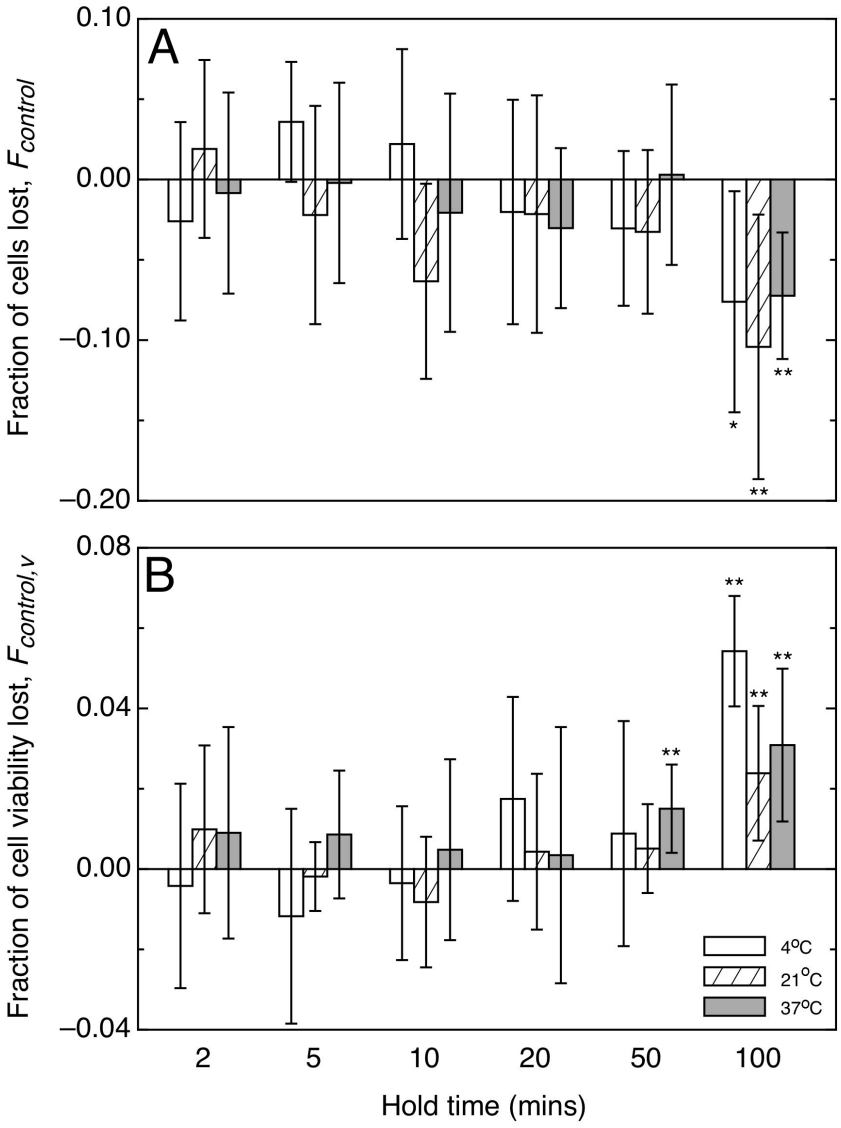

Figure 3.3: Impact of time-temperature on mES cells held in suspension. These results serve as controls to centrifuge samples. mES cell suspensions at 1×10^6 cells mL^{-1} were subjected to various time-temperature combinations to determine *Fraction of cells lost* (Panel A) and *Fraction of cell viability lost* (Panel B). Significant differences between initial and final values for each time-temperature exposure combination are indicated with * or ** denoting $p > 0.05$ and $p > 0.01$ respectively. Results are mean ± 2SE for 6 independent samples.

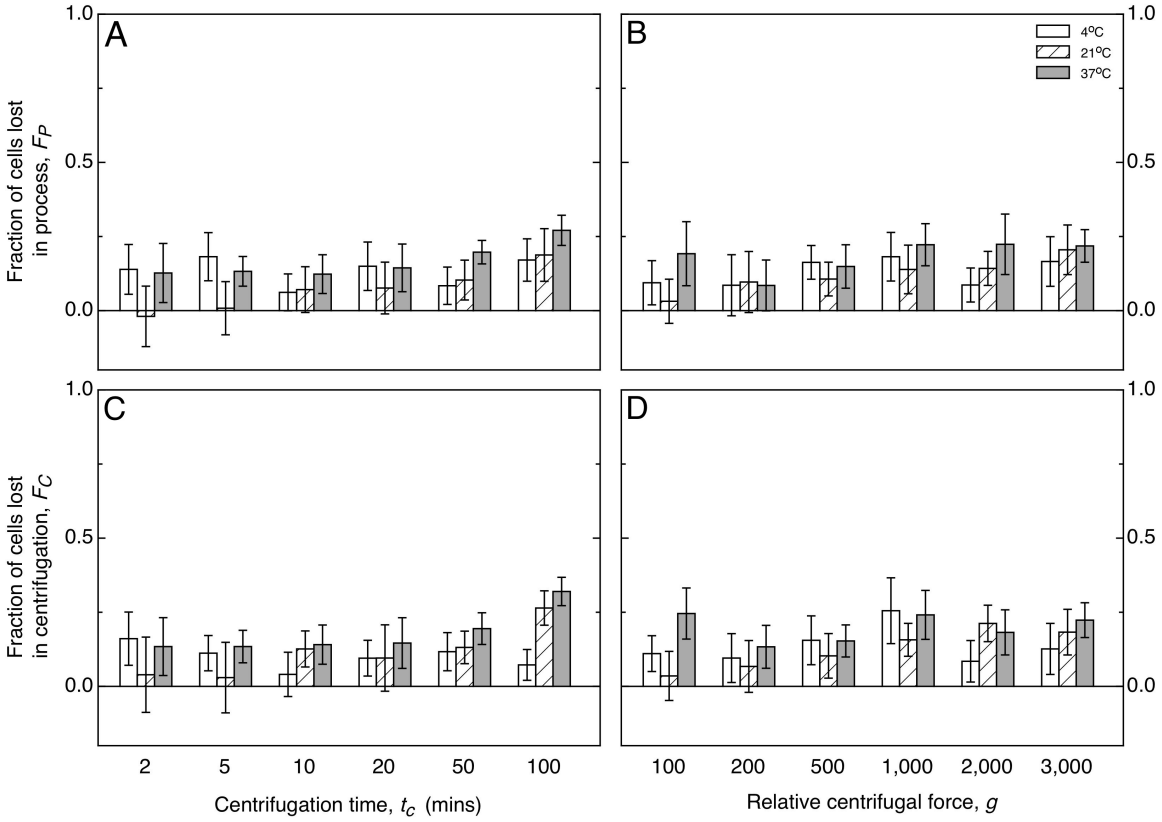

Figure 3.4: Impact of centrifugation time, process temperature and centrifugal force on mES cell numbers. mES cell suspensions were centrifuged by varying time at constant RCF (RCF = 200 g) conditions (Panels A & C), and varying RCF at constant time (20 mins) conditions (Panels B & D). The fraction of cells lost was evaluated on both a *process* (F_P; Panels A & B), and *centrifugation* (F_C; Panels C & D) basis. A 5–25% average cell loss occurring at all process temperatures and centrifugation conditions was observed, with losses peaking in high time and temperature combinations. Results are mean ± 2SE for 6 independent samples.

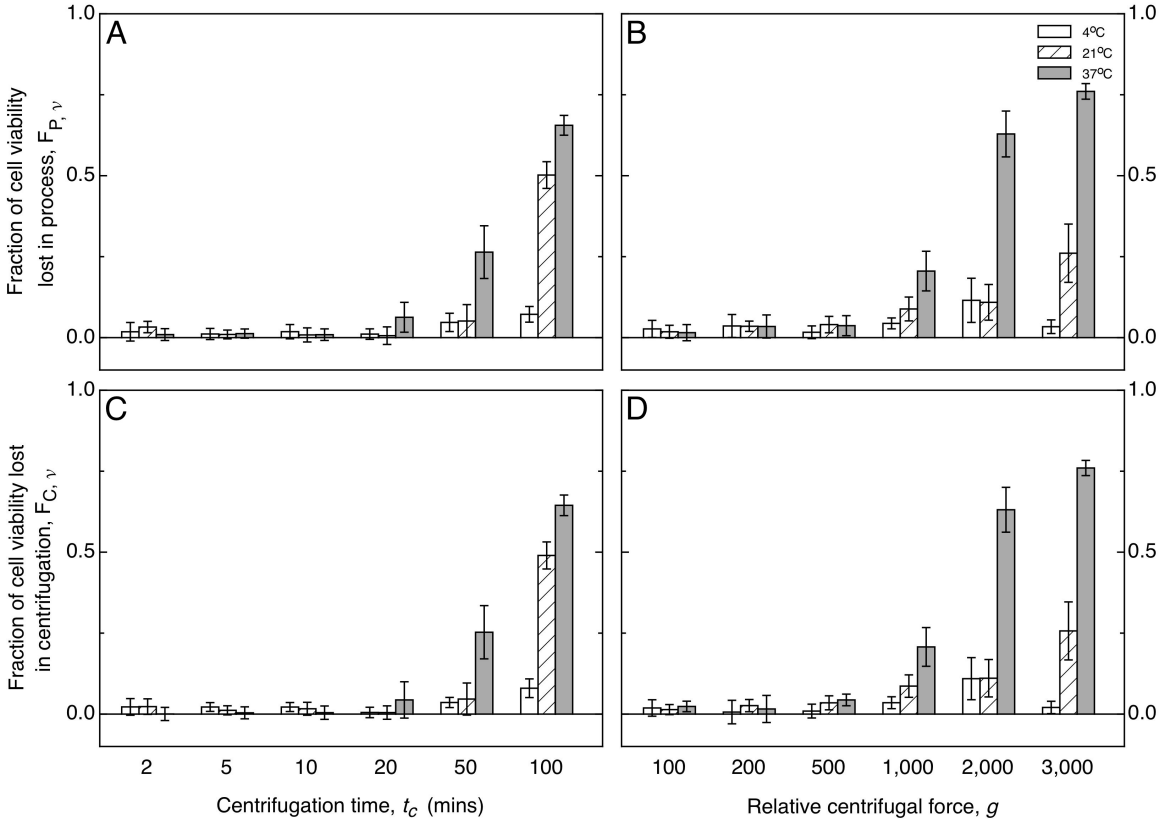

Figure 3.5: Impact of centrifugation time, process temperature and centrifugal force on mES cell viability. mES cell suspensions were centrifuged by varying time at constant RCF (RCF = 200 g) conditions (Panels A & C), and varying RCF at constant time (20 mins) conditions (Panels B & D). The fraction of cell viability loss was evaluated on both a *process* ($F_{P,\nu}$; Panels A & B), and *centrifugation* ($F_{C,\nu}$; Panels C & D) basis. The results indicate that cell damage is dependent on a combination of centrifugal force, centrifugation time and temperature. Results are mean ± 2SE for 6 independent samples.

3.3.1 Cell damage and the influence of process temperature

The degree of cell damage that occurs is measured by *Fraction of cells lost* and *Fraction of cell viability lost*. The former is characterised by the complete destruction of the cell plasma membrane resulting in the loss of intracellular contents to the surrounding medium (Al-Rubeai *et al.*, 1995). The latter is characterised by an increased permeability in cell membrane and its inability to mediate the flow of ions and molecules in and out of the cell whilst still maintaining the physical appearance of a viable cell; these cells are termed non-viable cells. In this study, the measure of *Fraction of cell viability lost* is in addition to the measure of *Fraction of cells lost*, as latter only declares the remaining population of cells after destructive cell damage and give no indication to the relative population of viable and non-viable cells.

Varying degrees of cell damage was detected in all centrifuged cell samples exposed to the different centrifugation conditions. Figure 3.4 illustrates the *Fraction of cells* (total cells) *lost* (i.e. total damage of cell plasma membrane) after centrifugation. In general, 5—25% of cells are lost depending on centrifugation time, processing temperature and centrifugal force. When considering cell loss as centrifugation time and relative centrifugal force is increased (Fig 3.4 C & D), a possible tendency for greater cell loss was noted as centrifugation time is increased to 100 mins when cells are processed at 21 and 37°C (Fig 3.4 C). The cell losses incurred in the remaining conditions were comparable to each other as RCF and centrifugation time were progressively increased.

Further to this observation, there is some possible evidence to suggest that processing cells at 21°C results in lower cell losses compared with processing at 4 and 37°C when the following rule is considered: Cells are not lost when the error bar for each respective condition crosses or touches the baseline $F_P = F_C = 0$. Where the error bar represents the range of values the calculated loss will lie for 95% ($\pm$2SE) of the time. From the data set, the synergistic effects of centrifugal force, centrifugation time and processing temperature on destructive cell damage may be ranked

in the following order of priority in terms of determining the extent of cell damage: time ($\geq$ 100 mins) $\gg$ temperature $\gg$ relative centrifugal force.

The extent of cell damage was assessed in the remaining recovered cells from each sample and is presented in Figure 3.5. In contrast to total cell loss data (Fig 3.4), there is a clear correlation between loss of cell viability and centrifugal force, centrifugation time and processing temperature. The relationship appears to manifest as a sigmodial function of the process variables. To explore this further it is valuable to look at the data for each temperature (Fig. 3.5 C & D):

At 4°C, cell viability losses were low across the board for both the varying time conditions at constant RCF, and varying RCF conditions at constant time. The loss in cell viability averaged 3%.

At 21°C, the largest change in cell viability was recorded at the highest levels of centrifugation time and force, 49 and 25% respectively (Fig 3.5 C). These values represent a magnitude increase in loss of cell viability over the losses observed at 4°C.

The greatest loss in cell viability was observed when cells were centrifuged at 37°C at the highest levels of centrifugation time and force, 76 and 64% respectively (Fig 3.5 D). When compared to the losses incurred at 21°, this is a 2.6 and 1.5-fold increase in fraction change of cell viability. The discrepancy between the values suggest that at extended centrifugation times at 21 and 37°C, the time dimension plays a crucial role in determining the the cells' susceptibility to damage.

Finally, at centrifugation times $\leqslant$ 20 mins and forces $\leqslant$ 500 g, low levels of change in cell viability are recorded across all process temperatures investigated. These two values serve as a practical upper limit for batch centrifugation and are used in Section 3.4.2 to aid in constructing of a window of operation for centrifugal cell recovery.

To recapitulate, the combined effects of low process temperature, low centrifugal force and short processing times result in low or no loss of cell viability. Low process

temperature minimises the extent of cell viability loss that occurs as centrifugation time or centrifugal force is increased.

No differences between cell damage (both viable cells lost and cell viability lost considerations) evaluated on a *process* and *centrifugation* basis was observed. The effects of cell gain or loss due to time-temperature exposure are ignored when evaluated on a *centrifugation* basis. Results from the experimental controls (Fig. 3.3) indicate that no significant changes in the mES cell suspension occurred up to 50 mins. The absence of any changes in cell number and cell viability effectively causes the *process* calculations to behave like the *centrifugation* calculations. However, at 100 mins, where a gain in cell numbers and a loss in cell viability was observed in the controls, the expected differences between either basis of calculation was not evident in the experimental results. This is likely due to a combination of large experiment-to-experiment variations and small gains and losses observed in the controls.

3.3.2 Lactate dehydrogenase activity

In order to evaluate where mES cells were being damaged during centrifugation, intracellular LDH released from damaged cells into the surrounding culture medium was monitored (Fig. 3.6). LDH activity was assayed in: (1) the supernatant fraction of the sample after centrifugal exposure (3,000 g $\times$ 20 min), and (2) the culture medium after pellet resuspension. Control samples were exposed to the same resuspension regime were also assayed.

Overall, the amounts of LDH detected within the control and supernatant samples were independent of the effects of temperature. The amounts of LDH detected within the supernatant samples were low and comparable to background values. The average values recorded across all three process temperatures examined for control samples was 330 RFU and 46 RFU for supernatant samples. The differences between the control and supernatant readings indicate that resuspension is responsible for cell damage.

LDH activity indicates for resuspended cell samples the degree of cell damage incurred during resuspension is dependent on process temperature. At 4°C, the amount of LDH detected from the resuspended sample (390 RFU) was not dissimilar to the value recorded for the control sample (360 RFU) at the same temperature. However, as process temperature was raised, increasing amounts of LDH was detected in the resuspended cell samples. At 21°C a value of 700 RFU was recorded, and 1720 RFU at 37°C. This increase corresponds to a 1.2 and 4.4 fold increase in LDH detected on 4°C. The data indicates that exposure of cells to a centrifugal field causes little or no damage, and resuspesnion operations together with increasing process temperatures account for the majority of the damage.

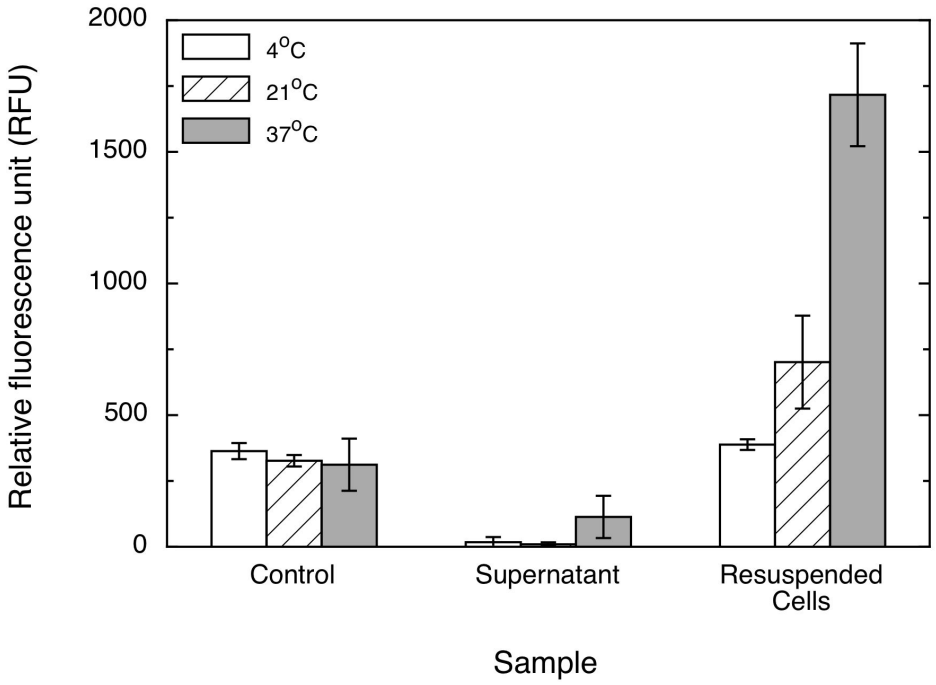

Figure 3.6: Contributions of centrifugal force and cell pellet resuspension to cell damage. mES cell samples were centrifuged at 3000 g for 20 mins at 4, 21 and 37°C. Supernatant samples were aspirated from the clarified medium immediately after centrifugation and assayed for LDH release. Resuspended cell samples were pellets resuspended back into the clarified supernatant *in situ* under constant resuspension conditions and assayed for LDH release. The data indicates the majority of cell damage occurs during resuspension and that cell damage increases with increasing temperature. Control samples not exposed to centrifugation ($RCF = 1\ g$; $t = 20$ mins) of equivalent time-temperature history were subjected to the same constant reuspension conditions, as was supernatant samples. Control samples were significantly different from supernatant samples, and resuspended samples with the exception of 4°C. Results are mean ± 2SE for 6 independent samples.

3.4 Constructing a window of operation

By predicting the clarification performance for the centrifuge and the amount of cell damage encountered for a specific set of centrifuge conditions, a Window of Operation for centrifugal recovery of mES cells was developed. The results from Figures 3.1 and 3.5 C & D together with equipment operating conditions in Table 3.2 were applied in constructing the window of operation.

Centrifuge clarification performance (Fig. 3.1) was evaluated to determine the relationship between clarification capacity (C) and fraction of cells recovered (F). This relationship governs the amount of cells that settle out of its suspending liquour for a given combination of centrifugal force (RCF) and centrifugation time (t_c). Based on this relationship and for a minimum acceptable value of 99% recovery of cells ($F = 0.99$), a centrifuge clarification capacity of 7.77×10^{-7} m s^{-1} has to be achieved. This value was then used to calculate a corresponding set of centrifugation conditions (RCF and t_c) using Equations (2.3) and (2.4). Combining both equations and solving for centrifugation time (t_c) gives Equation (2.12), thus a corresponding range of centrifugation time (t_c) can be obtained over a range of relative centrifugal forces (RCF). In this instance a range of 0—3000 g was used in the calculations. Figure 3.8 A illustrates the plotted set of RCF and t_t values; when operating to the right of this clarification line (shaded area) the minimum acceptable level of cell recovery is exceeded.

To construct the line representing the minimum acceptable level of *Fraction of cell viability lost* in the window of operation, a relationship between centrifugation force (RCF), centrifugation time (t_c) and *Fraction of cell viability lost* ($F_{P,\nu}$ or $F_{C,\nu}$) has to be established. Equations (2.13), (2.14) and (2.15) were examined to determine their suitability in modeling the required relationship between the cell viability and the centrifugation variables. Each function assumes a sigmoid shape and a 1^{st} order dependence on time, and no change in cell viability when not exposed to centrifugation (i.e. $F_{P,\nu}$ or $F_{C,\nu} = 0$, when $t_c = 0$ or RCF$= 0$). No attempt was made

to include in the model a function to allow for the influence of temperature on cell viability. Hence the *Fraction of cell viability lost* results was modeled as discrete temperature data sets.

3.4.1 Model development

The *Fraction of cell viability lost* evaluated for *centrifugation* was used to explore the relationship between $F_{C,\nu}$, RCF and t_c. The data together with preliminary range finding data for each process temperature investigated ($n = 12 + 6$ independent data points per process temperature) was organised into 3D Cartesian coordinates ($x = t, y = RCF$ and $z = \Delta\nu$, the *Fraction change in cell viability*) and the three different equations being examined (Eqn. (2.13), (2.14) & (2.15)) were used to convert the data.

Initial analysis revealed that the 1-exp function (Eqn. (2.13)), and the Michaelis-Menten type function (Eqn. (2.15)) and was best suited to describe each temperature profile ($R^2 = 0.965$ both functions where the R^2 value is the arithmetic mean value obtained over the 3 temperature fittings). The *tanh* function was excluded from further analysis due to its lower coefficient of determination ($R^2 = 0.960$), poor fit to the data set (Fig. 3.9 C & D), and due to the low incidence of such functions in biological systems. Although the 1-exp and Michaelis-Menten type functions have been applied to modeling growth, mass transport and enzyme kinetics, the former function was selected over the latter on the basis of simplicity and its better fit at low levels of cell damage (Fig. 3.9).

The line representing the minimum acceptable level of fraction of cell viability lost in the window of operation was determined for each process temperature and plotted. The plotted lines revealed a smaller area of available centrifuge operating conditions for 21°C when compared to operation at 37°C. This was contrary to the expectation that a reduction in process temperature has the effect of enlarging the operating area. The plotted operating area for the 4°C data set was the largest of

the three investigated temperatures. This unexpected result between the 21 and 37°C operating areas was traced back to the number of degrees of freedom provided in the 1-exp function. The discrepancy between the available operating areas of 21 and 37°C was resolved by reducing the number of degrees of freedom in the 1-exp function—from 3 to 1. This was acheived by applying the n and m coefficients determined at 37°C to the 4 and 21°C model to give:

$$\Delta\nu = \left(1 - e^{-a \cdot t_c \cdot RCF^{0.6}}\right)^{4.3} \tag{3.1}$$

Where a is the coefficient to be determined by the fitting algorithm. Table 3.3 summarises the value of coefficients evaluated for each temperature fit, and Figure 3.11 illustrates the fitted 3D profiles for each temperature data set. The performance of the 1-exp model was evaluated by charting the predicted model results against the actual experimental results for all temperatures in a parity plot (Fig. 3.10). The parity plot returned a goodness of fit coefficient of $R^2 = 0.940$. The parity plot suggests that the model underestimates the level of damage for a change in cell viability when less than 10%.

Using Equation (3.1) and the determined coefficients given in Table 3.3, a set of RCF and t_c values can be obtained for a minimum acceptable level of fraction of cell viability lost in the window of operation. Panel B in Figure 3.8 illustrates the plotted set of RCF and t_t values for a 1% loss in % cell viability at 21°C; when operating to the left of this line (shaded area) the minimum acceptable level of loss in cell viability after centrifugation is exceeded.

A thermodynamic assessment of the loss in cell viability during the cell resuspension can be performed with the fitted coefficient a from the 1-exp function when plotted in the Arrhenius form (Fig. 3.7)—where the logarithm of the determined rate constant, a, is plotted on the ordinate against the reciprocal of of the absolute temperature on the abscissa. The assessment provides a simple way to explain the

non-linear relationship between temperature and loss in cell viability during cell re-suspension. The fitted line ($R^2 = 0.988$) had a slope of -4,707.6 and corresponds to a calculated calculated activation energy (E_a) of 3.9×10^7 J kmol^{-1}. This value is proportional and within cited activation energies for thermal cell growth.

Table 3.2: Centrifuge characteristics and limits applied when generating the centrifuge clarification performance constraint (see Eqn. (2.12)). x and y represent the fraction of overall centrifugation time for acceleration and deceleration of the centrifuge rotor respectively. Centrifuge rotor acceleration and deceleration times were determined empirically for each RCF_{max} set point.

Description	Value	Units
Centrifuge characteristics		
Volume	1.70×10^{-6}	m^3
r_1	0.131	m
r_2	0.163	m
x	0.03 – 0.60	no units
y	0.04 – 0.70	no units
Constraints		
RCF	0 – 3,000	g
Maximum yield (F)	0.99	no units

Table 3.3: Table summarising curve fitting coefficients used in the 1-exp model. n and m coefficients remain constant and are based on the values generated from the 37°C fit.

Temperature (°C)	$a \times 10^{-3}$	n	m	R^2
4	0.18	0.6	4.3	0.951
21	0.57	0.6	4.3	0.923
37	1.08	0.6	4.3	0.964

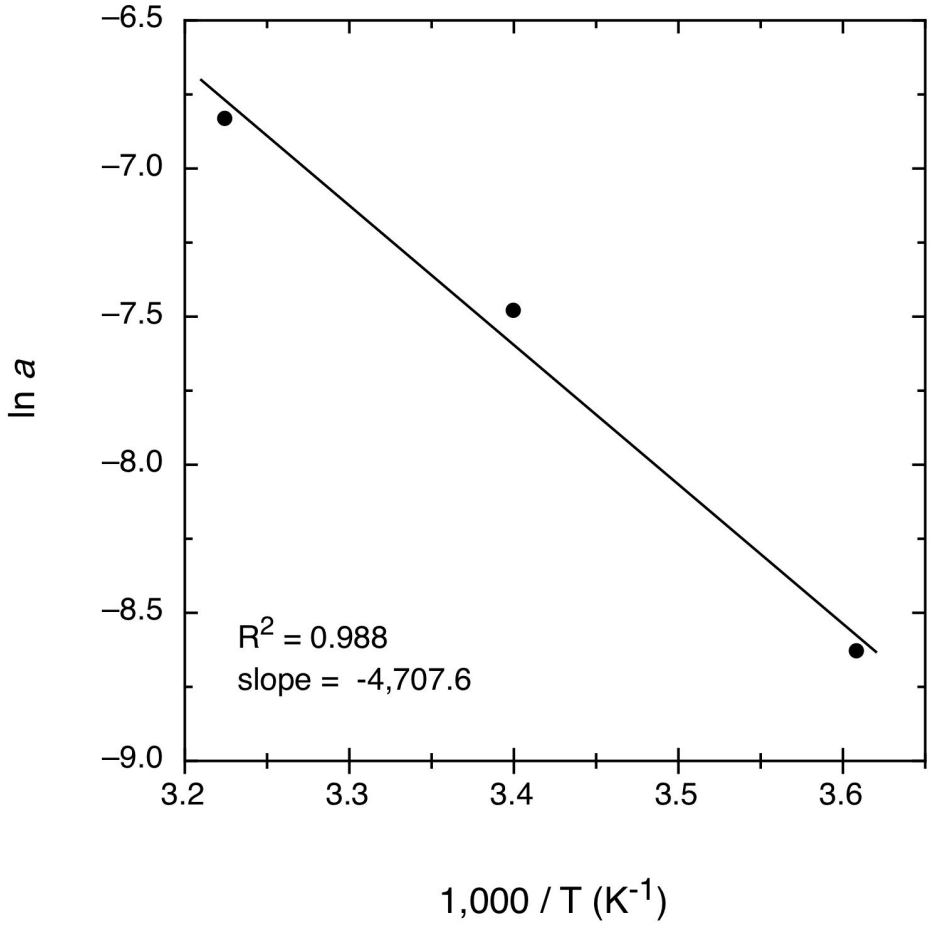

Figure 3.7: Thermodynamic assessment of the loss in cell viability during the resuspension process. The fitted coefficient a, from the 1-exp function was plotted in the Arrhenius form. The calculated activation energy (E_a) for the process is 3.9×10^7 J kmol^{-1}

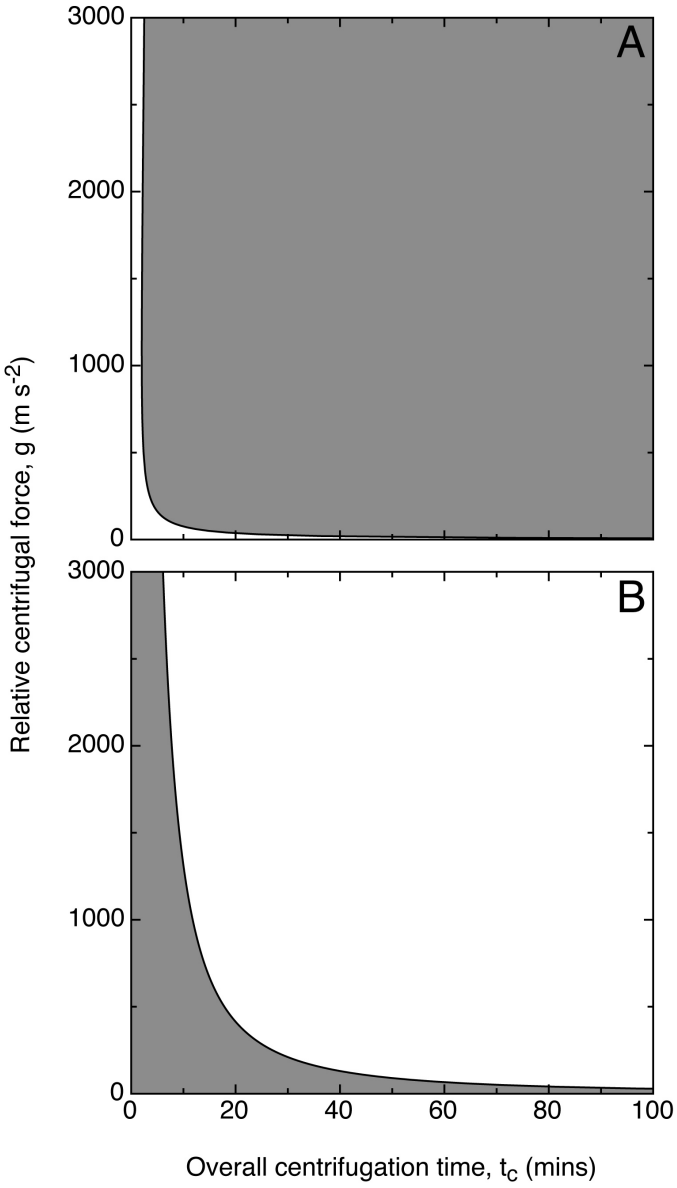

Figure 3.8: Operating constraints for constructing a window of operation for the centrifugal recovery of mES cells. The constraints are plotted for a 99% recovery of cells during clarification (Panel A), and a 1% loss in cell viability during centrifugation (Panel B) at 21°C. The shaded areas represent the available centrifuge operating conditions that meet or exceed the requirements.

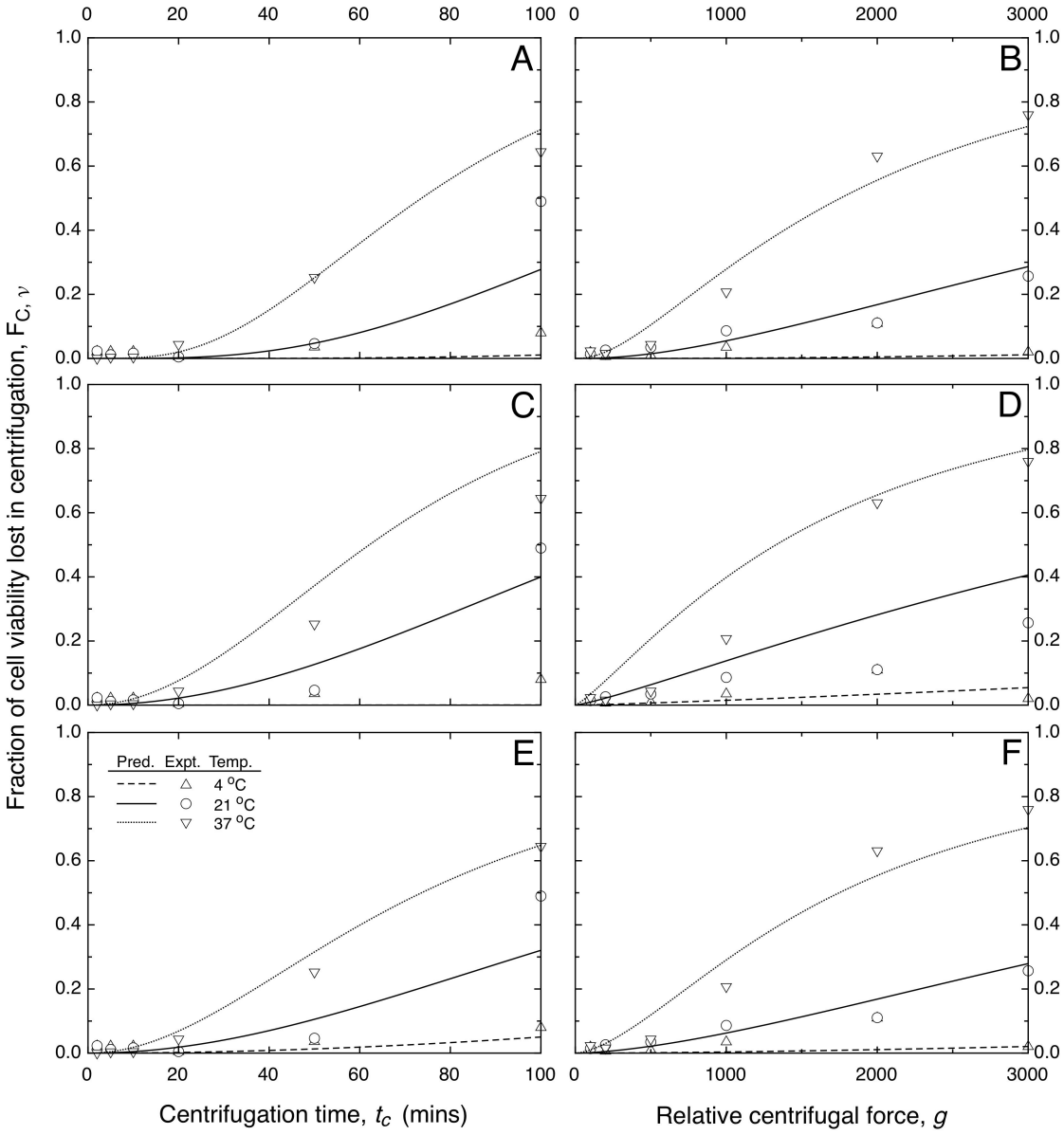

Figure 3.9: Model development to predict the *Fraction of cell viability lost* during centrifugation. 3 mathematical functions were explored to best fit the data set: 1-exp (Panels A & B), *tanh* (Panels C & D), and Michaelis-Menten (Panels E & F). The 1-exp function was selected over the *tanh* and Michaelis-Menten functions due to its simplicity and its better fit at low levels of cell damage.

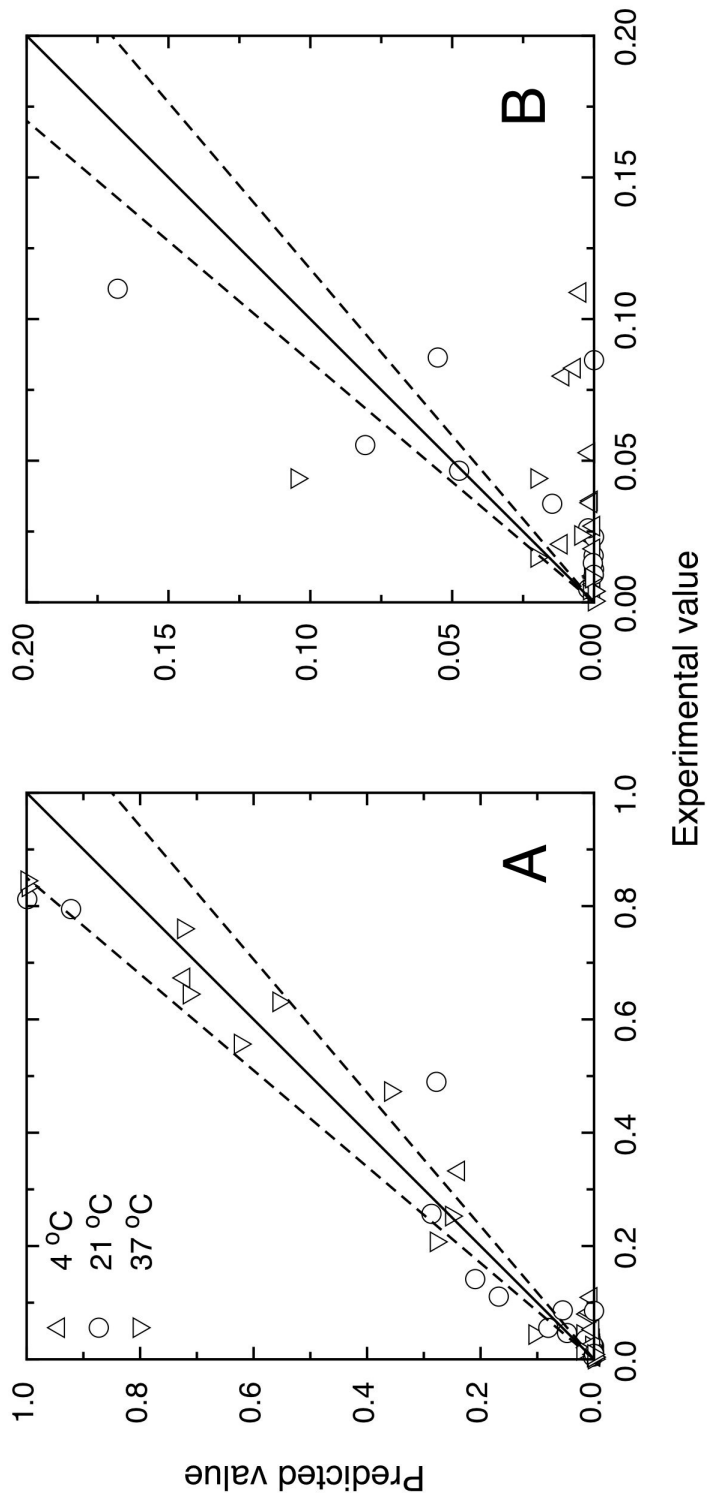

Figure 3.10: Parity plot of predicted change in cell viability for all process temperatures investigated. Parity plot for all data points (Panel A), and exploded view where experimental values are ≤ 0.2 (Panel B). The model yields a satisfactory fit ($R^2 = 0.940$). The dotted lines represents the $\pm 15\%$ variations from parity.

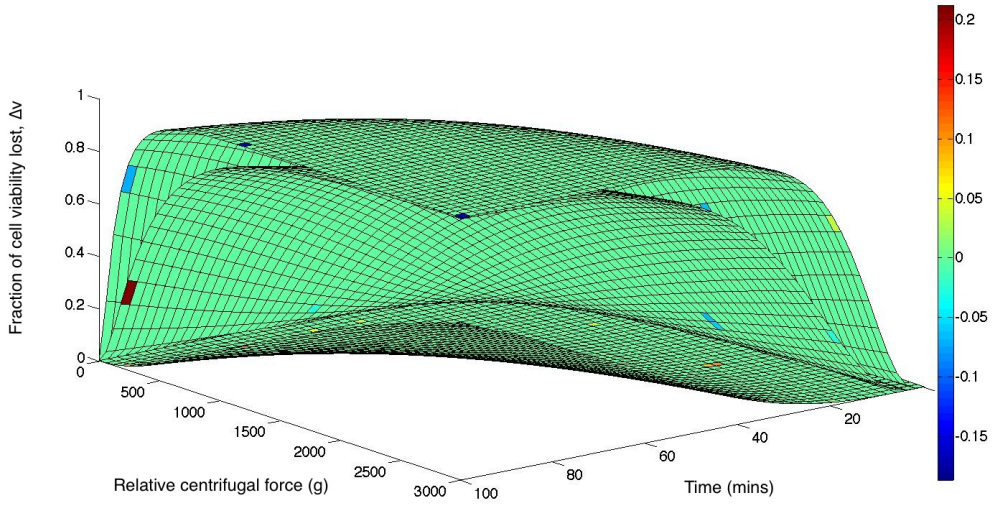

Figure 3.11: 3D plot of modeled *Fraction of cell viability lost* response surface for centrifugation at 4°C (bottom), 21°C (middle) and 37°C (top). The coloured spots on the mesh mark the the position of actual experimental data and its deviation from its predicted value as indicated in the colour bar.

3.4.2 Influence of processing temperature

A Window of Operation is constructed by superimposing lines which represent a minimum acceptable level of centrifuge performance onto common axes. Figure 3.12 illustrates the influence of processing temperature on the Window of Operation for centrifugal recovery of mES cells. Line (i) represents the clarification performance of the centrifuge and operating to the right of this line exceeds the requirement to recovery 99% of centrifuged cells. Line (ii) represents the fraction of cell viability lost during centrifugation and operating to the left of this line satisfies the requirement that there is a 1% or less change in cell viability during the centrifugation procedure. The L-shaped lines (i) and (ii) confine the unavailable and available operating conditions along the ordinate and abscissa of the plots respectively (Fig. 3.8A & B). When lines (i) and (ii) superimposed on each other, the area bounded by the elbows of both L-shaped lines suggest that for a given range of t values, there is large range of available RCF values that can be chosen from to satisfy the imposed minimum acceptable level of centrifuge performance. This is in contrast to the available operating conditions along the vertical and horizontal arms of the L-shaped area bounded by lines (i) and (ii). Operating along the tapered arms limits feasible operating conditions to narrow ranges of RCF or t to a correspondingly large range of t and RCF values respectively. The vertical and horizontal lines (iii) and (iv) represent the practical time (20 mins) and centrifugal force (500 g) upper limits for centrifugation.

In all cases, line (i) representing centrifuge clarification performance was presumed to be insensitive to changes in process temperature as indicated in the results in Table 3.1. When considering the influence of process temperature on the window of operation constructed by lines (i) and (ii), as processing temperature is raised, the area of the window decreases corresponding to a decrease of available centrifugation conditions. This decrease is brought about by the susceptibility of cells to non-destructive cell damage (cell viability losses) as temperature is increased. This

operating window can be further reduced by imposing practical centrifugal operating limits on time and centrifugal force; lines (iii) and (iv) respectively. When considering the sensitivity of the operating region bounded by lines (i), (ii), (ii) and (iv) to varying process temperatures, the available centrifuge operating conditions for processing cells at 4 and 21°C are similar and is approximately reduced by a third when processed at 37°C.

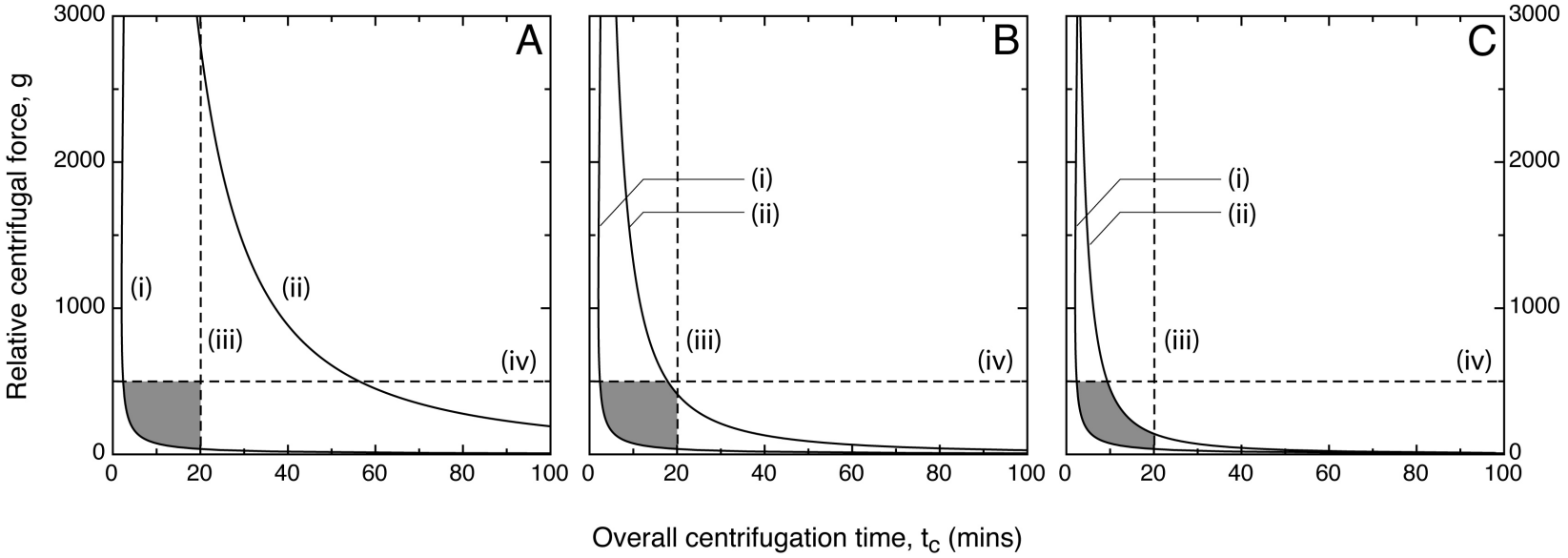

Figure 3.12: Windows of operation for batch centrifugation of mES cells. The available operating conditions are represented by the shaded area. The operating region is constructed by considering a 99% recovery of cells during clarification (Line (i)), a 1% change in cell viability during the centrifugation procedure (Line (ii)) and imposing practical time (20 mins) and centrifugal force (500 g) upper limits for centrifugation (Lines (iii) & (iv) respectively). Operating regions for centrifugation at 4, 21 and 37° are illustrated in panels A, B and C respectively.

3.5 Discussion

The physical impact of centrifugation on mES cells was examined by quantifying the degree of cell damage incurred during processing. Comparisons in cell concentration and cell viability before and after centrifugation provided the necessary cell damage information; the former indicative of destruction to the cells, and the latter indicative of the ratio between viable cells and non-viable cells in the remaining intact cell population. It was recognised early during preliminary centrifugation experiments that after centrifugation, it was inevitable that resuspension followed to disperse the collected cell pellet. The differing contributions of cell damage due to centrifugation, and due to resuspension were studied to some extent via monitoring LDH activity in the surrounding culture medium immediately after centrifugation, and after pellet resuspention. Although by this measure, the cells in the collected cell pellets were not directly damaged by centrifugal force (Fig. 3.6), it is probable that damage during resuspension is determined by the centrifugal force, centrifugation time and process temperature. Physical damage to cells in the collected cell pellet only occurred when they were exposed to the shear environment created to resuspend the cells after centrifugation. As the pipettor is cycled to disperse the pellet, a jet flow is established as fluid passes to and fro through the pipette tip. Cell damage is presumed to be caused by a combination of the energy dissipation rates encountered in the jet flow and elongation of cells and cell aggregates passing through the pipettor tip. The shear environment created by repeated cycling of the pipettor for each cell pellet sample was maintained at the same level, i.e. all samples were exposed to a similar resuspension/shear regime. It is appropriate to mention at this juncture the utility of the LDH activity assay in relation to bioprocessing. Unlike traditional methods of cell damage assay (e.g. trypan blue, PI staining) where cells –damaged or otherwise– have to be physically present to be quantified, the LDH activity assay allows for the level of cell damage to be determined without

cells having to be present. This is particularly useful in situations where cell samples are precious, limited or where cell samples are not available—situations that are commonly encountered during ES cell bioprocessing.

To help explain the results and facilitate the discussion of the likely processes that contribute to cell damage, an understanding of the events that occur at the cellular level has to be established, in particular, what is happening to and at the cell membrane. Born *et al.* (1992) and Zhang *et al.* (1993) reported that cell damage in laminar and turbulent flow is brought about by deformations caused to the cell membrane by: (1) the applied shear stress causing cells to form into prolate ellipsoids; and (2) eddies of sizes similar to or smaller than the cell interacting locally with the cell membrane. Cell damage occurs when these deformations cause a rise in cell membrane tension that exceeds the cell bursting membrane tension. In the cell pellet where cells are in close proximity to each other, membrane mediated intracellular adhesion events take place. The initial adhesion event is weak and reversible, and subsequent stabilisation of the adhesion is metabolically driven (Umbreit & Roseman, 1975). The stabilisation events are also time and temperature dependent where an increase in contact exposure time or temperature (up to 37°C) will result in a stronger adhesion or accelerate the stabilisation event (McClay *et al.*, 1981). Temperature also influences the fluidity of the cell membrane. A decrease in temperature leads to a decrease in membrane fluidity (Los & Murata, 2004), which results in a corresponding decrease in susceptibility to shear damage in the cell (Ramirez & Mutharasan, 1990). Cell damage can also occur during bubble disengagement at the bulk liquid-gas interface. Cells in contact with the collapsing thin film of a disengaging bubble are exposed to sufficiently high energy dissipation rates that can cause cell damage (Chisti, 2000; Garcia-Briones & Chalmers, 1994).

Cell damage resulting in cell loss during centrifugation is not desirable, and has the effect of lowering the unit operation's cell recovery efficiency and consequently overall process efficency. In order to circumvent cell loss that might arise during

centrifugation, a set of desirable centrifugation conditions is sought. In this study, data representing cell losses that arise during centrifugation (Fig. 3.4) is scattered and contains many variations making data analysis difficult. However, some sense was made out of the data by applying a rule based scoring system or by searching for trends in the data by inspection. The conclusions drawn from analysing the results in such a manner suggest: (1) centrifugation at 21°C gives rise to lower cell losses; and (2) extended centrifugation time is the dominant variable with respect to cell loss, and this is followed by temperature and centrifugal force (see Section 3.3.1). Although useful as process design and operational heuristics, these qualitative conclusions are not very helpful as they are unable to provide a definitive range of practical centrifuge operating conditions. An alternative method was explored to analyse the cell loss data to provide a quantitative answer.

The alternative method is based on a statistical consideration of all the data points examined. p-values generated from a two-tailed Student's t-test for each data point representing the probability of cell loss that might arise during centrifugation was plotted against centrifugation force and centrifugation time for all three process temperatures investigated (Fig. 3.13). Note that in each plot, the p-values are in logarithmic form to show clearly the spread of the data and to facilitate the fitting of the surface to all the data points. The fitted curved surface to the data points for each process temperature investigated (4, 21 and 37°C, Panels A, B and C respectively in Fig. 3.13) depicts the probability response surface for cell loss during centrifugation. The plane in each panel of the figure represents the 95% level of confidence ($z = log(0.05) = -1.3$) at which cell loss does not occur. Centrifuge operating conditions that lie on this plane and under the fitted probability response surface represents the set of operation conditions that will incur no cell loss during centrifugation. Visualising the data in this manner provides a high level of confidence and clarity in a simple-to-interpret quantitative graphical format when trying to determine suitable centrifuge operating conditions that results in no cell loss.

Figure 3.13: Likelihood of cell loss during centrifugal cell recovery is a function of centrifugal force and centrifugation time. p-values generated from the 2-tailed Student's t-test for each condition examined were plotted against centrifugal force and centrifugation time. A surface was fitted to the plotted data points and it depicts the probability response surface for cell loss during centrifugation. The plane in each panel represents the 95% level of confidence at which no cell loss occurs; the set of centrifuge operation conditions that lies on this plane and under the fitted probability response surface represents the set of centrifuge operation conditions that will incur no cell loss during centrifugation. Available centrifuge operation conditions at 4, 21 and 37° processing temperature are illustrated in panels A, B and C respectively.

Unlike cell damage resulting in cell loss, cell damage resulting in the loss of cell viability had a clearer and more well defined correlation to centrifuge operating conditions. The results in Figure 3.5 suggest that low temperatures preserve the cell quality irrespective of centrifugation time and centrifugal force. However, as process temperature is raised, cell quality decreases progressively as centrifugation time and centrifugal force increases. We propose a cell damage model in which the degree and mode of cell damage incurred during pellet resuspension is specified by the processing (centrifugation) conditions. The model is intended to reconcile cell damage data resulting in loss of cell viability and cell loss from the experiments (Fig. 3.4 & 3.13) and is deconstructed sequentially into the following four levels of detail as listed below:

1. Weak cells which are highly susceptible to destructive cell damage are eliminated first resulting in cell loss (Fig. 3.4).

2. For the remaining cells, i.e. those not eliminated by destructive cell damage, cell damage resulting in loss of cell viability occurs (Fig. 3.5). The changes in cell viability appear to be a function of centrifugation conditions; increasing changes in cell viability are incurred as centrifugation force, time and temperature are increased.

3. Cell damage resulting in loss of cell viability is minimised at low process temperatures due to the absence of the strong stabilised cell-to-cell adhesions, thus allowing for easy dispersal of the pellet within the shear field generated. Also at low temperatures, cell membranes were less susceptible to shear damage due to a decrease in cell membrane fluidity.

4. Cell damage resulting in loss of cell viability increases with increasing centrifugation time, centrifugal force and process temperature. Increasing centrifugation time allows the initial contact adhesion to become more established. It

is hypothesised that increasing temperature accelerates the rate of cell-to-cell contact stabilisation as this is metabolically driven. When a shear environment is generated to disperse the cell pellet, the cell pellet/aggregates persist longer due to stronger cell-to-cell adhesions and thus are exposed to the larger and more energetic eddies and elongation flow. Cell membranes at a high temperature are also more susceptible to shear damage.

As visible bubbles were not generated during the resuspension procedure, cell damage due to bubble disengagement was not considered within the proposed model. However, its effects cannot be rule out as bubbles invisible to the human eye may have formed during the resuspension procedure.

From the rule based analysis of Figure 3.4, there was weak evidence to suggest centrifugal processing cells at 21°C was better for cell conservation than at 4°C and 37°C. With this interpretation in mind, and from what is known about cellular responses to temperature variations, it is interesting to compare the likely cause of cell damage observed. As previously mentioned, cell damage occurs when cell membrane tension exceeds that of the cell bursting membrane tension. At 4°C, homeostatic activity within the cell is interrupted which results in uncontrollable cell swelling (Boutilier, 2001; Plesnila *et al.*, 2000). The cell swelling due to ion (K^+, Na^+, Ca^{2+} and Mg^{2+}) imbalance across the membrane (Hochachka, 1986) raises the cell membrane tension. At 37°C, cell membrane fluidity increases when compared to lower temperatures. The increase in membrane fluidity makes it more susceptible to membrane deformations that can also raise the cell membrane tension. An overall increase in cell membrane tension requires a lower energy input from the surrounding shear environment to exceed its bursting membrane tension. At 21°C, it appears a balance is struck between homeostatic activity, membrane fluidity and cell membrane tension that leads to cell damage.

Throughout the investigation, we noticed that cell pellets became more tightly packed as centrifugal force, centrifugation time and process temperature were pro-

gressively increased. The tight packing structure of the cell pellet is likely to be due to the increasing amounts of hydrostatic pressure exerted on the collected cells as centrifugal force is increased. The calculated range of hydrostatic pressure experienced by the cell pellet was 1.5—6.8 atmospheres (Hydrostatic head pressure calculated using $P = \rho gh$. 1 atm = 101.3 kN m^{-2}) and this corresponds to 200—3,000 g of centrifugal force. It seems unlikely that the range of hydrostatic pressures encountered during centrifugation results in cell damage (Fig. 3.6). The range of hydrostatic pressures encountered during centrifugation are also unlikely to disrupt cytoskeletal organisation; the cytoskeleton plays a central role in maintaining cell shape/structure, cellular division and intracellular transport. For cytoskeletal disruption to occur, hydrostatic pressures in the range of hundreds of atmospheres (200—700 atmospheres) have to be applied (Crenshaw *et al.*, 1996; Salmon *et al.*, 1976).

The concept of Windows of Operation has been applied to various scenarios in bioprocessing to help optimise and understand bioprocess design and operation. This study demonstrates for the first time, a developed methodology involving its use to describe a range of possible operating conditions for the centrifugal recovery of ES for a regenerative medicine bioprocess. The strength of the concept of a Window of Operation lies in the ability to organise and present multivarate complex information into a simple graphical visualisation to aid in bioprocess design decisions. For instance, from the results in Figure 3.4 and Figure 3.5 it would be difficult to determine a set of optimal centrifugation conditions that is able to satisfy a specified bioprocess design requirement, and assess its robustness to changes within the system. A Window of Operation for centrifugal recovery of mES cells was generated by predicting centrifuge performance with regards to clarification, cell damage and process temperature, and combined with a minimum acceptable level of centrifuge performance, a simple graphical area is defined. Figure 3.12 illustrates the sensitivity of the available centrifuge operating conditions to a designer by varying

processing temperature subject to the particular operating limits applied.

The work accomplished in this chapter has examined the physical impact of centrifugation on mES cells by monitoring the degree of cell damage incurred. Monitoring cell damage however, dose not provide any information to the changes in the identity (e.g. biological characteristics) of the cell that might have occurred during centrifugation. The following chapter will examine the impact of centrifugation on biological characteristics of the mES cell.

Chapter 4

Results and Discussion: Impact of Centrifugation on the phenotype of mES Cells

4.1 Introduction

Two major sets of results are reported in this chapter. These results relate to the study of the impact of centrifugation during bioprocessing on the phenotype of the mES cells. The first set relates to the study of undifferentiated expansion of mES cells after exposure to a range of centrifugal forces (see Section 4.2). The second is concerned with the formation of embryoid bodies (EBs) and the differentiation potential of EBs formed from mES cells exposed to different levels of centrifugal force (see Section 4.3).

4.2 Undifferentiated expansion of mES cells

In this section, the impact of centrifugation on mES cell proliferation and pluripotency were determined. Following exposure to different levels of centrifugal force, pelleted cells were resuspended (see Section 2.3.2.2 for resuspension procedure) and plated onto pre–gelatinised plates at a density of 10,000 viable cells cm^{-2}. Cells were allowed to proliferate in media containing leukemia inhibitory factor (LIF) for two days before being analysed. LIF plays a central role in maintaining pluripotency in mES cells (Boeuf *et al.*, 1997).

4.2.1 Viable cell concentration

The viable cell concentration of mES cell samples taken after centrifugation and compared with a non-centrifuged control is shown in Figure 4.1 (NB: Fig 4.1 reports total viable cell concentration alongside GFP expression data. Viable cell concentration data is discussed in this section and GFP expression data is discussed in Section 4.2.2). The data indicates a reduction in viable cell concentration as centrifugal force is increased beyond 500 g. The viable cell concentration for the non-centrifuged control was measured at 13.5×10^4 viable cells cm^{-2}. No significant difference ($p = 0.499$) in viable cell concentration was observed between cells

measured for the control and after exposure to 500 g of centrifugal force and cell re-suspension (12.9×10^4 viable cells cm^{-2}). A decrease in viable cell concentration was observed as centrifugal force was increased beyond 500 g. When compared to the control sample (two-tailed Student's t test, 10% confidence level), mES cells exposed to 1,000, 2,000 and 3,000 g of centrifugal force recorded a 16% ($p = 0.012$), 17% ($p = 0.072$) and 27% ($p = 0.003$) decrease in viable cell concentration respectively.

The viable cell concentration analysis suggests that proliferation would be inhibited when attempting to culture mES cells exposed to centrifugal forces 1,000 g or greater.

4.2.2 *Oct4*-GFP expression

The transcription factor Oct4 is inextricably linked to the fate of a cell, and *Oct4* gene expression is required to maintain stem cell pluripotency and sustain self-renewal (Niwa *et al.*, 2000). As a result, *Oct4* expression is widely used by investigators as a defining endogenous marker of stem cell pluripotency. The *Oct4*-GFP mES cell line used in this study expresses green fluorescent protein (GFP) under the regulatory control of the *Oct4* gene. As a consequence, GFP expression may be used as a direct measure of stem cell pluripotency. Cells not expressing GFP are classified as differentiated mES cells. The impact of centrifugation on mES pluripotency was determined by evaluating the abundance of GFP in the viable cells of each treated sample and comparing it to an equivalent non-centrifuged control (Fig 4.1). Three sub-populations of viable cells were identified as: GFP$^-$, high (i.e. normal) GFP$^+$ and low (i.e. significantly reduced) GFP$^+$ expression.

The percentage population of spontaneously differentiated background cells (i.e. GFP$^-$ cells) was similar in the control sample and all centrifuged samples, averaging $\sim 6\%$. This value is in agreement with the $<8\%$ of spontaneously differentiated background cells observed in undifferentiated expansion culture of mES cells (Veraitch *et al.*, 2008). Because the percentage population of GFP$^-$ cells remains consistent

as centrifugal force is progressively increased, GFP^- results suggest that centrifugal force has no impact on the remaining GFP^+ pluripotent mES cells.

However, on closer inspection of GFP^+ cells, changes in high and low GFP^+ cell populations were recorded. The analysis of shifts in high and low GFP^+ expression is described in Section 2.2.3. mES cell population shifts from high GFP^+ to low GFP^+ cells indicates a loss of pluripotency in mES cells, i.e. cells are differentiating. The GFP^+ expression data in Figure 4.1 indicates that mES cells progressively lose pluripotency up to 2,000 g of centrifugal force exposure. These shifts are thought to be caused by the physical stresses associated with the centrifugal force and subsequent resuspension of the collected cell pellet. Physical stresses and cell stress responses have been reported to induce differentiation in ES cells (Lin *et al.*, 2005; Maimets *et al.*, 2008; Shimizu *et al.*, 2008; Yamamoto *et al.*, 2005). When exposed to 3,000 g, mES cell pluripotency does not seem to be affected; it is hypothesised that at this exposure level, the hydrodynamic shear damage to the cells associated with pellet resuspension dominates over stressed induced differentiation and selects against less pluripotent cells, resulting in a high proportion of high GFP^+ cells after two days of culture. The percentage yield of high GFP^+ in the 3,000 g sample (53%) was not significantly different from the percentage yield of high GFP^+ in the control sample (48%). The percentage yield of GFP (Y_{GFP}) expressing cells is given in Equation (2.1).

The shifts in yield of high GFP^+ expression suggests that mES cell pluripotency can be influenced centrifugation.

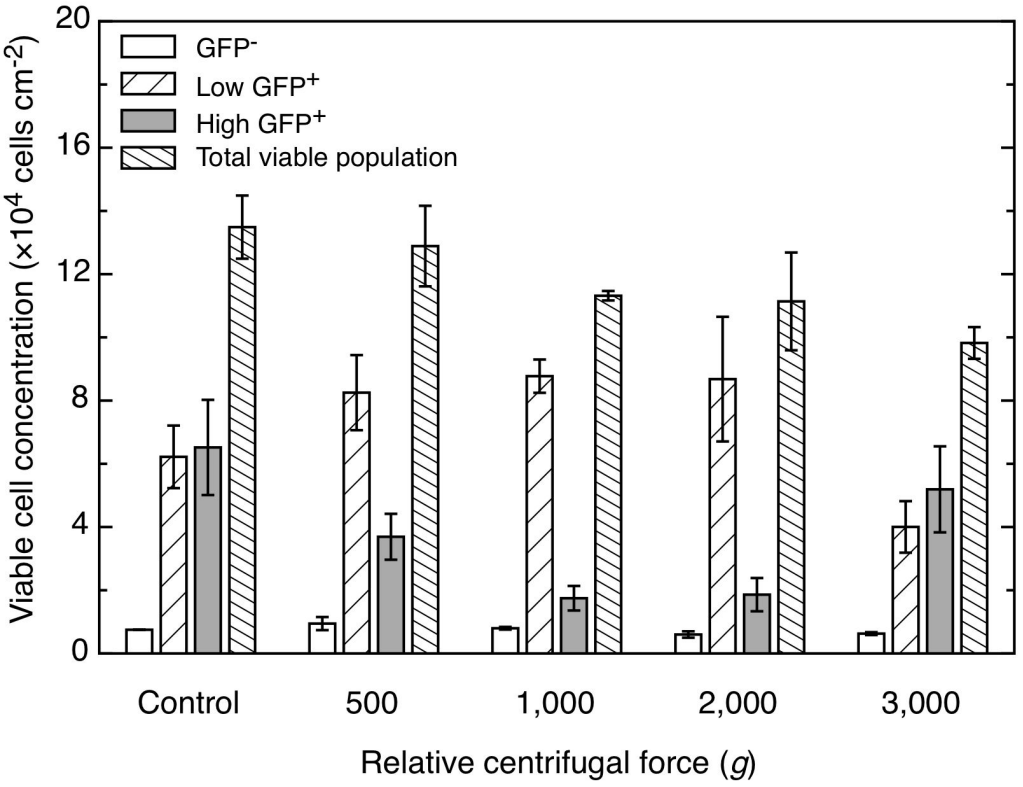

Figure 4.1: Effect of centrifugal force on mES cells during undifferentiated expansion. Cells were exposed to a range of centrifugal forces for 3 minutes at 21°C the resuspended cells were subsequently expanded in culture. Cell concentration and *Oct4*-GFP expression was determined after two days of culture in complete media. Results are mean ± 2SE for 3 independent wells for each centrifugation condition studied.

4.2.3 Gene expression analysis of mES cell pluripotency

Oct4, *Nanog*, *Rex1* and *Utf1* are genes expressed in undifferentiated mES cells and therefore are used as markers of pluripotency (Ben-Shushan *et al.*, 1998; Mitsui *et al.*, 2003; Niwa *et al.*, 2000; Okuda *et al.*, 1998; Yates & Chambers, 2005). To determine if varying levels of centrifugal force applied during centrifugation affected the pluripotency of mES cells, gene expression for *Oct4*, *Nanog* and *Rex1* was analysed using RT-PCR (Fig. 4.2). Neither *Oct4* nor *Nanog* nor *Rex1* expression were affected by the different centrifugal force exposures as their expression levels were similar to the control sample. The results indicate that mES cells were not affected by centrifugation and were able to maintain their pluripotentcy. Gene expression for *Oct4*, *Nanog* and *Utf1* gene expression was subsequently quantified using qPCR.

Figure 4.3 shows the relative change in gene expression levels of *Oct4*, *Nanog* and *Utf1* of mES cells exposed to 500, 1,000, 2,000 and 3,000 g of centrifugal force relative to the non-centrifuged control sample. No significant changes in the levels of *Oct4* and *Nanog* expression were detected between control and centrifuged samples. Similarly, differences in expression levels of *Utf1* in centrifuged samples were not significant when compared to the control except for the sample exposed to centrifugation at 500 g (0.4 fold change; $p = 0.034$).

Although *Utf1* is used as a marker for pluripotency, its exact role within the regulatory network that controls self-renewal and differentiation in ES cells is unclear. So far, Utf1 has been identified to be a stable chromatin-associated protein involved in the initiation of differentiation, and has been implicated in maintaining a specific epigenetic profile in ES cells (van den Boom *et al.*, 2007). It has also been reported to participate in cell proliferation by promoting cell cycle progression in early embryos (Nishimoto *et al.*, 2005). A possible explanation in the variation in expression of *Utf1* observed at 500 g may lie in its regulation. As *Utf1* is transcriptionally activated by the synergistic action of Oct4 and Sox2 (Nishimoto *et al.*, 1999), it is thought that the tight regulation of *Utf1* makes it highly sensitive to the

minute changes in levels of Oct4 and Sox2 present. Also, we have in the research group unpublished data to suggest that large variations in *Utf1* expression levels across mES clones from the same cell line with similar *Oct4* expression levels is possible. Further examination into the use of Utf1 as a definitive marker for stem cell pluripotency is required to confirm the variation observed in Figure 4.3 C.

The gene expression analysis of *Oct4*, *Nanog* and *Rex1* suggests that centrifugation does no affect mES cell pluripotency.

The discrepancy between the findings drawn from the *Oct4*-GFP analysis and pluripotency marker analysis is connected with the resolution of the assay used. *Oct4*-GFP analysis resolves pluripotency at the protein level whereas qPCR resolves pluripotecy at the gene expression level and results from either assay technique are valid. Protein translation and folding rates are presumed not to be a limiting factor in the analysis as they are in the order of seconds to minutes and milliseconds respectively. Crucial to studying the impact of centrifugation is the ability to detect subtle changes in pluripotency with respect to changes in centrifugation. Analysis of Oct4 at the protein level based on relative GFP fluorescence using flow cytometry occurs on a per cell basis and allows for a population of mES cells to be distinguished between low or high levels of Oct4. In contrast, Oct4 analysis at the transcription level is unable to afford this distinction as cells are assayed as an entire population. This example illustrates the importance of an understanding of the system and selecting an appropriate analytical method to quantify it. Alternatively, the effects of centrifugation on mES cell pluripotency can be evaluated by making chimeras. (Chimeras are produced from mixing cells from two different organisms, in this case centrifuged mES cells can be injected into blastocysts and implanted into a host and allowed to develop). While chimera formation is laborious and beyond the scope of this thesis, it is possible that the variations seen in pluripotency of centrifuged mES cells are of no consequence *in vivo*, as other yet to be identified extrinsic biological factors will come into play.

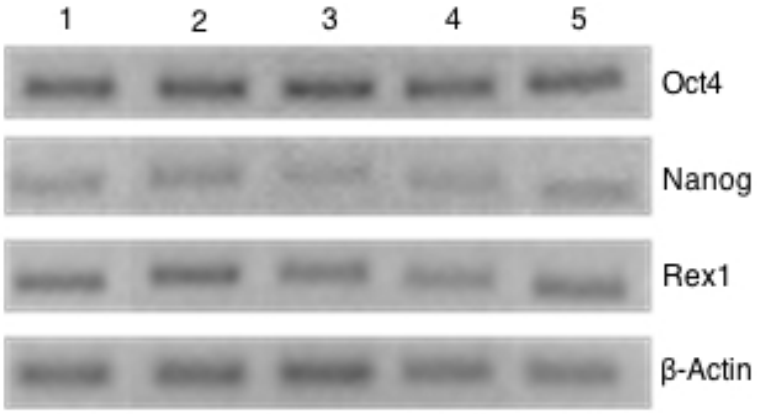

Figure 4.2: RT-PCR analysis of mES cells exposed to different levels of centrifugal force. Following centrifugation, cells were allowed to proliferate in culture for two days before being analysed for the presence of the pluripotent markers *Oct4*, *Nanog* and *Rex1*; with *β-actin* as the internal control. All samples were positive for the pluripotent markers. Lanes 1, 2, 3 4 and 5 correspond to the control sample and samples centrifuged at 500, 1,000, 2,000 and 3,000 g.

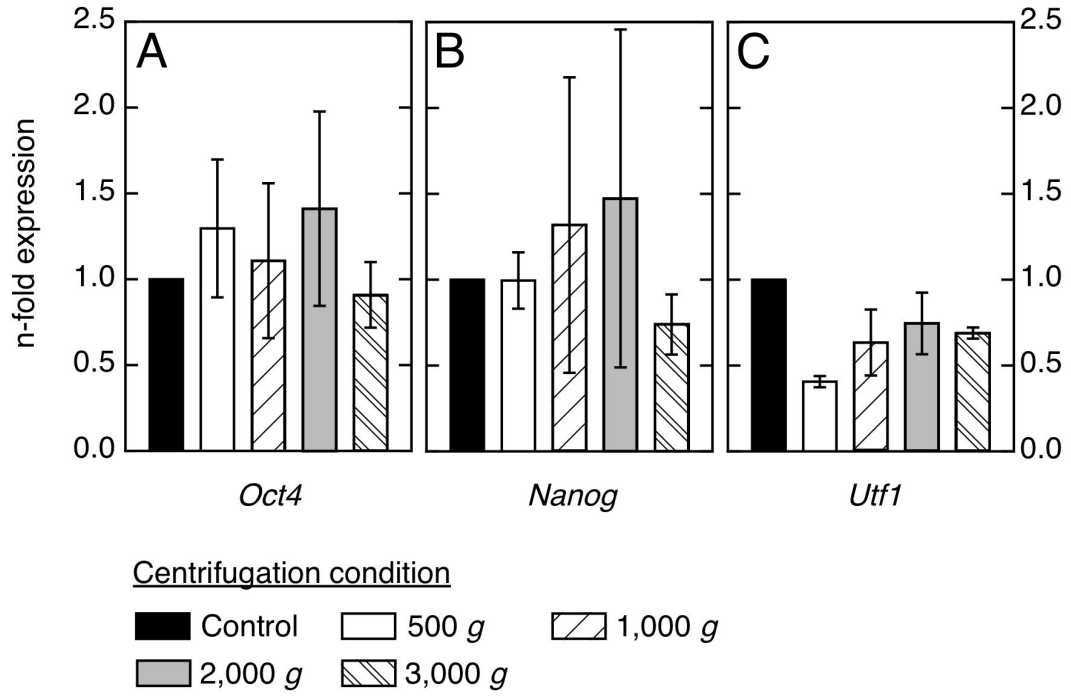

Figure 4.3: Gene expression analysis of mES cells exposed to different levels of centrifugal force. Following centrifugation and resuspension, cells were allowed to proliferate for two days and transcription levels of pluripotency markers *Oct4* (Panel A), *Nanog* (Panel B) and *Utf1* (Panel C) were determined using qPCR. Expression levels were standardised to *β-actin* and normalised to the uncentrifuged control sample. Results are mean ± SE of two independent samples analysed in triplicate.

4.3 Embryoid body expansion and differentiation

In this section, mES cells were examined for their ability to form and propagate as EBs (3-D spherical cell aggregates), and their ability to retain pluripotent differentiation capacity after being exposed to centrifugal force. After exposure to different levels of centrifugal force and subsequent resuspension, mES cells were plated onto non-tissue culture treated petri dishes. Plated cells were allowed to form EBs under static suspension culture conditions in LIF-free complete medium and propagated over 8 days. Culture medium exchange was performed every two days, during which EB samples were collected. Collected EBs were trypsinised and assayed for cell number, cell viability and used for quantitative PCR analysis.

4.3.1 Growth characteristics

Cell growth curves for mES cells exposed to each centrifugation condition (including the non-centrifuge control) was established by plotting cell viability and viable cell density against time (Fig. 4.4, Panels A & B respectively). Viable cell density data for each centrifugation condition was normalised to a starting cell density of 5×10^5 viable cells mL^{-1} to provide a means of comparing cell growth characteristics over the course of the experiment.

Analysis of the non-centrifuged control culture (0 g) revealed that mES cells were capable of being maintained in static culture conditions for up to 8 days whilst maintaining a high overall cell viability ($> 80\%$). The non-centrifuged control culture exhibited a 3-phase growth pattern: (1) a cell death phase from days 0 to 2, where 68% of available viable cells on inoculation were lost by day 2. This decline in viable cell number is likely to be attributed to a combination of cell death brought on by the failure of the attachment dependent mES cells to spontaneously aggregate after inoculation (Koyanagi-Katsuta *et al.*, 2000), and cell loss during the gravity settling step of the media exchange procedure; (2) a growth phase from days 2 to

4, where the surviving viable cells (likely to be nascent EBs at this stage) grew to a high viable cell density on day 4 representing a 4.8 fold increase in viable cells from day 2; and (3) a maintenance phase from days 4 to 8 as indicated by the high % cell viability throughout; and where viable cell numbers dipped slightly and remained constant.

The growth characteristics of cultures inoculated from mES cells exposed to different levels of centrifugal force (500, 1,000, 2,000 and 3,000 g) revealed a similar cell death phase (days 0 to 2) and growth phase (days 2 to 4) pattern to the non-centrifuged control culture. On closer inspection of the viable cell data we note that more cells were lost in the cell death phase in centrifuged cultures when compared to the non-centrifuged control. The remaining cells in centrifuged cultures at the end of the growth phase recovered to viable cell densities similar or greater than the non-centrifuged control. For all centrifuged cultures, cell loss during the death phase averaged 83% on inoculation and the gain in cells during the growth phase averaged 12.3 fold. Also, cell viabilites recorded over these two phases (on days 2 and 4) indicate a decreasing trend in cell viability as centrifugal force is is progressively increased at the end of the death phase, and a recovery to non-centrifuged control levels at the end of the exponential growth phase.

When viewed together, viable cell density and cell viability data give the impression that centrifuged cells are more prolific than the non-centrifuged control cells. The calculated normalised specific growth rates (μ) and normalised doubling times (t_d) of all centrifugation conditions examined also support this observation. From Table 4.1 which summarises these calculated values, non-centrifuge control cultures (0 g) recorded the lowest specific growth rate (0.033 ± 0.007 hour^{-1}) and the highest doubling time (21.2 ± 4.5 hours) in comparison to centrifuged cultures. Based on the differences observed in viable cell densities, specific growth rates and doubling times between centrifuged and non-centrifuged control cells, it would be reasonable to suggest that: (1) all starting cell samples comprise of a mixture of cells with vary-

ing proliferation capacities, and (2) on centrifugation and subsequent resuspension, the less prolific cells are eliminated thus giving rise to a population of more prolific cells that serve as the initial inoculum (See section 3.5 on page 88 for description of presumed cell loss action during cell pellet resuspension).

Viable cell densities recorded on days 6 and 8 for centrifuged cells are indicative of a second death phase, and is in contrast to the maintenance phase recorded for the non-centrifuge control culture over the same period. Unlike the first death phase observed in all centrifugation conditions, the second death phase is not due to an inability of the attachment dependent mES cells to aggregate because phase contrast images indicate the presence of EBs (Fig. 4.5). The discrepancy between culture phases of centrifuged cells and non-centrifuged control cultures over this period maybe explained in terms of nutrient and oxygen transport limitations within the EB. In particular, within EBs of the centrifuged mES cells that are composed of highly prolific cells. The high consumption rate associated with rapidly proliferating cells coupled with a nutrient and oxygen transport limitation may account for the second death phased observed in centrifuged cells. The influence of transport limitation on viable cell yield from EB cultures is verified in a study by Carpenedo *et al.* (2007). The study reports a reduction in apoptotic core and dead cell cluster formation within EBs cultured in continuous flow conditions when compared to static culture conditions.

Because of the scatter in the data, it is difficult to comment precisely at this juncture if progressively increasing exposure to centrifugal force and the associated resuspension procedure results in a corresponding increase in cell proliferation and viable cell loss. However, the evidence given from the cell viability recorded on day 2 seems to suggest so (see Appendix A for additional information) . The source of scatter is likely to be due to the inherent variability encountered during the sampling and assay of EBs. To refine the observations made on the date presented in Figure 4.4, additional studies involving a higher sampling frequency (2—3 samples day^{-1})

and independent replicate runs ($\geq$3) would be required.

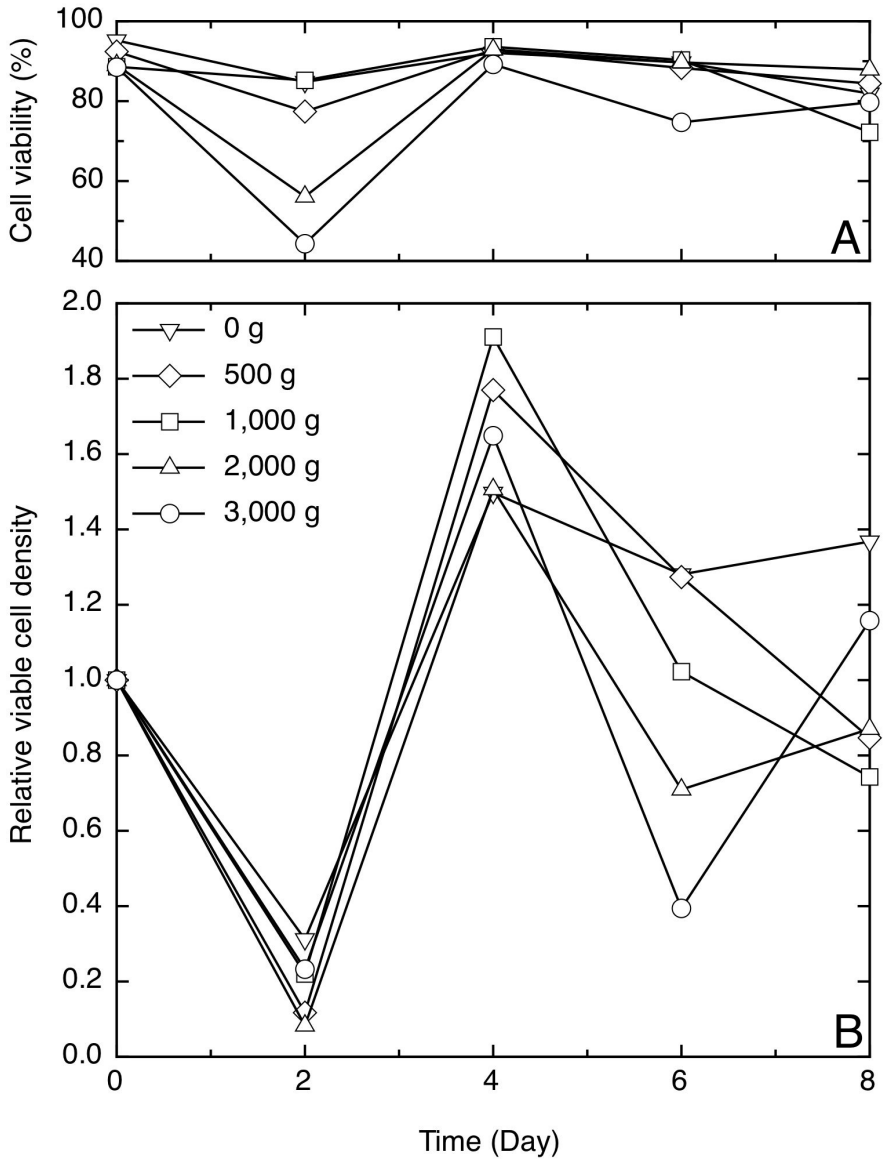

Figure 4.4: Growth curves of static EB culture inoculated with mES cells exposed to different levels of centrifugal force. Cell viability (Panel A) and viable cell density (Panel B) were determined over the course of 8 days with culture medium exchanged every two days. Viable cell densites for each centrifugation condition was normalised to a starting cell density of 5×10^5 viable cells mL^{-1}. Results are means of triplicate samples for a single experimental run. Error bars have been omitted for clarity.

Table 4.1: Normalised specific growth rates (μ) and doubling times (t_d) for static EB cultures inoculated with mES cells exposed to different levels of centrifugal force. μ and t_d were calculated using Equations (2.20) and (2.21) and data from the growth phase (days 2 to 4) of each batch culture. Results are means ± 2SE of triplicate samples from a single experimental run. *Arguably, it is not possible to accurately calculate specific growth rates and doubling times from two data points in a growth curve. However, the the calculated values presented in this table given an indication as to how the EB cultures are performing and the values are comparable to literature values Cormier* et al. *(2006).*

Condition	Specific growth rate (hour^{-1})	Doubling time (hour)
0 g	0.033 ± 0.007	21.2 ± 4.5
500 g	0.057 ± 0.007	12.3 ± 1.5
1,000 g	0.045 ± 0.015	15.4 ± 5.2
2,000 g	0.060 ± 0.032	11.5 ± 6.0
3,000 g	0.041 ± 0.008	17.0 ± 3.2

4.3.2 EB formation

To assess the effect of centrifugal force and subsequent resuspension on mES cells used for EB formation, mES cells exposed to different levels of centrifugal force together with a non-centrifuged control were observed using phase contrast microscopy (Fig. 4.5). Phase contrast images (4× magnification) were captured prior to culture medium exchange. EB diameter (Table 4.2) and EB concentration (Fig. 4.6) were determined from the phase contrast images using ImageJ image analysis software (v.138x). A minimum of 100 EBs were analysed per sample. The images captured on days 4 and 8 of all centrifugation conditions depict features characteristic of static suspension EB culture. EBs appear to have a wide range of sizes, and are either irregular or roughly circular in shape. These characteristics stem from the variation in the number of cells incorporated into each EB during cell aggregation (Kurosawa, 2007). Based on the phase contrast images EBs formed appear to be non-cyctic in morphology due to the dark/opaque centers, however, this can only be confirmed though histological examination of EB samples.

By day 4 (Fig. 4.5 A–E), centrifuged and non-centrifuged control mES cells formed medium sized EBs, averaging 151 μm in diameter. A higher proportion of smaller EBs were apparent in the culture centrifuged at 2,000 g (Fig. 4.5D) when compared to the non-centrifuged control and centrifuged cultures at 500, 1,000 and 3,000 g. This higher proportion of smaller EBs within the culture accounts for the significantly ($p = 0.041$) smaller average EB diameter (141 μm; Table 4.2), and an $\sim$2 fold higher EB concentration (Fig. 4.6) when compared to the non-centrifuged control. A combination of slow spontaneous EB aggregation and poor EB handling resulting in fragmentation during the previous medium exchange is presumed to be the cause of the higher proportion of smaller EBs visible in the 2,000 g culture.

By day 8 (Fig. 4.5 F–J), EBs from centrifuged and non-centrifuged control cultures grew to an average diameter of 190 μm, representing an average gain of 39 $\pm$ 9 μm on day 4 EB diameters for all centrifugation conditions investigated. The

gain in EB diameter can be attributed to both cell growth and EB agglomeration. The EB diameters of EBs formed from mES cells exposed to centrifugation were not significantly different from the non-centrifuge control (Table 4.2). However, an ∼2 fold greater concentration of EBs in the culture centrifuged at 500 g was visible when compared to the non-centrifuge control (Fig. 4.6); a similar explanation to above is used account for the high EB cell concentration observed. Phase contrast images of this centrifugation condition (Fig. 4.5G) suggest that the proportion of smaller EBs present are low; and as a consequence of a low incidence of smaller EBs, the calculated overall average EB diameter is not significantly altered. For all intents and purposes, despite the higher proportions of EBs observed in Fig. 4.5 D & G, they about the same as their respective control.

The image analysis indicates that mES cells exposed to centrifugal forces up to 3,000 g are capable of forming EBs without affecting the average EB diameter.

While the term embryoid body (EB) has been used to describe ES cell assemblies, it should not be confused from the term ES cell aggregates that is sometimes found in literature. In general, EBs are assembled from ES cells that are allowed to spontaneously aggregate and spontaneously differentiate under non-differentiating medium conditions (e.g. mES EB formation using LIF free culture medium). This spontaneous differentiation is driven by the cell-to-cell interactions within the EB that recapitulates the early developmental changes observed in embryogenesis. As a result of theses interactions, ES cells within the EB begin to differentiate and give rise to progenitor cells that make up the three primary germ layers. In contrast, ES cell aggregates are ES cell assemblies that consist of progenitor cells committed towards a particular cell lineage. The lineage committed progenitor cells are formed via directed differentiation of ES cells (or EBs), and is typically achieved by adding specific growth factors to the culture medium that induce cells to differentiate along a particular pathway (Dontu *et al.*, 2003; Okada *et al.*, 2004; Youn *et al.*, 2005).

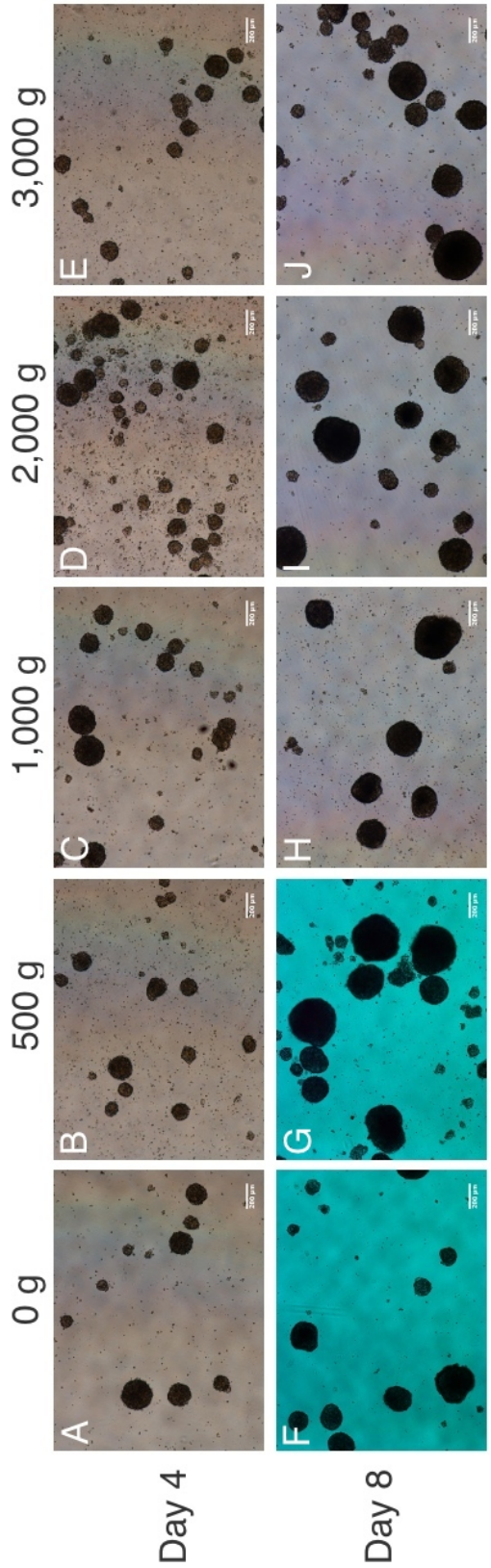

Figure 4.5: Phase contrast images (4× magnification) of static suspension EB cultures inoculated with mES cells expose to different levels of centrifugal force. EB morphology at day 4 (Panels A–E) and day 8 (Panels F–J) are depicted. A higher proportion of smaller EBs are observed in Panels D and F when compared to their respective uncentrifuged controls. Scale bar: 200 μm.

Table 4.2: Average EB size after 4 and 8 days of static culture. mES cells used to form embryoid bodies were exposed to a range of centrifugal forces. EB diameters were measured using ImageJ image analysis software (v1.38x). Average EB diameters of centrifuged cultures were compared to the non-centrifuge control culture (0 g). Results reported are mean ± 2SE determined from a minimum of 100 EBs.

	Day 4		Day 8	
Condition	Diameter (μm)	p-value	Diameter (μm)	p-value
0 g	155 ± 10	–	194 ± 23	–
500 g	160 ± 16	0.608	202 ± 21	0.647
1,000 g	148 ± 11	0.365	169 ± 19	0.098
2,000 g	141 ± 8	0.041	188 ± 21	0.705
3,000 g	151 ± 11	0.628	194 ± 23	0.964

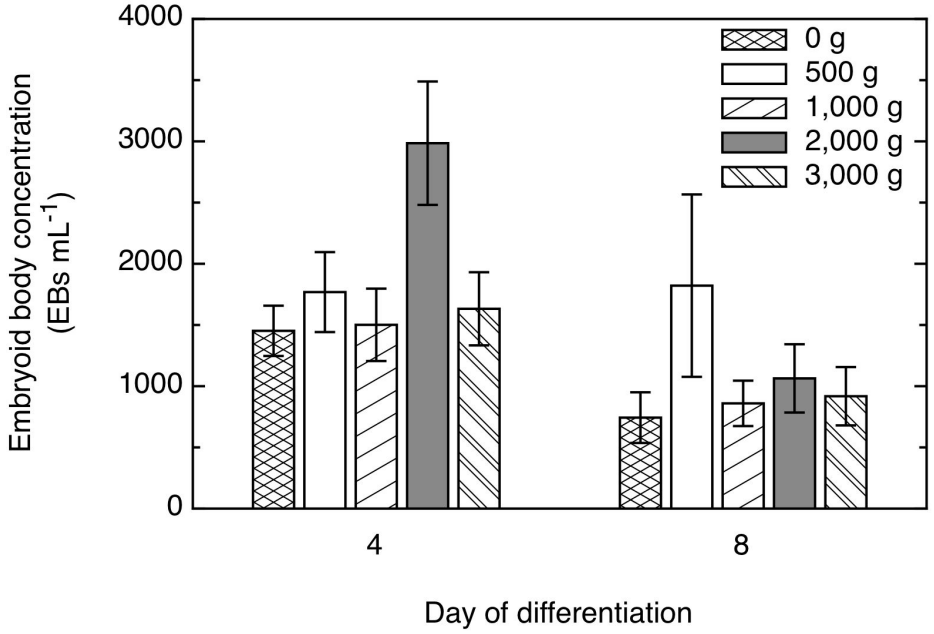

Figure 4.6: EB concentrations determined after 4 and 8 days of static culture. mES cells used to form EBs were exposed to a range of centrifugal force. Results reported are mean ± 2SE.

4.3.3 EB gene expression analysis

To demonstrate that EBs formed from mES cells exposed to centrifugation were capable of differentiation, their differentiation status was evaluated after 8 days of static suspension EB culture. The pluripotent differentiation capacity of EBs are typically assessed on their ability to give rise to cells that make up the three primary germ layers, namely the endoderm, mesoderm and ectoderm layers. Endoderm cells form the outer layer of the EB which surrounds a central core composed of mesoderm and ectoderm cells. Gene expression of the germ layer markers SRY-box containing gene 17 (*Sox17*), Brachyury (*T*) and β3-tubulin (*Tubb3*) were assessed quantitatively using PCR (Fig. 4.7), and are early developmental markers of endoderm, mesoderm and neuroectoderm respectively (Nakanishi *et al.*, 2007). Sox17 is a transcription factor that participates in extraembryonic endoderm specification (Shimoda *et al.*, 2007), *T* expression occurs during early stage mesoderm development (Wilkinson *et al.*, 1990), and βIII-tubulin is a neuron specific microtuble isoform that is synthesised in postmitotic neuroblasts (Lee *et al.*, 1990).

Sox17, *T* and *βIII-tubulin* were expressed in all centrifuged and non-centrifuged control cultures thereby confirming in all cases the development of the three primary germ layers that typify EB differentiation *in vitro*. This result was anticipated as it is generally assumed that EBs are capable of recapitulating the early developmental changes in embryogenesis where the markers for endoderm, mesoderm and ectoderm layers are invariably expressed (Choi *et al.*, 2005; Doetschman *et al.*, 1985). Higher levels of *Sox17* were detected in EBs formed from mES cells exposed to 2,000 and 3,000 g when compared to EBs formed from cells exposed to 500 and 1,000 g, and the non-centrifuged control. *T* expression was elevated in EBs formed from mES cells exposed to 3,000 g, and all other conditions showed insignificantly higher expression levels when compared to the non-centrifuged control. *Tubb3* expression levels were similar under all centrifugation conditions to the non-centrifuge control. The increased expression of endoderm and mesoderm expression at higher levels of

centrifugation suggest that differentiation is induced sooner. Because the enveloping endoderm provides the cell signals required for differentiation (Maye *et al.*, 2000), it is possible that the elevated levels of *T* expression is a consequence of the high levels of *Sox17*. Signals from the endoderm are also responsible for creating cavities within EBs, i.e. formation of cystic EBs by inducing apoptosis of cells at the core (Coucouvanis & Martin, 1995), thus also possibly contributing to the second cell death phase observed in centrifuged EB cultures (Fig. 4.4). The comparable expression of *Tubb3* at all centrifugation conditions examined indicates that centrifugation did not inhibit or delay differentiation into the neuroectoderm.

The gene expression analysis shows that in general, mES cells exposed to various centrifugal forces prior to EB culture do not lose their pluripotent potential to differentiate. Although the data suggests that higher levels of centrifugal force and the subsequent effects of resuspension of the cells used to prepare the EBs induce early differentiation of endoderm and mesoderm, further studies are required to verify these results. There is a possibility that early induction of differentiation is related to the selection of more prolific cells by the centrifugation procedure. These additional studies maybe conducted in a monolayer differentiation culture system to reduce the complex 3D cell-to-cell interaction and signaling environment associated with an EB and better study the effects of centrifugation. A monolayer culture system also allows for better culture synchronisation and makes cells more amendable to manipulation with factors (West *et al.*, 2006).

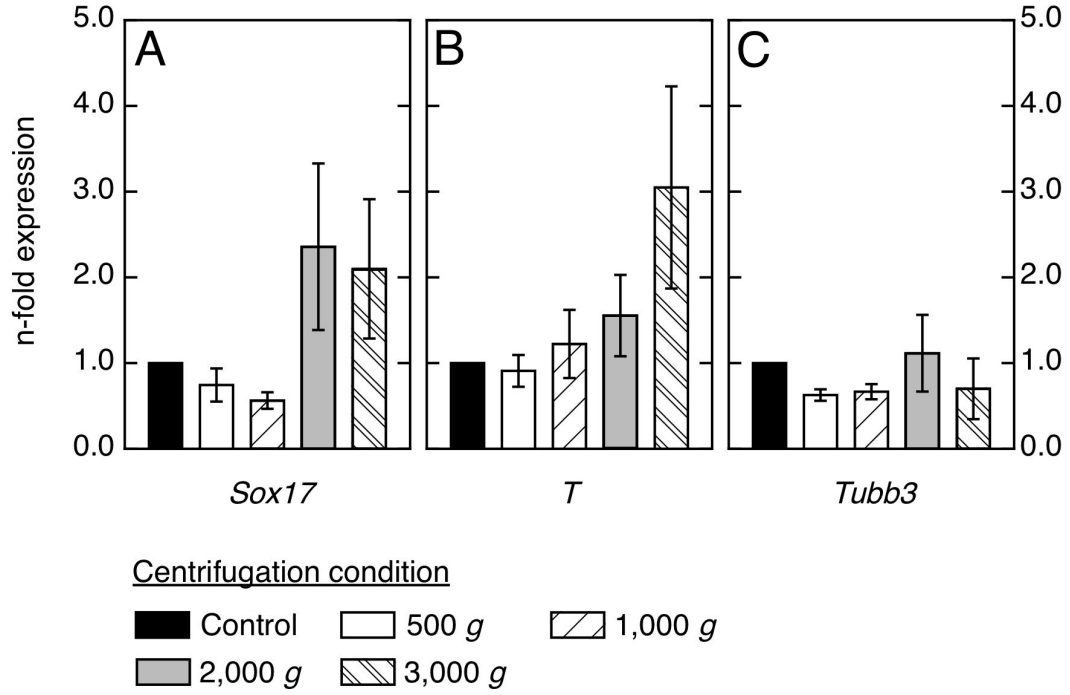

Figure 4.7: Gene expression analysis of static EB cultures inoculated with mES cell exposed to different levels of centrifugal force. After 8 days of static culture, transcript levels of germ layer markers *Sox17* (Panel A), *T* (Panel B) and *Tubb3* (Panel C) were determined using qPCR. Expression levels were standardised to *β-actin* and normalised to the control sample. Results are mean ± SE of two independent samples analysed in triplicate

4.4 Discussion

It is generally acknowledged that pluripotent ES cells in culture are an artifact of their *in vitro* conditions because these cells rapidly differentiate *in situ* during embryo development (Avery *et al.*, 2006). Like a double edged sword, the plasticity in the biological properties of ES cells which allows them to differentiate, makes them susceptible to external bio-physical and biochemical cues. Typical ES cell expansion and differentiation culture protocols necessitate the use of centrifugation to effect cell separation from its suspending bulk medium for routine sub-culture (cell expansion) or subsequent use downstream (cell differentiation). The results presented in this chapter highlight the sensitivity of mES cells to centrifugation. In doing so, hopes to identify critical parameters which may become helpful in designing effective strategies to maintain or exploit ES cell properties, and maximise overall bioprocess productivity.

From the point of using centrifugation for collecting cells for routine sub-culture or subsequent downstream use, the results show that the proliferation of undifferentiated and differentiated mES cell populations can be affected by centrifugation. In addition, exposing mES cells to centrifugation also affects its pluripotency and differentiation status. Clearly gaining high yields of mES cells of the desired phenotype (i.e. undifferentiated or differentiated cells) is linked to centrifugation. Control over centrifugation conditions has to be exerted to ensure reproducibility and stability of cultures over multiple sub-cultures or extended periods of culture. The results strongly suggest that restricting exposure to no more than low levels of centrifugal force is necessary to safeguard the stability of the desired biological characteristics of mES cells during sub-culture. Excessive centrifugation is detrimental to the culture of mES cells.

From the point of using centrifugation to exploit mES cell properties, the results suggest that by judiciously selecting an appropriate centrifugation speed, mES cells can be persuaded towards a desired outcome. The outcome though, maybe a

compromise of overall bioprocess productivity and is probably the more important operating parameter. Two examples are given here: (1) in the undifferentiated mES cell expansion study, cells exposed to 3,000 g of centrifugal force exhibited a 27% decrease in viable cell concentration when compared to the non-centrifuged control. At the same time no change in pluripotency was exhibited. In a scenario where large volumes of mES cells have to be processed, operating the centrifuge at 3,000 g reduces the time required to achieve a desired level of clarification for an equivalent volume of cells to be processed when compared to lower levels of centrifugal force. It is possible that while still maintaining a high level of pluripotency, the savings in centrifugation time outweighs the diminished cell proliferation. Furthermore, the savings in processing time also decreases the exposure of the sensitive mES cells to the surrounding ambient conditions that can cause culture variations (e.g. growth rates, phenotype) (Veraitch *et al.*, 2008); and (2) in the EB expansion and differentiation study, increasing levels of centrifugal force promoted cell proliferation and a possibility of early induction of endoderm and mesoderm differentiation. Where high levels of viable cells are desired to maximise overall bioprocess yield, high cell proliferation rates are beneficial. However, the benefits of an increased proliferation rate within an EB is curtailed by a probable nutrient transport limitation resulting in reduced viable cell numbers when compared to the non-centrifuged control. Thus in order to maximise overall cell numbers a compromise between centrifugal force and cell proliferation rates has to be established. Alternatively, highly prolific EBs may be cultured in continuous flow conditions to improve nutrient and gas diffusion that promotes cell viability (Carpenedo *et al.*, 2007). Where endoderm and mesoderm cells are desired, high centrifugal forces are advantageous. The use of the bioprocessing environment to direct ES cell differentiation is not new and has been described by Yamamoto *et al.* (2005) and Shimizu *et al.* (2008); however these efforts have only been confined to culture conditions only.

Undoubtedly, the combined effects of centrifugation and resuspension are able

to influence yield and the desired biological characteristics of mES cells. The shear environment generated during resuspension works on two levels to influence mES cell attributes: (1) it first eliminates cells (e.g. cell damage resulting in loss in cells or viability) that are susceptible to the shear environment, and (2) it provides the physical stress cues for the remaining cells to be transduced. Because exposure to centrifugal force has been shown not to eliminate cells (Fig. 3.6), its influence on mES cell attributes is assumed to be exclusively mechanical, i.e. it provides physical stress cues only (The effects of oxygen concentration has been omitted from this consideration). Although little is known about the specifics of how varying levels of physical stress are able to modify mES cell pluripotency and differentiation, it appears that cell cytoskeleton plays a crucial role in the signal transduction of these mechanical forces (Ingber, 1997; Sadoshima & Izumo, 1997). Additionally, cell stress responses to the shear environment have to be considered (Lin *et al.*, 2005; Maimets *et al.*, 2008). Concerning the shear environment and bioprocessing, they are inextricably linked and together represent major challenges in developing robust and scalable processes for cell based regenerative medicines (Zoro *et al.*, 2008).

In hindsight, the EB expansion and differentiation study was probably limited by the chosen experimental method employed. Because of the relatively low culture volumes involved ($\sim$ 12 mL), it is highly likely that cell and fluid losses were introduced during the medium exchange procedure over the course of the experiment. In particular, as EBs were allowed to gravity settle out of the spent medium before being replaced, it is likely that nascent EBs would have been discarded together with the spent medium (Fig. 4.4, day 2 cell counts: cell loss observed could be due to a combination of cells spontaneously aggregating to form EBs and nascent EBs that are unable to settle out of the spent medium). In addition to medium exchange losses, cell sampling losses due to the extensive handling of the EBs samples required for cell enumeration have to be taken into account. Despite these shortcomings, it would not be unreasonable to assume that the errors associated

with cell and fluid losses were systemic errors that were propagated evenly across all centrifuge conditions investigated. Owing to the fact that systemic errors and cell loss were incurred, the reliability of the results reported (e.g. EB formation and gene expression analysis data) could possibly been affected.

Chapter 5

Conclusions and Research opportunities

5.1 Conclusions

Paramount to the successful manufacture of any cell based regenerative medicine on an industrial scale is a fundamental understanding of the bioprocessing environment and its impact on cells. Where ES cells are to be utilised as a renewable source for cell therapy, this understanding has to be extended not only to preventing cell loss, but also its impact on ES cell expansion and differentiation. It is envisaged that centrifugation will play a central role in the primary recovery of ES cells in whole cell bioprocessing as centrifuges are generally easy to operate and scale. It is recognised that the scale of ES cell bioprocesses is determined by the useful amount of therapeutic material required for therapy and may fall into the following two scale categories: (1) 10s of milliliters to liters; and (2) 10s to 100s of liters. The two ES scale of operations mirror closely the scale of operations encountered in autologous or allogenic whole cell bioprocessing.

The research in this thesis aims to highlight crucial areas in ES cell bioprocessing ahead of the industrial need as determined by market demands. A mES cell line was selected as a mimic for ES cell types that will be used in cell based regenerative medicines; the work accomplished centers about using milliliter volumes of mES cell suspensions to demonstrate techniques useful in the characterisation and analysis of centrifuge performance, and to study the bioprocessing impact of centrifugation on mES cells. The results from this study hope to serve as a starting point for investigators who are seeking identify critical centrifugation process variables to design cell recovery stratagems for both terminally differentiated and hES cells at various processing scales. At a more strategic level, the work undertaken within this thesis serves to create and establish an awareness of the bioprocessing challenges faced within this emerging area of science.

The results indicate that centrifugal force, centrifugation time and process temperature affects the population of mES cells as recovered after pellet resuspension. Cell damage during centrifugation resulting in loss of cells or cell viability is probably

not caused directly by direct exposure to centrifugal force, but by the environment generated during cell pellet resuspension. With the level of cell damage incurred being determined by centrifugal force, centrifugation time and process temperature. To minimise cell damage whilst optimising centrifuge performance, a Window of Operation for centrifugal cell recovery of mES cells was generated by predicting clarification and cell damage with regards to centrifugation conditions and process temperature. The resultant Window of Operation points to a requirement to minimise the exposure of cells to harsh centrifugation conditions (e.g. high centrifugal force, centrifugation time and process temperature) to limit cell damage. It is useful to highlight at this juncture a common minimum centrifugal force and centrifugation time that minimises cell damage at 4, 21 and 37^{o}C process temperatures; for a $> 99\%$ recovery of cells and a $< 1\%$ change in cell viablilty, the centrifuge can be operated at 5–9 mins $\times$ 300–500 g. These centrifugation condtions are similar to standard laboratory practices used for the recovery of animal cells.

In addition to cell damage, the combined effects of centrifugal force and mechanical stresses stemming from the shear environment generated during the resuspension procedure seems to affect the biological characteristics of mES cells during expansion and differentiation. The results strongly suggest that restricting exposure to no more than low levels of centrifugal force is necessary to safeguard the stability of desired plastic mES cell characteristics. During mES cell expansion, cell proliferation and cell pluripotency were influenced by increasing levels of centrifugal force as indicated by viable cell numbers and *Oct4*-GFP expression respectively. During mES cell differentiation, the growth characteristics and differentiation status of EBs appear to be altered as centrifugal force is progressively increased. Exposure of cells to increasing levels of centrifugal force did not appear to affect the cell's ability to form EBs in static suspension culture.

5.2 Research opportunities

The list of exciting research opportunities involving the use of ES cells is vast and diverse. Currently, the bulk of research in this area relates to the elucidation and understanding of ES cell biology and is beyond the intent of this thesis. The research opportunities highlighted below are restricted to the arena of bioprocessing:

- Cell damage with respect to process temperature. From the rule based interpretation of Fig. 3.4, the data suggests that processing cells at 21°C results in lower cell losses when compared to processing at higher (37°C) or lower (4°C) temperatures. It was hypothesised that a balance between homeostatic activity, membrane fluidity and cell membrane tension is struck in order to minimise cell loss (see Section 3.5 on page 88). Studies examining this hypothesis would provide useful information to facilitate bioprocess design and bioprocess scheduling decisions. In particular, the use of low process temperatures as a stratagem in preserving cells over extended periods (Hunt *et al.*, 2005). The study may also be further extended to examining the effects of rewarming injury to cells (Healy *et al.*, 2006; Rauen *et al.*, 2000).

- Scalability. Where biological material under investigation is precious and not available in large quantities , data generated at the milliliter (or microliter) scale to predict manufacturing scale process performance is invaluable in terms of cost savings and then different bioprocess scenarios and variables that can be investigated. The research undertaken in this thesis centres about the use of milliliter volumes of mES cell suspension to generate quantitative centrifugation data in order to facilitate bioprocess design decisions. The research undertaken can be further extended to cover correlating and validating the milliliter scale data to predict full scale centrifuge performance. This is achieved by understanding the properties of the biological properties and how the dominant flow regime within the industrial scale centrifuge (batch or continuous) affects

these properties. See review by Titchener-Hooker *et al.* (2008) on microscale biochemical engineering analysis.

- Tangential flow filtration (TFF). Studies examining the performance of TFF for ES cell recovery and how the flow regime during TFF recovery (e.g. pressure, shear, pump damage etc) influence ES cell pluripotency and differentiation potential. The data could be compared against centrifugal recovery data as centrifugation and TFF are in competition, and maybe used to build a database or design heuristics that would facilitate the design and development of future whole ES cell bioprocess. The study may also be further extended by comparing the process cost-benefit gains associated with each unit operation when governed by a particular scale of operation.

- Validated holding steps built into any industrial bioprocess allows for process flexibility in case of contingencies. Lowering process temperatures to no lower than freezing is also another common stratagem in preserving cells over extended periods (Hunt *et al.*, 2005). Studies of the impact of time-temperature exposure to ES cells in holding steps prior to subsequent processing would provide useful information to facilitate bioprocess design decisions. Additionally, the effects of rewarming causing injury to cells may also need to be assessed (Healy *et al.*, 2006; Rauen *et al.*, 2000).

- Hydrodynamic forces encountered during bioprocessing are able to induce a variety of cell responses (Chisti, 2001) and are present from cell culture, to pumping and pipe transfer operations and primary recovery. Where the bioprocessing of ES cells are concerned, the microenvironment has been reported to affect pluripotency or differentiation (Saha *et al.*, 2005; Shimizu *et al.*, 2008; Yamamoto *et al.*, 2005) — these studies though only relate to culture conditions. Studies related to quantifying ES cell responses (i.e. cell loss, changes in pluripotency potential or differentiation status) when exposed to a specific

magnitude of force and flow regime when not in culture will aid in development of a bioprocessing equipment sector which is able to cater to the specialised demands of processing ES cells (Mason & Hoare, 2006).

- The epigenetic impact of bioprocessing on ES cells. Epigenetics relates to the process whereby a substance and/or environment changes gene expression without a change in DNA sequence. The features and factors that affect gene expression have been identified and include transcription factors, microRNAs, DNA methylation and histone mediated changes in chromatin structure (Bibikova *et al.*, 2008). Where ES cells are concerned, there is an increasing body of evidence for an epigenetic basis for pluripotency and differentiation potential (Atkinson & Armstrong, 2008; Collas *et al.*, 2008; Gan *et al.*, 2007). However, as the precise epigenetic mechanisms are currently not well understood, it is important to recognise and possibly identify the bioprocess engineering conditions that can significantly influence the epigenome and affect the safety and efficacy of cells used for therapy.

Appendix A

Additional data for EB growth characteristics

Extracted from the EB growth curve data (Fig. 4.4), the information presented in Table A.1 contains further supporting evidence that centrifugal force influence EB cell proliferation and cell loss.

Table A.1: Table summarising the percentage (%) drop in cell viability in EBs after 2 days of static suspension culture, and fold change in viable cells in EBs from day 2 to day 4 (increase), and day 4 to day 6 (decrease). EBs were formed from mES cells exposed to a range of centrifugal force.

		Fold change in viable cell from:	
Condition	% drop in cell viability	Day 2 to Day 4	Day 4 to Day 6
0 g	10.9	4.79	0.86
500 g	16.2	15.11	0.72
1,000 g	3.9	8.69	0.54
2,000 g	36.9	18.17	0.47
3,000 g	49.9	7.09	0.24

References

Adachi, T., Osako, Y., Tanaka, M., Hojo, M. & Hollister, S.J. (2006). Framework for optimal design of porous scaffold microstructure by computational simulation of bone regeneration. *Biomaterials*, **27**, 3964–72.

Aflatoonian, B. & Moore, H. (2006). Germ cells from mouse and human embryonic stem cells. *Reproduction*, **132**, 699–707.

Al-Rubeai, M. & Singh, R. (1998). Apoptosis in cell culture. *Curr Opin Biotechnol*.

Al-Rubeai, M., Singh, R., Goldman, M. & Emery, A. (1995). Death mechanisms of animal cells in conditions of intensive agitation. *Biotechnol Bioeng*, **45**, 463–472.

Ambler, C. (1961). Theory of centrifugation. *Industrial & Engineering Chemistry*, **53**, 430–433.

Améen, C., Strehl, R., Björquist, P., Lindahl, A., Hyllner, J. & Sartipy, P. (2008). Human embryonic stem cells: current technologies and emerging industrial applications. *Critical Reviews in Oncology/Hematology*, **65**, 54–80.

Amit, M., Carpenter, M.K., Inokuma, M.S., Chiu, C.P., Harris, C.P., Waknitz, M.A., Itskovitz-Eldor, J. & Thomson, J.A. (2000). Clonally derived human embryonic stem cell lines maintain pluripotency and proliferative potential for prolonged periods of culture. *Dev Biol*, **227**, 271–8.

Aoi, T., Yae, K., Nakagawa, M., Ichisaka, T., Okita, K., Takahashi, K., Chiba, T. & Yamanaka, S. (2008). Generation of pluripotent stem cells from adult mouse liver and stomach cells. *Science*, **321**, 699–702.

Atala, A. (2004). Tissue engineering and regenerative medicine: concepts for clinical application. *Rejuvenation Res*, **7**, 15–31.

Atala, A., Bauer, S.B., Soker, S., Yoo, J.J. & Retik, A.B. (2006). Tissue-engineered autologous bladders for patients needing cystoplasty. *Lancet*, **367**, 1241–6.

Atkinson, S. & Armstrong, L. (2008). Epigenetics in embryonic stem cells: Regulation of pluripotency and differentiation. *Cell Tissue Res*, **331**, 23–29.

Aumailley, M. & Gayraud, B. (1998). Structure and biological activity of the extracellular matrix. *J Mol Med*, **76**, 253–65.

Avery, S., Inniss, K. & Moore, H. (2006). The regulation of self-renewal in human embryonic stem cells. *Stem Cells Dev*, **15**, 729–40.

Bainbridge, J.W.B., Smith, A.J., Barker, S.S., Robbie, S., Henderson, R., Balaggan, K., Viswanathan, A., Holder, G.E., Stockman, A., Tyler, N., Petersen-Jones, S., Bhattacharya, S.S., Thrasher, A.J., Fitzke, F.W., Carter, B.J., Rubin, G.S., Moore, A.T. & Ali, R.R. (2008). Effect of gene therapy on visual function in Leber's congenital amaurosis. *N Engl J Med*, **358**, 2231–9.

Beattie, G.M., Lopez, A.D., Bucay, N., Hinton, A., Firpo, M.T., King, C.C. & Hayek, A. (2005). Activin a maintains pluripotency of human embryonic stem cells in the absence of feeder layers. *Stem Cells*, **23**, 489–495.

Belfort, G., Davis, R.H. & Zydney, A.L. (1994). The behaviour of suspensions and marcomolecular solutions in cross-flow microfiltration. *Journal of Membrane Science*, **96**, 1–58.

Ben-Shushan, E., Thompson, J.R., Gudas, L.J. & Bergman, Y. (1998). Rex-1, a gene encoding a transcription factor expressed in the early embryo, is regulated via Oct-3/4 and Oct-6 binding to an octamer site and a novel protein, Rox-1, binding to an adjacent site. *Mol Cell Biol*, **18**, 1866–78.

Bibikova, M., Laurent, L.C., Ren, B., Loring, J.F. & Fan, J.B. (2008). Unraveling epigenetic regulation in embryonic stem cells. *Cell Stem Cell*, **2**, 123–134.

Blayer, S., Woodley, J.M., Lilly, M.D. & Dawson, M.J. (1996). Characterization of the chemoenzymatic synthesis of N-Acetyl-D-neuraminic acid (Neu5Ac). *Biotechnol Prog*, **12**, 758–763.

Boeuf, H., Hauss, C., Graeve, F.D., Baran, N. & Kedinger, C. (1997). Leukemia inhibitory factor-dependent transcriptional activation in embryonic stem cells. *J Cell Biol*, **138**, 1207–1217.

Boneva, R.S. & Folks, T.M. (2004). Xenotransplantation and risks of zoonotic infections. *Annals of Medicine*, **36**, 504–17.

Born, C., Zhang, Z., Al-Rubeai, M. & Thomas, C. (1992). Estimation of disruption of animal cells by laminar shear stress. *Biotechnol Bioeng*, **40**, 1004–1010.

Boultonstone, J. & Blake, J.R. (1993). Gas-bubbles bursting at a free surface. *J Fluid Mech*, **254**, 437–466.

Boutilier, R.G. (2001). Mechanisms of cell survival in hypoxia and hypothermia. *J Exp Biol*, **204**, 3171–81.

Boychyn, M., Doyle, W., Bulmer, M., More, J. & Hoare, M. (2000). Laboratory scaledown of protein purification processes involving fractional precipitation and centrifugal recovery. *Biotechnol Bioeng*, **69**, 1–10.

Boychyn, M., Yim, S., Shamlou, P.A. & Bulmer, M. (2001). Characterization of flow intensity in continuous centrifuges for the development of laboratory mimics. *Chemical Engineering Science*, **56**, 4759–4770.

Boychyn, M., Yim, S.S.S., Bulmer, M., More, J., Bracewell, D.G. & Hoare, M. (2004). Performance prediction of industrial centrifuges using scaledown models. *Bioprocess and Biosystems Engineering*, **26**, 385–91.

Brittan, M. & Wright, N.A. (2002). Gastrointestinal stem cells. *J Pathol*, **197**, 492–509.

Brons, I.G.M., Smithers, L.E., Trotter, M.W.B., Rugg-Gunn, P., Sun, B., de Sousa Lopes, S.M.C., Howlett, S.K., Clarkson, A., Ahrlund-Richter, L., Pedersen, R.A. & Vallier, L. (2007). Derivation of pluripotent epiblast stem cells from mammalian embryos. *Nature*, **448**, 191–195.

Bruder, S.P., Jaiswal, N. & Haynesworth, S.E. (1997). Growth kinetics, self-renewal, and the osteogenic potential of purified human mesenchymal stem cells during extensive subcultivation and following cryopreservation. *J Cell Biochem*, **64**, 278–94.

Bursac, P., Fabry, B., Trepat, X., Lenormand, G., Butler, J.P., Wang, N., Fredberg, J.J. & An, S.S. (2007). Cytoskeleton dynamics: Fluctuations within the network. *Biochem Biophys Res Commun*, **355**, 324–30.

Carpenedo, R.L., Sargent, C.Y. & McDevitt, T.C. (2007). Rotary suspension culture enhances the efficiency, yield, and homogeneity of embryoid body differentiation. *Stem Cells*, **25**, 2224–34.

Casadevall, N., Nataf, J., Viron, B., Kolta, A., Kiladjian, J., Martin-Dupont, P., Michaud, P., Papo, T., Ugo, V., Teyssandier, I., Varet, B. & Mayeux, P. (2002). Pure red-cell aplasia and antierythropoietin antibodies in patients treated with recombinant erythropoietin. *New Engl J Med*, **346**, 469–475.

Chan, G., Booth, A.J., Mannweiler, K. & Hoare, M. (2006). Ultra scale-down studies of the effect of flow and impact conditions during E. coli cell processing. *Biotechnol Bioeng*, **95**, 671–683.

Cheema, S.K., Chen, E., Shea, L.D. & Mathur, A.B. (2007). Regulation and guidance of cell behavior for tissue regeneration via the siRNA mechanism. *Wound Repair Regen*, **15**, 286–295.

Chen, S., Zhang, Q., Wu, X., Schultz, P. & Ding, S. (2004). Dedifferentiation of lineage-committed cells by a small molecule. *J Am Chem Soc*, **126**, 410–411.

Chen, Y., He, Z.X., Liu, A., Wang, K., Mao, W.W., Chu, J.X., Lu, Y., Fang, Z.F., Shi, Y.T., Yang, Q.Z., Chen, D.Y., Wang, M.K., Li, J.S., Huang, S.L., Kong, X.Y., Shi, Y.Z., Wang, Z.Q., Xia, J.H., Long, Z.G., Xue, Z.G., Ding, W.X. & Sheng, H.Z. (2003). Embryonic stem cells generated by nuclear transfer of human somatic nuclei into rabbit oocytes. *Cell Res*, **13**, 251–63.

Chirino, A. & Mire-Sluis, A. (2004). Characterizing biological products and assessing comparability following manufacturing changes. *Nat Biotech*, **22**, 1383–1391.

Chisti, Y. (2000). Animal-cell damage in sparged bioreactors. *Trends Biotechnol*, **18**, 420–432.

Chisti, Y. (2001). Hydrodynamic damage to animal cells. *Crit Rev Biotechnol*, **21**, 67–110.

Choi, D., Lee, H.J., Jee, S., Jin, S., Koo, S.K., Paik, S.S., Jung, S.C., Hwang, S.Y., Lee, K.S. & Oh, B. (2005). In vitro differentiation of mouse embryonic stem cells: Enrichment of endodermal cells in the embryoid body. *Stem Cells*, **23**, 817–27.

Chong, S.L., Mou, D.G., Ali, A.M., Lim, S.H. & Tey, B.T. (2008). Cell growth, cell-cycle progress, and antibody production in hybridoma cells cultivated under mild hypothermic conditions. *Hybridoma*, **27**, 107–111.

Collas, P., Noer, A. & Sorensen, A.L. (2008). Epigenetic basis for the differentiation potential of mesenchymal and embryonic stem cells. *Transfus Med Hemother*, **35**, 205–215.

Cordewener, F.W., Dijkgraaf, L.C., Ong, J.L., Agrawal, C.M., Zardeneta, G., Milam, S.B. & Schmitz, J.P. (2000). Particulate retrieval of hydrolytically degraded poly(lactide-co-glycolide) polymers. *J Biomed Mater Res*, **50**, 59–66.

Cormier, J.T., zur Nieden, N.I., Rancourt, D.E. & Kallos, M.S. (2006). Expansion of undifferentiated murine embryonic stem cells as aggregates in suspension culture bioreactors. *Tissue Eng*, **12**, 3233–45.

Coucouvanis, E. & Martin, G.R. (1995). Signals for death and survival: A two-step mechanism for cavitation in the bertebrate embryo. *Cell*, **83**, 279–287.

Crenshaw, H.C., Allen, J.A., Skeen, V., Harris, A. & Salmon, E.D. (1996). Hydrostatic pressure has different effects on the assembly of tubulin, actin myosin II, vinculin, talin, vimentin and cytokeratin in mammalian tissue cells. *Exp Cell Res*, **227**, 285–297.

Daar, A.S. & Greenwood, H.L. (2007). A proposed definition of regenerative medicine. *J Tissue Eng Regen Med*, **1**, 179–84.

Dazzi, F., Ramasamy, R., Glennie, S., Jones, S. & Roberts, I. (2006). The role of mesenchymal stem cells in haemopoiesis. *Blood Reviews*, **20**, 161–171.

Ding, S. & Schultz, P.G. (2004). A role for chemistry in stem cell biology. *Nat Biotech*, **22**, 833–40.

Doetschman, T.C., Eistetter, H., Katz, M., Schmidt, W. & Kemler, R. (1985). The in vitro development of blastocyst-derived embryonic stem cell lines: Formation of visceral yolk sac, blood islands and myocardium. *Journal of Embryology and Experimental Morphology*, **87**, 27–45.

Dontu, G., Abdallah, W.M., Foley, J.M., Jackson, K.W., Clarke, M.F., Kawamura, M.J. & Wicha, M.S. (2003). In vitro propagation and transcriptional profiling of human mammary stem/progenitor cells. *Genes Dev*, **17**, 1253–1270.

Dua, H., Shanmuganathan, V., Powell-Richards, A., Tighe, P. & Joseph, A. (2005). Limbal epithelial crypts: A novel anatomical structure and a putative limbal stem cell niche. *British Journal of Ophthalmology*, **89**, 529–532.

Dunn, J.C. (2008). Analyses of cell growth in tissue-engineering scaffolds. *Regen Med*, **3**, 421–4.

Dunnett, S.B., Björklund, A. & Lindvall, O. (2001). Cell therapy in Parkinson's disease - stop or go? *Nat Rev Neurosci*, **2**, 365–9.

Elliott, R.B., Escobar, L., Tan, P.L.J., Muzina, M., Zwain, S. & Buchanan, C. (2007). Live encapsulated porcine islets from a type 1 diabetic patient 9.5 yr after xenotransplantation. *Xenotransplantation*, **14**, 157–161.

Engel, E., Michiardi, A., Navarro, M., Lacroix, D. & Planell, J.A. (2008). Nanotechnology in regenerative medicine: The materials side. *Trends Biotechnol*, **26**, 39–47.

Engler, A.J., Sen, S., Sweeney, H.L. & Discher, D.E. (2006). Matrix elasticity directs stem cell lineage specification. *Cell*, **126**, 677–89.

Evans, M.J. & Kaufman, M.H. (1981). Establishment in culture of pluripotential cells from mouse embryos. *Nature*, **292**, 154–6.

Fox, S.R., Patel, U.A., Yap, M.G.S. & Wang, D.I.C. (2004). Maximizing interferon-gamma production by chinese hamster ovary cells through temperature shift optimization: Experimental and modeling. *Biotechnol Bioeng*, **85**, 177–84.

Freyman, T., Yannas, I. & Gibson, L. (2001). Cellular materials as porous scaffolds for tissue engineering. *Prog Mater Sci*, **46**, 273–282.

Fujita, J. (1999). Cold shock response in mammalian cells. *J Mol Microbiol Biotechnol*, **1**, 234–255.

Gan, Q., Yoshida, T., McDonald, O.G. & Owens, G.K. (2007). Concise review: Epigenetic mechanisms contribute to pluripotency and cell lineage determination of embryonic stem cells. *Stem Cells*, **25**, 2–9.

Gao, D. & Critser, J.K. (2000). Mechanisms of cryoinjury in living cells. *ILAR journal / National Research Council, Institute of Laboratory Animal Resources*, **41**, 187–96.

Garcia-Briones, M.A. & Chalmers, J. (1994). Flow parameters associated with hydrodynamic cell injury. *Biotechnol Bioeng*, **44**, 1089–1098.

Giovannetti, G.T. & Jaggi, G. (2007). Beyond borders. Ernst & Young's global biotechnology report 2007.

Glofcheski, D.J., Borrelli, M.J., Stafford, D.M. & KRUUV, J. (1993). Induction of tolerance to hypothermia and hyperthermia by a common mechanism in mammalian cells. *J Cell Physiol*, **156**, 104–11.

Gorantla, V.S., Barker, J.H., Jones, J.W., Prabhune, K., Maldonado, C. & Granger, D.K. (2000). Immunosuppressive agents in transplantation: Mechanisms of action and current anti-rejection strategies. *Microsurgery*, **20**, 420–9.

Green, D. & Ware, C. (1997). Fas-ligand: Privilege and peril. *Proc Natl Acad Sci USA*, **94**, 5986–5990.

Halperin, G., Tauber-Finkelstein, M. & Shaltiel, S. (1984). Hydrophobic chromatography of cells: Adsorption and resolution on homologous series of alkylagaroses. *J Chromatogr*, **317**, 103–18.

Hanna, J., Markoulaki, S., Schordert, P., Carey, B., Beard, C., Wernig, M., Creyghton, M., Steine, E., Cassady, J. & Foreman, R. (2008). Direct reprogrammnig of terminall differentiated mature B lymphocytes to pluripotency. *Cell*, **133**, 250–264.

Hayflick, L. (1979). The cell biology of aging. *J Invest Dermatol*, **73**, 8–14.

Healy, D.A., Daly, P.J., Docherty, N.G., Murphy, M., Fitzpatrick, J.M. & Watson, R.W.G. (2006). Heat shock-induced protection of renal proximal tubular epithelial cells from cold storage and rewarming injury. *J Am Soc Nephrol*, **17**, 805–12.

Hochachka, P.W. (1986). Defense strategies against hypoxia and hypothermia. *Science*, **231**, 234–41.

Hoganson, D.M., Pryor, H.I. & Vacanti, J.P. (2008). Tissue engineering and organ structure: A vascularized approach to liver and lung. *Pediatr Res*, **63**, 520–526.

Hollister, S.J. (2005). Porous scaffold design for tissue engineering. *Nature Materials*, **4**, 518–24.

Horas, U., Pelinkovic, D., Herr, G., Aigner, T. & Schnettler, R. (2003). Autologous chondrocyte implantation and osteochondral cylinder transplantation in cartilage repair of the knee joint. A prospective, comparative trial. *The Journal of Bone and Joint Surgery American Volume*, **85-A**, 185–92.

Hubbell, J.A. (1995). Biomaterials in tissue engineering. *Biotechnology (NY)*, **13**, 565–76.

Hunt, L., Hacker, D.L., Grosjean, F., Jesus, M.D., Uebersax, L., Jordan, M. & Wurm, F.M. (2005). Low-temperature pausing of cultivated mammalian cells. *Biotechnol Bioeng*, **89**, 157–63.

Hutchinson, N., Bingham, N., Murrell, N., Farid, S. & Hoare, M. (2006). Shear stress analysis of mammalian cell suspensions for prediction of industrial centrifugation and its verification. *Biotechnol Bioeng*, **95**, 483–491.

Ingber, D.E. (1997). Tensegrity: The architectural basis of cellular mechanotransduction. *Annu Rev Physiol*, **59**.

Jiao, Y.P. & Cui, F.Z. (2007). Surface modification of polyester biomaterials for tissue engineering. *Biomed. Mater.*, **2**, R24–37.

Kawase, Y. & Moo-Young, M. (1990). Mathematical models for design of bioreactors: Applications of Kolmogoroff's theory of isotropic turbulence. *The Chemical Engineering Journal*, **43**, B19–B41.

Kemp, P. (2006). History of regenerative medicine: Looking backwards to move forwards. *Regen Med*, **1**, 653–69.

Kempken, R., Preissmann, A. & Berthold, W. (1995). Assessment of a disc stack centrifuge for use in mammalian cell separation. *Biotechnol Bioeng*, **46**, 132–138.

King, J., Griffiths, P., Zhou, Y. & Titchener-Hooker, N. (2004). Visualising bioprocesses using '3D-windows of operation'. *J Chem Technol Biot*, **79**, 518–525.

Klein, M.A., Kadidlo, D., McCullough, J., McKenna, D.H. & Burns, L.J. (2006). Microbial contamination of hematopoietic stem cell products: Incidence and clinical sequelae. *Biol Blood Marrow Transplant*, **12**, 1142–9.

Koyanagi-Katsuta, R., Akimitsu, N., Arimitsu, N., Hatano, T. & Sekimizu, K. (2000). Apoptosis of mouse embryonic stem cells induced by single cell suspension. *Tissue & cell*, **32**, 66–70.

Kuhlmann, M. & Covic, A. (2006). The protein science of biosimilars. *Nephrol Dial Transplant*, **21 Suppl 5**, v4–8.

Kunas, K. & Papoutsakis, E.T. (1990). Damage mechanisms of suspended animal cell in agitated bioreactors with and without bubble entrainment. *Biotechnol Bioeng*, **36**.

Kurosawa, H. (2007). Methods for inducing embryoid body formation: In vitro differentiation system of embryonic stem cells. *J Biosci Bioeng*, **103**, 389–398.

Lander, R., Daniels, C. & Meacle, F. (2005). Efficient, scalable clarification of diverse bioprocess streams using a novel pilot-scale tubular bowl centrifuge. *BioProcess Int*, **3**, 32–40.

Langer, R. & Vacanti, J.P. (1993). Tissue engineering. *Science*, **260**, 920–6.

Lee, J., Cuddihy, M. & Kotov, N.A. (2008). Three-dimensional cell culture matrices: State of the art. *Tissue Engineering: Part B*, **14**, 61–86.

Lee, M., Tuttle, J.B., Rebhun, L., Cleveland, D.W. & Frankfurter, A. (1990). The expression and posttranslational modification of a neuron-specific β-tubulin isotype during chick embryogenesis. *Cell Motil Cytoskeleton*, **17**, 118–132.

Lerou, P.H. & Daley, G.Q. (2005). Therapeutic potential of embryonic stem cells. *Blood Reviews*, **19**, 321–31.

Lightfoot, E.N. & Moscariello, J.S. (2004). Bioseparations. *Biotechnol Bioeng*, **87**, 259–73.

Lima, C., Pratas-Vital, J., Escada, P., Hasse-Ferreira, A., Capucho, C. & Peduzzi, J.D. (2006). Olfactory mucosa autografts in human spinal cord injury: A pilot clinical study. *The Journal of Spinal Cord Medicine*, **29**, 191–203; discussion 204–6.

Lin, T., Chao, C., Saito, S., Mazur, S.J., Murphy, M.E., Appella, E. & Xu, Y. (2005). p53 induces differentiation of mouse embryonic stem cells by suppressing nanog expression. *Nat Cell Biol*, **7**, 165–71.

Liu, A.Y., Bian, H., Huang, L.E. & Lee, Y.K. (1994). Transient cold shock induces the heat shock response upon recovery at 37°C in human cells. *J Biol Chem*, **269**, 14768–75.

Livak, K.J. & Schmittgen, T.D. (2001). Analysis of relative gene expression data using real-time quantitative PCR and the $2^{-\Delta\Delta C_T}$ method. *Methods*, **25**, 402–8.

Lokmic, Z. & Mitchell, G.M. (2008). Engineering the microcirculation. *Tissue Eng Pt B-Rev*, **14**, 87–103.

Los, D.A. & Murata, N. (2004). Membrane fluidity and its roles in the perception of environmental signals. *Biochim Biophys Acta*, **1666**, 142–157.

Lu, J., Hou, R., Booth, C.J., Yang, S.H. & Snyder, M. (2006). Defined culture conditions of human embryonic stem cells. *Proc Natl Acad Sci USA*, **103**, 5688–93.

Ludwig, T.E., Levenstein, M.E., Jones, J.M., Berggren, W.T., Mitchen, E.R., Frane, J.L., Crandall, L.J., Daigh, C.A., Conard, K.R., Piekarczyk, M.S., Llanas, R.A. & Thomson, J.A. (2006). Derivation of human embryonic stem cells in defined conditions. *Nat Biotech*, **24**, 185–7.

Ma, N., Koelling, K.W. & Chalmers, J.J. (2002). Fabrication and use of a transient contractional flow device to quantify the sensitivity of mammalian and insect cells to hydrodynamic forces. *Biotechnol Bioeng*, **80**, 428–437.

Maa, Y.F. & Hsu, C.C. (1996). Effect of high shear on proteins. *Biotechnol Bioeng*, **51**, 458–465.

MacLoughlin, P., Malone, D., Murtagh, J. & Kieran, P. (1998). The effects of turbulent jet flows on plant cell suspension cultures. *Biotechnol Bioeng*, **58**, 595–604.

Maimets, T., Neganova, I., Armstrong, L. & Lako, M. (2008). Activation of p53 by nutlin leads to rapid differentiation of human embryonic stem cells. *Oncogene*, 1–11.

Maiorella, B., Dorin, G., Carion, A. & Harano, D. (1991). Crossflow microfiltration of animal cells. *Biotechnol Bioeng*, **37**, 121–126.

Mason, C. & Dunnill, P. (2008a). A brief definition of regenerative medicine. *Regen Med*, **3**, 1–5.

Mason, C. & Dunnill, P. (2008b). Getting regenerative medicine onto the UK health agenda. *Unpublished*.

Mason, C. & Hoare, M. (2006). Regenerative medicine bioprocessing: the need to learn from the experience of other fields. *Regen Med*, **1**, 615–623.

Mason, C. & Hoare, M. (2007). Regenerative medicine bioprocessing: Building a conceptual framework based on early studies. *Tissue Eng*, **13**, 301–311.

Massia, S.P. & Hubbell, J.A. (1990). Covalent surface immobilization of Arg-Gly-Asp- and Tyr-Ile-Gly-Ser-Arg-containing peptides to obtain well-defined cell-adhesive substrates. *Anal Biochem*, **187**, 292–301.

Maybury, J., Hoare, M. & Dunnill, P. (2000). The use of laboratory centrifugation studies to predict performance of industrial machines: Studies of shear-insensitive and shear-sensitive materials. *Biotechnol Bioeng*, **67**, 265–273.

Maybury, J.P., Mannweiler, K., Titchener-Hooker, N.J., Hoare, M. & Dunnill, P. (1998). The performance of a scaled down industrial disc stack centrifuge with a reduced feed material reqirement. *Bioprocess Eng*, **18**, 191–199.

Maye, P., Becker, S., Kasameyer, E., Byrd, N. & Grabel, L. (2000). Indian hedgehog signaling in extraembryonic endoderm and ectoderm differentiation in es embryoid bodies. *Mech Dev*, **94**, 117–132.

Mazur, P. (1970). Cryobiology: The freezing of biological systems. *Science*, **168**, 939–49.

McClay, D.R., Wessel, G.M. & Marchase, R.B. (1981). Intercellular recognition: Quantitation of initial binding events. *Proc Natl Acad Sci USA*, **78**, 4975–9.

Metcalfe, A.D. & Ferguson, M.W.J. (2007). Tissue engineering of replacement skin: The crossroads of biomaterials, wound healing, embryonic development, stem cells and regeneration. *Journal of the Royal Society, Interface / The Royal Society*, **4**, 413–37.

Mitsui, K., Tokuzawa, Y., Itoh, H., Segawa, K., Murakami, M., Takahashi, K., Maruyama, M., Maeda, M. & Yamanaka, S. (2003). The homeoprotein Nanog is required for maintenance of pluripotency in mouse epiblast and ES cells. *Cell*, **113**, 631–42.

Moore, K.A. & Lemischka, I.R. (2006). Stem cells and their niches. *Science*, **311**, 1880–5.

Moore, M., Jabbari, E., Ritman, E., Lu, L., Currier, B., Windebank, A. & Yaszemski, M. (2004). Quantitative analysis of interconnectivity of porous biodegradable scaffolds with micro-computed tomography. *Journal of Biomedical Materials Research Part A*, **71A**, 258–267.

Morrison, S.J. & Kimble, J. (2006). Asymmetric and symmetric stem-cell divisions in development and cancer. *Nature*, **441**, 1068–1074.

Mountford, J.C. (2008). Human embryonic stem cells: Origins, characteristics and potential for regenerative therapy. *Transfus Med*, **18**, 1–12.

Nagy, A., Rossant, J., Nagy, R., Abramow-Newerly, W. & Roder, J.C. (1993). Derivation of completely cell culture-derived mice from early-passage embryonic stem cells. *Proc Natl Acad Sci USA*, **90**, 8424–8.

Nakanishi, M., Hamazaki, T.S., Komazaki, S., Okochi, H. & Asashima, M. (2007). Pancreatic tissue formation from murine stem cells *in vitro*. *Differentiation*, **75**, 1–11.

Nesic, D., Whiteside, R., Brittberg, M., Wendt, D., Martin, I. & Mainil-Varlet, P. (2006). Cartilage tissue engineering for degenerative joint disease. *Advanced Drug Delivery Reviews*, **58**, 300–22.

Ng, T., Marx, G., Littlewood, T. & Macdougall, I. (2003). Recombinant erythropoietin in clinical practice. *Postgraduate Medical Journal*, **79**, 367–76.

Nishimoto, M., Fukushima, A., Okuda, A. & Muramatsu, M. (1999). The gene for the embryonic stem cell coactivator UTF1 carries a regulatory element which selectively interacts with a complex composed of Oct-3/4 and Sox-2. *Mol Cell Biol*, **19**, 5453–5465.

Nishimoto, M., Miyagi, S., Yamagishi, T., Sakaguchi, T., Niwa, H., Muramatsu, M. & Okuda, A. (2005). Oct-3/4 maintains the proliferative embryonic stem cell state via specific binding to a variant octamer sequence in the regulatory region of the UTF1 locus. *Mol Cell Biol*, **25**, 5084–94.

Niwa, H., Miyazaki, J. & Smith, A.G. (2000). Quantitative expression of Oct-3/4 defines differentiation, dedifferentiation or self-renewal of ES cells. *Nat Genet*, **24**, 372–6.

O'Ceallaigh, S., Herrick, S.E., Bennett, W.R., Bluff, J.E., Ferguson, M.W.J. & McGrouther, D.A. (2007). Perivascular cells in a skin graft are rapidly repopulated by host cells. *J Plast Reconstr Aes*, **60**, 864–875.

Okada, Y., Shimazaki, T., Sobue, G. & Okano, H. (2004). Retinoic-acid-concentration-dependent acquisition of neural cell identity during in vitro differentiation of mouse embryonic stem cells. *Dev Biol*, **275**, 124–142.

Okuda, A., Fukushima, A., Nishimoto, M., Orimo, A., Yamagishi, T., Nabeshima, Y., Kuro-o, M., i Nabeshima, Y., Boon, K., Keaveney, M., Stunnenberg, H.G. & Muramatsu, M. (1998). UTF1, a novel transcriptional

coactivator expressed in pluripotent embryonic stem cells and extra-embryonic cells. *EMBO J*, **17**, 2019–32.

Oshima, H., Rochat, A., Kedzia, C., Kobayashi, K. & Barrandon, Y. (2001). Morphogenesis and renewal of hair follicles from adult multipotent stem cells. *Cell*, **104**, 233–45.

Papoutsakis, E.T. (1991). Fluid-mechanical damage of animal cells in bioreactors. *Trends Biotechnol*, **9**, 427–37.

Perotti, M., Toddei, F., Mirabelli, F., Vairetti, M., Bellomo, G., McConkey, D.J. & Orrenius, S. (1990). Calcium-dependent DNA fragmentation in human synovial cells exposed to cold shock. *FEBS Lett*, **259**, 331–4.

Plesnila, N., Muller, E., Guretzki, S., Ringel, F., Staub, F. & Baethmann, A. (2000). Effect of hypothermia on the volume of rat glial cells. *J Physiol (Lond)*, **523 (1)**, 155–62.

Pollock, K., Stroemer, P., Patel, S., Stevanato, L., Hope, A., Miljan, E., Dong, Z., Hodges, H., Price, J. & Sinden, J.D. (2006). A conditionally immortal clonal stem cell line from human cortical neuroepithelium for the treatment of ischemic stroke. *Exp Neurol*, **199**, 143–55.

Radisic, M., Deen, W., Langer, R. & Vunjak-Novakovic, G. (2005). Mathematical model of oxygen distribution in engineered cardiac tissue with parallel channel array perfused with culture medium containing oxygen carriers. *American Journal of Physiology- Heart and Circulatory Physiology*, **288**, H1278–1H289.

Ramirez, O.T. & Mutharasan, R. (1990). The role of the plasma membrane fluidity on the shear sensitivity of hybridomas grown under hydrodynamic stress. *Biotechnol Bioeng*, **36**, 911–920.

Rauen, U., Petrat, F., Li, T. & Groot, H.D. (2000). Hypothermia injury/cold-induced apoptosis - evidence of an increase in chelatable iron causing oxidative injury in spite of low O_2^-/H_2O_2 formation. *FASEB J*, **14**, 1953–1964.

Russotti, G., Brieva, T., Toner, M. & Yarmush, M. (1996). Induction of tolerance to hypothermia by previous heat shock using human fibroblasts in culture. *Cryobiology*, **33**, 567–580.

Sadoshima, J. & Izumo, S. (1997). The cellular and molecular response of cardiac myocytes to mechanical stress. *Annu Rev Physiol*, **59**.

Saha, S., Ji, L., de Pablo, J. & Palecek, S.P. (2005). Inhibition of human embryonic stem cell differentiation by mechanical strain. *J Cell Physiol*, **206**, 126–137.

Sakurai, T., Itoh, K., Liu, Y., Higashitsuji, H., Sumitomo, Y., Sakamaki, K. & Fujita, J. (2005). Low temperature protects mammalian cells from apoptosis initiated by various stimuli in vitro. *Exp Cell Res*, **309**, 264–272.

Salmon, E.D., Goode, D., Maugel, T.K. & Bonar, D.B. (1976). Pressure-induced depolymerization of spindle microtubles. *J Cell Biol*, **69**, 443–454.

Salte, H., King, J.M.P., Baganz, F., Hoare, M. & Titchener-Hooker, N.J. (2006). A methodology for centrifuge selection for the separation of high solids density cell broths by visualisation of performance using windows of operation. *Biotechnol Bioeng*, **95**, 1218–27.

Seal, B., Otero, T. & Panitch, A. (2001). Polymeric biomaterials for tissue and organ regeneration. *Materials Science & Engineering R*, **34**, 147–230.

Seow, T., Korke, R., Liang, R., Ong, S., Ou, K., Wong, K., Hu, W. & Chung, M. (2001). Proteomic investigation of metabolic shift in mammalian cell culture. *Biotechnol Prog*, **17**, 1137–1144.

Shah, M., Foreman, D.M. & Ferguson, M.W. (1992). Control of scarring in adult wounds by neutralising antibody to transforming growth factor β. *Lancet*, **339**, 213–4.

Sherwood, J.K., Riley, S.L., Palazzolo, R., Brown, S.C., Monkhouse, D.C., Coates, M., Griffith, L.G., Landeen, L.K. & Ratcliffe, A. (2002). A three-dimensional osteochondral composite scaffold for articular cartilage repair. *Biomaterials*, **23**, 4739–51.

Shieh, S.J. & Vacanti, J.P. (2005). State-of-the-art tissue engineering: From tissue engineering to organ building. *Surgery*, **137**, 1–7.

Shimizu, N., Yamamoto, K., Obi, S., Kumagaya, S., Masumura, T., Shimano, Y., Naruse, K., Yamashita, J.K., Igarashi, T. & Ando, J. (2008). Cyclic strain induces mouse embryonic stem cell differentiation into vascular smooth muscle cells by activating PDGF receptor β. *J Appl Physiol*, **104**, 766–72.

Shimoda, M., Kanai-Azuma, M., Hara, K., Miyazaki, S., Kanai, Y., Monden, M. & ichi Miyazaki, J. (2007). Sox17 plays a substantial role in late-stage differentiation of the extraembryonic endoderm in vitro. *J Cell Sci*, **120**, 3859–69.

Shortt, A.J., Secker, G.A., Notara, M.D., Limb, G.A., Khaw, P.T., Tuft, S.J. & Daniels, J.T. (2007). Transplantation of ex vivo cultured limbal epithelial stem cells: A review of techniques and clinical results. *Survey of ophthalmology*, **52**, 483–502.

Smith, A.G. (2001). Embryo-derived stem cells: of mice and men. *Annu Rev Cell Dev Biol*, **17**, 435–462.

Sneddon, J.B. & Werb, Z. (2007). Location, location, location: The cancer stem cell niche. *Cell Stem Cell*, **1**, 607–11.

Soker, S., Machado, M. & Atala, A. (2000). Systems for therapeutic angiogenesis in tissue engineering. *World Journal of Urology*, **18**, 10–18.

Soutschek, J., Akinc, A., Bramlage, B., Charisse, K., Constien, R., Donoghue, M., Elbashir, S., Geick, A., Hadwiger, P., Harborth, J., John, M., Kesavan, V., Lavine, G., Pandey, R.K., Racie, T., Rajeev, K.G., Röhl, I., Toudjarska, I., Wang, G., Wuschko, S., Bumcrot, D., Koteliansky, V., Limmer, S., Manoharan, M. & Vornlocher, H.P. (2004). Therapeutic silencing of an endogenous gene by systemic administration of modified siRNAs. *Nature*, **432**, 173–8.

Stadtfeld, M., Brennand, K. & Hochedlinger, K. (2008). Reprogramming of pancreatic β cells into induced pluripotent stem cells. *Curr Biol*, **18**, 890–894.

Stevens, M.M. & George, J.H. (2005). Exploring and engineering the cell surface interface. *Science*, **310**, 1135–8.

Takahashi, K. & Yamanaka, S. (2006). Induction of pluripotent stem cells from mouse embryonic and adult fibroblast cultures by defined factors. *Cell*, **126**, 663–676.

Takahashi, K., Tanabe, K., Ohnuki, M., Narita, M., Ichisaka, T., Tomoda, K. & Yamanaka, S. (2007). Induction of pluripotent stem cells from adult human fibroblasts by defined factors. *Cell*, **131**, 861–872.

Taylor, G.I. (1934). The formation of emulsions in definable fields of flow. *Proceedings of the Royal Society of London. Series A, Containing Papers of a Mathematical and Physical Character*, **146**, 501–523.

Tesar, P.J., Chenoweth, J.G., Brook, F.A., Davies, T.J., Evans, E.P., Mack, D.L., Gardner, R.L. & McKay, R.D.G. (2007). New cell lines from

mouse epiblast share defining features with human embryonic stem cells. *Nature*, **448**, 196–199.

Thomson, J.A., Itskovitz-Eldor, J., Shapiro, S.S., Waknitz, M.A., Swiergiel, J.J., Marshall, V.S. & Jones, J.M. (1998). Embryonic stem cell lines derived from human blastocysts. *Science*, **282**, 1145–7.

Titchener-Hooker, N.J., Dunnill, P. & Hoare, M. (2008). Micro biochemical engineering to accelerate the design of industrial-scale downstream processes for biopharmaceutical proteins. *Biotechnol Bioeng*, **100**, 473–87.

Tögel, F. & Westenfelder, C. (2007). Adult bone marrow-derived stem cells for organ regeneration and repair. *Dev Dyn*, **236**, 3321–31.

Trounson, A. (2006). The production and directed differentiation of human embryonic stem cells. *Endocrine Reviews*, **27**, 208–219.

Umbreit, J. & Roseman, S. (1975). A requirement for reversible binding between aggregating embryonic cells before stable adhesion. *J Biol Chem*, **250**, 9360–8.

van den Boom, V., Kooistra, S.M., Boesjes, M., Geverts, B., Houtsmuller, A.B., Monzen, K., Komuro, I., Essers, J., Drenth-Diephuis, L.J. & Eggen, B.J.L. (2007). UTF1 is a chromatin-associated protein involved in ES cell differentiation. *J Cell Biol*, **178**, 913–24.

van der Laan, L.J., Lockey, C., Griffeth, B.C., Frasier, F.S., Wilson, C.A., Onions, D.E., Hering, B.J., Long, Z., Otto, E., Torbett, B.E. & Salomon, D.R. (2000). Infection by porcine endogenous retrovirus after islet xenotransplantation in SCID mice. *Nature*, **407**, 90–4.

van Reis, R., Leonard, L., Hsu, C. & Builder, S. (1991). Industrial scale harvest of proteins from mammalian cell culture by tangential flow filtration. *Biotechnol Bioeng*, **38**, 413–422.

Vanreis, R. & Zydney, A. (2007). Bioprocess membrane technology. *Journal of Membrane Science*, **297**, 16–50.

Veraitch, F.S., Scott, R., Wong, J.W., Lye, G.J. & Mason, C. (2008). The impact of manual processing on the expansion and directed differentiation of embryonic stem cells. *Biotechnol Bioeng*, **99**, 1216–29.

Wang, Z.Q., Kiefer, F., Urbánek, P. & Wagner, E.F. (1997). Generation of completely embryonic stem cell-derived mutant mice using tetraploid blastocyst injection. *Mech Dev*, **62**, 137–45.

Waugh, R.E. (1982). Temperature dependence of the yield shear resultant and the plastic viscosity coefficient of erythrocyte membrane. *Biophysical Journal*, **39**, 6.

Weiss, R.A., Weiss, M.A., Beasley, K.L. & Munavalli, G. (2007). Autologous cultured fibroblast injection for facial contour deformities: A prospective, placebo-controlled, phase III clinical trial. *Dermatol Surg*, **33**, 263–268.

West, J.A., Park, I.H., Daley, G.Q. & Geijsen, N. (2006). In vitro generation of germ cells from murine embryonic stem cells. *Nature Protocols*, **1**, 2026–36.

Westra, A. & Dewey, W.C. (1971). Variation in sensitivity to heat shock during the cell-cycle of chinese hamster cells in vitro. *Int. J. of Radiation Biol.*, **19**, 467–477.

Wilkinson, D.G., Bhatt, S. & Herrmann, B.G. (1990). Expression pattern of the mouse T gene and its role in mesoderm formation. *Nature*, **343**, 657–9.

Williams, R.L., Hilton, D.J., Pease, S., Willson, T.A., Stewart, C.L., Gearing, D.P., Wagner, E.F., Metcalf, D., Nicola, N.A. & Gough, N.M. (1988). Myeloid leukaemia inhibitory factor maintains the developmental potential of embryonic stem cells. *Nature*, **336**, 684–687.

Wilson, C.J., Clegg, R.E., Leavesley, D.I. & Pearcy, M.J. (2005). Mediation of biomaterial-cell interactions by adsorbed proteins: A review. *Tissue Eng*, **11**, 1–18.

Wobus, A.M. & Boheler, K.R. (2005). Embryonic stem cells: Prospects for developmental biology and cell therapy. *Physiol Rev*, **85**, 635–678.

Woodley, J. & Titchener-Hooker, N. (1996). The use of windows of operation as a bioprocess design tool. *Bioprocess Eng*, **14**, 263–268.

Yamamoto, K., Sokabe, T., Watabe, T., Miyazono, K., Yamashita, J.K., Obi, S., Ohura, N., Matsushita, A., Kamiya, A. & Ando, J. (2005). Fluid shear stress induces differentiation of Flk-1-positive embryonic stem cells into vascular endothelial cells in vitro. *Am J Physiol Heart Circ Physiol*, **288**, H1915–24.

Yannas, I.V. (2001). *Tissue and organ regeneration in adults*. Springer, 1st edn.

Yannas, I.V. (2004). Synthesis of tissues and organs. *ChemBioChem*, **5**, 26–39.

Yates, A. & Chambers, I. (2005). The homeodomain protein Nanog and pluripotency in mouse embryonic stem cells. *Biochem Soc Trans*, **33**, 1518–21.

Ying, Q.L., Nichols, J., Evans, E.P. & Smith, A.G. (2002). Changing potency by spontaneous fusion. *Nature*, **416**, 545–8.

Youn, B.S., Sen, A., Kallos, M.S., Behie, L.A., Girgis-Gabardo, A., Kurpios, N., Barcelon, M. & Hassell, J.A. (2005). Large-scale expansion of mammary epithelial stem cell aggregates in suspension bioreactors. *Biotechnol Prog*, **21**, 984–993.

Zandstra, P.W. & Nagy, A. (2001). Stem cell bioengineering. *Annual review of biomedical engineering*, **3**, 275–305.

Zeng, X. & Rao, M.S. (2007). Human embryonic stem cells: Long term stability, absence of senescence and a potential cell source for neural replacement. *Neuroscience*, **145**, 1348–1358.

Zhang, Z., Al-Rubeai, M. & Thomas, C. (1993). Estimation of disruption of animal cells by turbulent capillary flow. *Biotechnol Bioeng*, **42**, 987–993.

Zhou, Y.H. & Titchener-Hooker, N.J. (1999). Visualizing integrated bioprocess designs through "windows of operation". *Biotechnol Bioeng*, **65**, 550–7.

Zimmermann, T.S., Lee, A.C.H., Akinc, A., Bramlage, B., Bumcrot, D., Fedoruk, M.N., Harborth, J., Heyes, J.A., Jeffs, L.B., John, M., Judge, A.D., Lam, K., Mcclintock, K., Nechev, L.V., Palmer, L.R., Racie, T., Röhl, I., Seiffert, S., Shanmugam, S., Sood, V., Soutschek, J., Toudjarska, I., Wheat, A.J., Yaworski, E., Zedalis, W., Koteliansky, V., Manoharan, M., Vornlocher, H.P. & Maclachlan, I. (2006). RNAi-mediated gene silencing in non-human primates. *Nature*, **441**, 111–4.

Zoro, B.J.H., Owen, S., Drake, R.A.L. & Hoare, M. (2008). The impact of process stress on suspended anchorage-dependent mammalian cells as an indicator of likely challenges for regenerative medicines. *Biotechnol Bioeng*, **99**, 468–74.